IWF

ANNUAL REPORT 2002

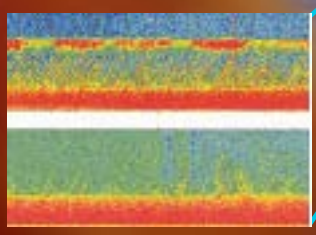

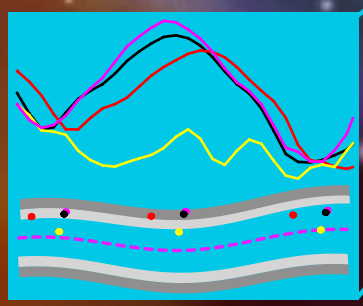

SPACE RESEARCH INSTITUTE GRAZ
AUSTRIAN ACADEMY OF SCIENCES

ANNUAL REPORT 2002

SPACE RESEARCH INSTITUTE GRAZ
AUSTRIAN ACADEMY OF SCIENCES

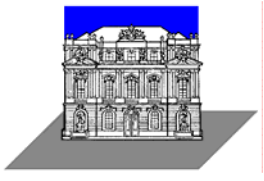

Institut für Weltraumforschung
Österreichische Akademie der Wissenschaften
Schmiedlstraße 6
8042 Graz, Austria
Tel.: +43 316 4120-400
Fax: +43 316 4120-490
office.iwf@oeaw.ac.at
http://www.iwf.oeaw.ac.at

Cover Image:

Measurements in the Earth's magnetosphere by the Cluster tetrahedron of spacecraft: left: radio signatures of plasmaspheric structures (see Fig. 3.11, p. 24); right: bifurcated current sheets (see Fig. 3.8, p. 22).

Table of Contents

1 Introduction

The Space Research Institute (Institut für Weltraumforschung, IWF) of the Austrian Academy of Sciences (Österreichische Akademie der Wissenschaften, ÖAW) understands itself as a focus of Austrian space activities. It cooperates closely with space agencies all over the world, with the two academic universities located in Graz, with the Austrian Space Agency (ASA), and with numerous other national and international institutions. A particularly intense cooperation exists with the European Space Agency (ESA). IWF participates in various interplanetary missions as well as in missions dedicated to the exploration of our own planet Earth and its neighborhood. In particular:

- *Cassini/Huygens* is currently on the way to Saturn and its satellite system.
- *Cluster* is exploring the space-time structure of the terrestrial magnetic field and the magnetospheric plasma in unprecedented detail.
- *DoubleStar,* the first European-Chinese space mission cooperation, will support the *Cluster* mission.
- *Rosetta* will investigate the coma and the nucleus of a comet. For the first time a soft landing on a cometary nucleus will be tried.
- *Mars Express* will investigate water on Mars by an on-board radar system.
- *Venus Express* will investigate the atmosphere and ionosphere of the Earth's nearest planetary neighbor, Venus.
- *BepiColombo* will investigate in detail the innermost planet Mercury, using a fleet of two orbiters and one lander.
- *Envisat's* radar altimeter will be calibrated by a transponder system, owned by IWF, at a cross-over site on the Greek island Gavdos.
- *GOCE* will determine with high accuracy and resolution the structure of the terrestrial gravitational field. These measurements are expected to contribute significantly to a better understanding of the Earth's interior, global ocean circulation, heat transport mechanisms, and to a worldwide unification of regional height systems.

In addition, IWF performs a wealth of theoretical investigations, data analysis, and laboratory experiments on gravitational and magnetic fields, on atmospheres and on surface properties of solar system bodies. Moreover, at Lustbühel Observatory in Graz one of the most accurate laser ranging stations of the world is operated. Its data are used to determine the orbits of more than 30 satellites. Also located at Lustbühel Observatory is a system of antennas used to monitor the radio emissions of Jupiter and the Sun. Finally, a network of nine permanent GPS stations is operated by IWF in order to monitor geodynamical movements in Austria and its vicinity.

IWF is located in an attractive building, the "Forschungszentrum Graz" (Research Center Graz) of the Austrian Academy of Sciences (see Fig. 1.1). Its managing director, Prof. Dr. Hans Sünkel, is at the same time vice rector for research of the Graz University of Technology.

IWF is structured into three departments:

- Experimental Space Research
  (Head: Prof. Dr. Wolfgang Baumjohann)
- Extraterrestrial Physics
  (Head: Prof. Dr. Helmut O. Rucker)
- Satellite Geodesy
  (Head: Prof. Dr. Hans Sünkel)

Fig. 1.1: A view inside the "Forschungszentrum Graz".

The bulk of financial support for our research comes from the Austrian Academy of Sciences (Österreichische Akademie der Wissenschaften, ÖAW). Substantial support is also provided by other national institutions, the Austrian Space Agency (ASA), the Austrian Science Fund (Fonds zur Förderung der wissenschaftlichen Forschung, FWF), the Austrian Council for Research and Technology Development (Rat für Forschung und Technologieentwicklung, RFTE), and by the Austrian Academic Exchange Service (Österreichischer Akademischer Austauschdienst, ÖAD) and its partner institutions in other countries. Last but not least, European Institutions like the European Space Agency (under the PRODEX and GOCE Programs) and the European Union (under the INTAS and 5th Framework Programs) contribute substantially.

2 Solid Earth

How is the actual status of the surface of the Earth and its near vicinity? Can permanent monitoring lead to a possible prediction of future global changes and, if yes, how?

Questions for our “blue planet” which find the answer in a nearly unlimited bulk of data provided by artificial satellites of different kind and layout, equipped with special sensors for different tasks. They outline a global image of our planet with, up to now, unknown resolution, which allows for the investigation of detailed structures. The task remains how to decorrelate individual phenomena and to pick out the specific elements which are required for the understanding of the basic physical processes.

For example, the precise knowledge of the Earth’s gravity field and its temporal changes contributes to the detection of the mechanisms leading to the building of the Earth’s crust, the evolution of the green house effect and the realization of ocean currents. The repeated determination of precise station coordinates via GPS and Satellite Laser Ranging leads to the definition of a temporally changing velocity field, which enables the investigation of the underlying driving forces and the energy transport in the Earth’s interior.

2.1 Gravity Field

The gravity field of the Earth is the sum of the gravitational and centrifugal force, with the first being the response to the Earth’s interior density distribution and the latter caused by its rotation. Up to now the gravitational part is far from being well known on a global scale, which is reflected in the low accuracy of current global gravity Earth models. A quantum leap forward, as far as accuracy as well as resolution of these satellite derived gravity models are concerned, will be made in the near future by three dedicated gravity field satellite missions, namely *Champ*, *Grace* and *GOCE*. The *GOCE* mission (Gravity Field and Steady-State Ocean Circulation Explorer) will be the prime focus of attention, as the number one ranked mission in ESA’s Earth Explorer program.

GOCE Mission

The sensor fusion concept of the *GOCE* satellite (Fig. 2.1) will enable an accuracy gain over the whole wavelength spectrum of the gravity field, making use of two complementing measuring devices: satellite-to-satellite tracking (SST) in high-low mode using GPS and providing the long to medium wavelength information, plus the satellite’s core instrument itself for performing satellite gravity gradiometry (SGG) yielding information in the short wavelength range. In technical terms, this gravity field information is represented by harmonic coefficients of a spherical harmonics series expansion up to degree and order 300, which corresponds to shortest half wavelengths of less than 70 km. The derived geoid model will become known with an accuracy of better than 1 cm on a global scale.

The selected *GOCE* orbit is nearly circular with a nominal mean satellite altitude of 250 km, the orbit inclination at the given altitude is i=96.5° (sun-synchronous orbit). The repeat period for the ground tracks for global coverage is equal or larger than 2 months, and in the two measurement phases of 6 months

each the huge amount of tens of millions of orbit data will have to be processed. A three-axis gravity gradiometer as the core instrument on board the satellite will provide local gravity field information along the orbit in terms of second order derivatives of the gravitational potential along the orbit.

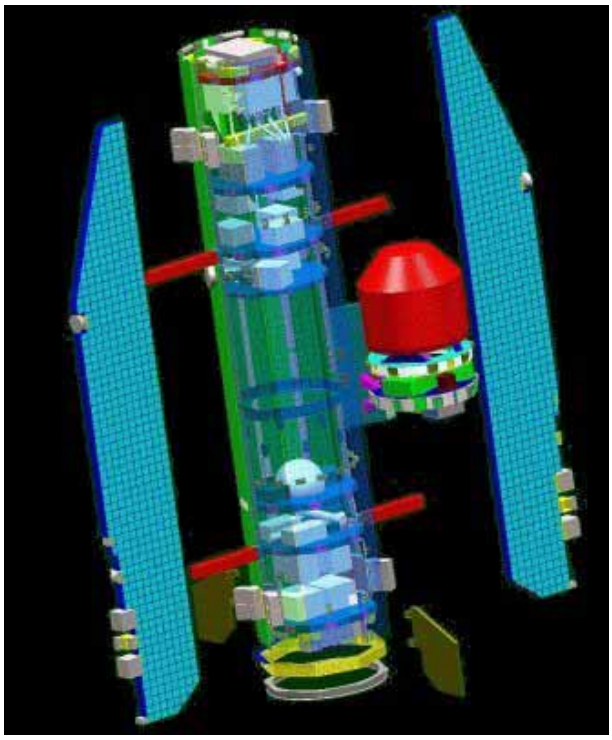

Fig. 2.1: Exploded view of the GOCE satellite showing the gradiometer instrument (in red) and the micro-thrusters located at the ends of the body.

Additionally it will provide linear and angular accelerations of the spacecraft, which will be compensated for by ion and cold gas thrusters such that the spacecraft remains in a perfect free fall motion with perfectly controlled rotation. The transformation of the GPS phase measurements plus the observed second order derivatives of the gravitational field (expressed in terms of Eötvös units, 1 E = 1 mGal/10 km), into Milligal, is the scientific focus in the course of the *GOCE* data processing. Numerics, statistics, and especially tailored processing algorithms, making extensive use of parallel computer hard- and software, will be the scientific working tools to accomplish this laborious and extremely demanding task. The long history in participation in several ESA project studies enables our GOCE team to be well prepared in facing this forthcoming challenge.

E2mGal+ Activities

The *E2mGal+* project is following the previous *"From Eötvös to Milligal" (E2mGal)* project, which continues the long sequence of *GOCE* related studies on behalf of the European Space Agency. The work offered in this project was performed by the TUG/ÖAW consortium, the Austrian Competence Center for satellite based gravity field determination, located in Graz, Austria. The scientific team consists of two academic institutions:

- Institute of Geodesy, Department of Theoretical Geodesy, Graz University of Technology (TUG)
- Space Research Institute (IWF), Department of Satellite Geodesy, Austrian Academy of Sciences (ÖAW)

The TUG/ÖAW consortium was supported by the scientific consulting of the Institute of Astronomical and Physical Geodesy of the Technical University of Munich (Germany) and the Institute of Theoretical Geodesy of the University of Bonn (Germany).

One of the focal points in the project study was the demanding task of accomplishing the satellite-to-satellite tracking concepts, i.e. the implementation of the SST high-low component, focusing in particular on temporal variation phenomena and their influence on the *GOCE* orbit. In the course of the project, we developed from scratch our own ARCSST software for arcwise SST *GOCE* data processing, which integrates the orbit together with the variational equations and takes into account many temporal variations of the Earth's gravity field. Furthermore, another alternative procedure to compute the spherical harmonics coefficients based on the Jacobi Energy integral (energy conservation law) approach was developed. In order to assess the sensitivity of both methods to the orbital noise, a realistic orbital error description in terms of

propagated position variance/covariance matrices together with the corresponding position noise distribution was provided by TU Munich, where simulations of *GOCE* Precise Orbit Determination (POD) was carried out based on the kinematic POD approach.

Fig. 2.2 shows the obtained results in terms of RMS per coefficient per degree for different gravity field estimation runs. From this we can deduce that in the noise-free scenario the energy balance approach shows a better accuracy than the numerical integration technique. However, a major difference is the run-time, which is in the present configuration approximately 20 times longer for the numerical integration approach.

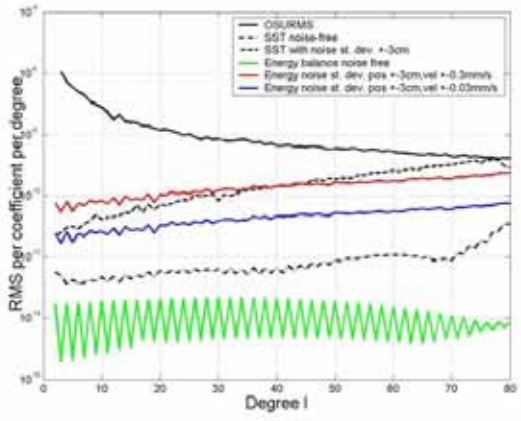

Fig. 2.2: RMS plot for different SST solutions.

As far as the noisy scenario is concerned, from Fig. 2.2 we see that, in order to obtain roughly the same accuracy as the numerical integration, the velocities have to be known with an accuracy of at least 10^{-4} m/s, and even then we have a lower accuracy compared to the numerical integration approach in the spectral range up to degree 35. Summarizing, the numerical integration approach has proven itself to be superior to the energy balance approach when noise with a realistic amplitude is introduced, although it requires more computational time.

In the further context of the *E2mGal+* project, we performed a detailed study of the temporal variations of the Earth's gravity field caused mainly by the influence of the Sun and the Moon on the mass redistribution. Our investigations mainly focused on the ocean tides, since they are one of the main contributors to variations of the gravity field on a short time scale. As a second time varying component, we also considered seasonal variations caused by other phenomena such as ocean topography or land hydrology variations.

In the course of the *GOCE* data processing, there are two main strategies to deal with temporal variation effects. The optimum approach would be to model these contributions based on external geophysical models and to reduce them from the *GOCE* observations. However, the quality of this strategy is highly related to the accuracy of the external models. If we follow this strategy, the crucial point will be the accuracy of the external models. Therefore, in these studies we did not only investigate the absolute contribution of temporal variations to the Earth's gravity field, but also the magnitude of residuals between different, independently generated state-of-the-art geophysical models. For the analysis of semi-diurnal and diurnal ocean tide signals the ocean tide models CSR4.0, AG95.1 and SR95B were assessed. All models are given as in-phase and quadrature 0.5° x 0.5° equiangular grids. Considering the long periodic temporal variations, for the land hydrology contribution assessment, we selected the SiB2 model, generated by the Colorado State University, as well as the ISBA model provided by Meteo-France for further studies. The soil moisture and snow cover data are given as representative values on a 1° x 1° equiangular grid. For the ocean topography the ECCO model as well as the POCM, also known as the Semtner & Chervin model was used, with a nominal lateral resolution of 1/4° x 1/4°.

Fig. 2.3 shows the RMS amplitude of geoid heights, related to the lunar semidiurnal M_2 constituent of the ocean tide model AG95.1.

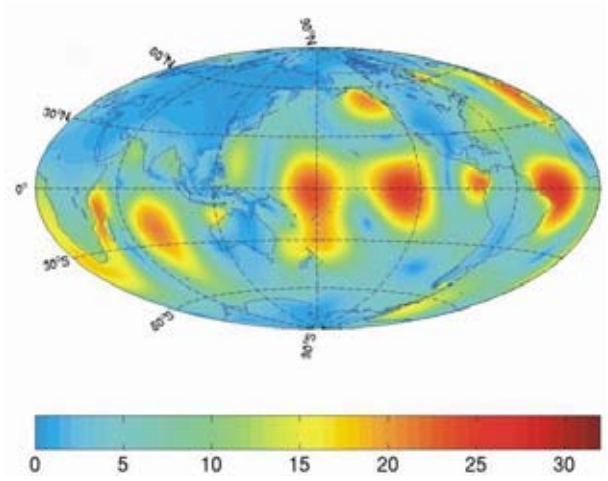

Fig. 2.3: RMS of geoidal height [mm] of M_2 constituent based on ocean tide model AG95.1

Evidently, the principal lunar ocean tide component M_2 causes gravity field signals up to 3 cm. In order to estimate the magnitude of potential modeling errors, occurring if such models are used for the external reduction of ocean tide signals, Fig. 2.4 shows the corresponding deviations of the CSR4.0 from the AG95.1 ocean tide model.

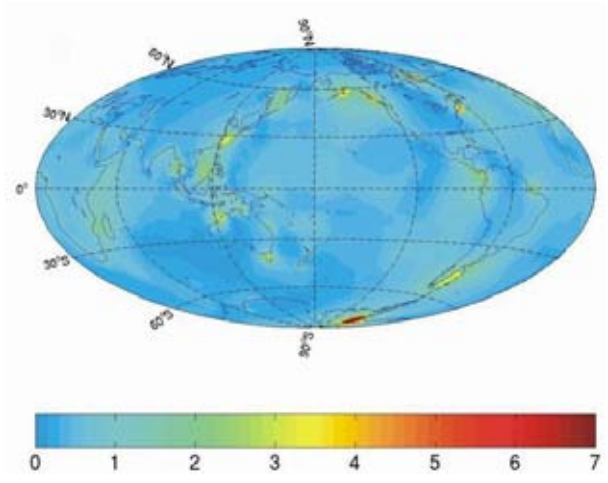

Fig. 2.4: Geoid height differences [mm] of M_2 constituent between AG95.1 and CSR4.0.

Although most of the ocean regions are modeled very well, there remain some large differences predominantly in the coastal areas, which are mainly due to the fact that in the CSR4.0 some new regional off-shore models are included, which are not inherent in AG95.1.

The land hydrology and the ocean topography have complementing definition domains. Therefore, a merge of the two temporal variation effects to one global model suggests itself in order to perform a combined sensitivity analysis. Fig. 2.5 shows the cumulative annual gravity anomaly signal based on the SiB2 soil moisture and snow cover model combined with the ocean model ECCO complete up to degree 50 masking those regions where the signal is below the 1 μGal-level. Compared with only the SiB2 component, it becomes obvious that the land hydrology contributes by far larger signals to the gravity field than the non-steric (caused by water mass changes) ocean topography effect.

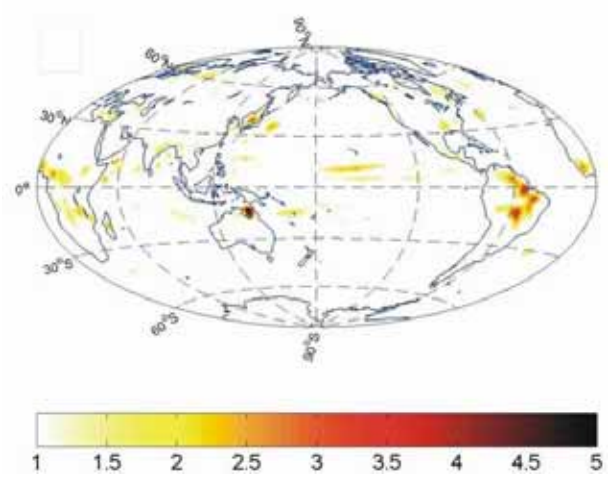

Fig. 2.5: Sensitivity analysis: Cumulative gravity anomaly contributions [μGal] up to degree 50 of SiB2+ECCO models.

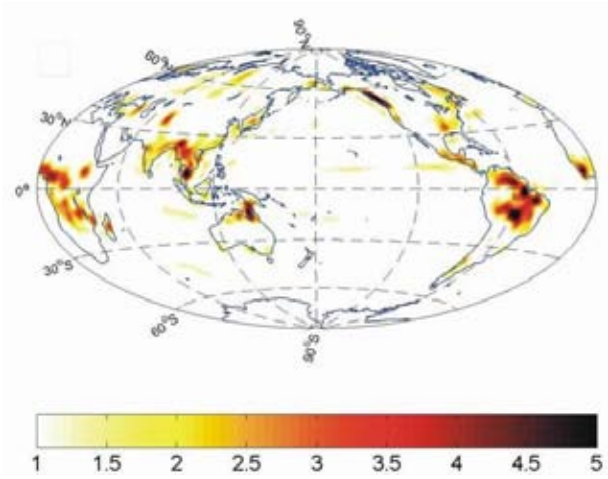

Fig. 2.6: Discrepancies between SiB2-ISBA and ECCO-POCM, resp. Cumulative GOCE gravity error level at degree 50:1 μGal.

Correspondingly, also in the difference plot Fig. 2.6 of the annual component, comparing

SiB2 and ISBA over the continents as well as POCM and ECCO over the oceans, the dominating influence of land hydrology is evident. Small additional signals, due to the non-steric ocean topography, occur in the Pacific Ocean, but the amplitudes are small compared with the errors in the land hydrology component.

In the further context of the project, we assessed the contribution of these temporal variation effects to the gravity field in terms of RMS, and it has been noticed that most of the energy of the temporal variations phenomena is contributed to the long-wavelength components of the Earth's gravity field, and therefore the major signals can be expected to be inherent in the high-low SST observations, while the signals contributed to the SGG component are in the order of the noise level of the gradiometer. Therefore, these effects deserve special treatment when we process SST data and have to be somehow modeled in advance (which is to a great extent dependant on the quality of our a priori models). Alternatively, these parameters have to be estimated together with the static gravity field unknowns. In this case, we speak about the parameterization of these effects. We performed different combinations of the static and dynamic coefficients and different solutions were investigated with the goal to find the optimum combination of our static as well as the dynamic coefficients, which will deliver an optimum gravity field determination from the SST observations.

The summary of different tests is presented in Fig. 2.7 where several runs corresponding to different reduction and/or prediction procedures in the treatment of these phenomena are presented. The parameterization process was restricted to the prediction of lower degrees only, since the contribution of the higher degrees falls below the SST noise level.

At first, an idealized scenario was assessed, where only the static coefficients up to degree and order 20 and the 8 main ocean tide constituents up to degree and order 10 were included in the orbit, and a combined prediction of static and dynamic coefficients was performed in a noise-free scenario. We noticed that even in this simplified case, the solar constituents are predictable with very low accuracy, despite of the well-conditioned normal equation system, and correspondingly the results are even getting worse if additional noise is included, leading to errors in the order of ±1 m in terms of static geoid heights (the purple curve in Fig. 2.7).

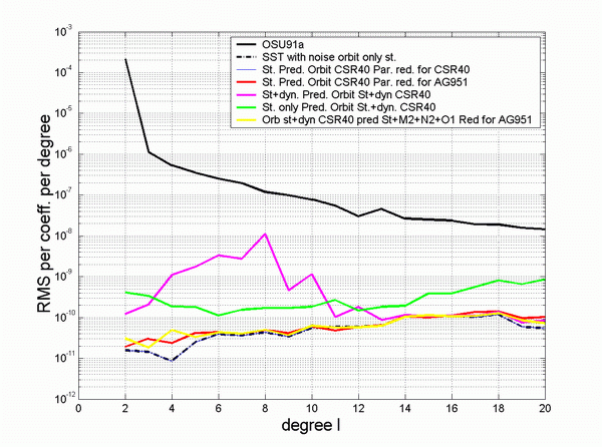

Fig. 2.7: Degree RMS for different ARCSST runs including the POD noise.

In the case that only the static coefficients are parameterized in the course of the adjustment process, we obtained slightly improved results of about ±25 cm (the green curve Fig. 2.7). Therefore, a reduction of the ocean tides by means of an external model was simulated, and naturally the accuracy of the results largely depends on the quality of the model applied. The red curve shows the obtained accuracy in terms of RMS when a "wrong" model is used in the reduction process, leading to ±2.5 cm geoidal height error. The best result was achieved when only selected constituents are parameterized, namely M_2, N_2 and O_1, but still discrepancies in the order of ±1.5 cm in terms of geoid height errors occurred. This corresponds to the yellow curve in Fig. 2.7.

Therefore, we conclude that in the real *GOCE* SST data processing an external model reduc-

tion, supported by the prediction of selected ocean tide constituents, is currently the best strategy.

The *E2Mgal+* project was completed and presented at ESA/ESTEC in Noordwijk, The Netherlands, on October 1, 2002.

2.2 Geodynamics & Meteorology

Disaster prevention is one of the most important challenges for our society to preserve life and property. Disaster prediction relies on experience, which in our days is not only based on history but on well certified data sets. The more accurate these sets are, the better short wave and even secular processes can be monitored. Precise coordinates are the prerequisite for geodynamical investigations, for real-time products for fast dynamic changes such as e.g. changes in the atmosphere. Besides, we also have to include the monitoring of the sea-surface as their status is intimately connected with geodynamical events (e.g. Tsunamis) and climate changes, which enables indirect conclusions about the net-effects of these influences. We cannot cover the whole field but we try to give valuable contributions in the global context.

Reference Frame

We operate a data and analysis center where all data of the Austrian as well as of the *CERGOP-2* GPS reference stations are stored and where the coordinates of a selected set of European stations are computed on a regular basis (daily/weekly). The results are included in the European weekly solution, which determines the actual, time varying reference system of Europe. In addition, we are responsible for monitoring sudden changes of coordinates in southeast Europe (down to Israel), which may indicate a response to geodynamical activities (Fig. 2.8), the part of Europe showing the most seismic activities during the last decades. This perfectly fits into our program of monitoring crustal movements.

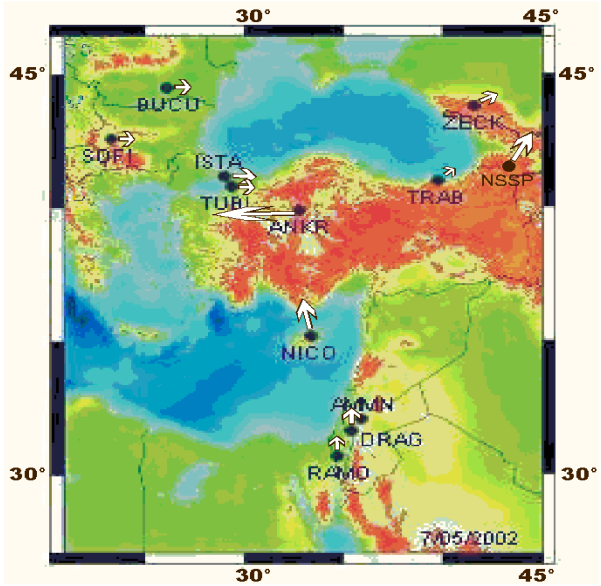

Fig. 2.8: EUREF stations (velocities) controlled by IWF.

CERGOP-2/Environment

A considerable part of the efforts was devoted to the 5th FP EU project *CERGOP-2/Environment*, which got an "okay" in April 2002. The start of this project is scheduled for January 2003.

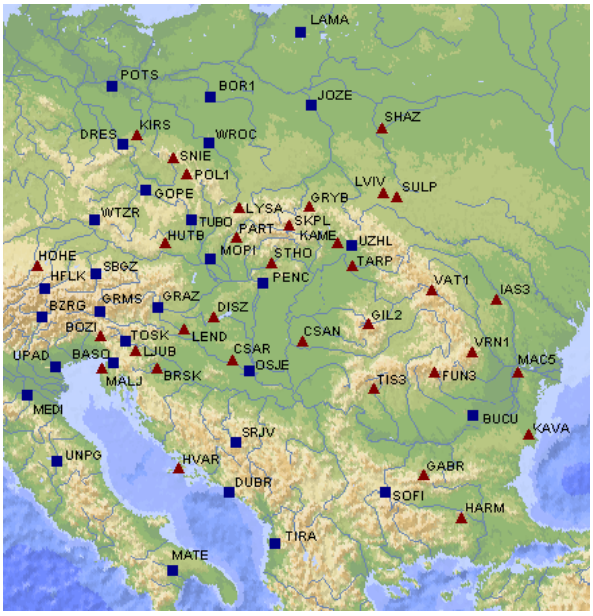

Fig. 2.9: The geodynamic reference frame CEGRN.

The aim of the project with all-together 14 partners from 13 countries of the Central

European Initiative is the establishment, maintenance and monitoring of a reference frame for geodynamical research covering about 15% of the European area. Local investigations in seismic active regions (7 work packages) will supplement the objectives. The final output will be a timely varying velocity field, which gives the basis for geodynamical investigations in this region, i.e. allocation of the underlying forces and the energy transfer leading to earthquakes. Fig. 2.9 shows the present distribution of GPS monitoring stations. This project is also highly correlated with the planned INTERREG initiative for monitoring the complete alpine region.

GAVDOS

The 5th FP EU project *GAVDOS* started in December 2001 with 9 partners, the coordinator is the Technical University of Crete. The project title is "Establishment of a European radar altimeter calibration and sea-level monitoring site for *Jason*, *Envisat* and EURO-GLOSS". We are responsible for Work Package (WP) 3 "Use of a transponder for determining the radial and along track component of satellite orbits", leading to an independent method for altimeter calibration and orbit determination.

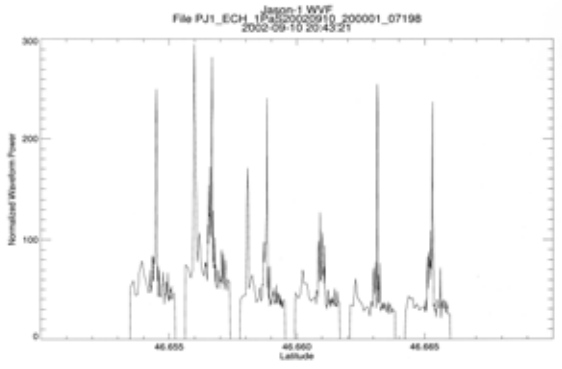

Fig. 2.10: Response of the Jason-1 altimeter to transponder signals.

The failure of first test measurements led to a complete check and update of the equipment, subsequent test-measurement to *Jason* and *Envisat* were successful (Fig. 2.10).

During a working meeting in Toulouse with the *Jason* team it was decided to use the altimeter calibration mode 2 for further test, which implies a partial re-design of the transponder. Further successful observations to *Envisat* were carried out during December 2002 and a detailed discussion with Rutherford Appleton Lab (UK) for software support arranged during the recent *Envisat* meeting in Frascati prior to the deployment at Gavdos (see Fig. 2.11).

Fig. 2.11: Location of Jason-1 (blue) and Envisat (red) sub-tracks over Gavdos.

ISDR (former IDNDR)

The program *ISDR* (International Strategy of Disaster Reduction) is the successor of the UN Project *IDNDR* (International Decade of Natural Disaster Reduction, 1990-2000). This program of the National Science Research Ministry, managed by ÖAW, gave us the required additional funding for establishing a reference network in Austria for monitoring local crustal movements. During the year 2002 we could actuate two more stations near Kitzbühel and Trafelberg, the latter providing collocation with the geodynamic base station of the Central Institute of Meteorology and Geodynamics (Fig. 2.12).

Fig. 2.12: The new geodynamic station Trafelberg (November 2002).

Altogether the Federal Office for Metrology and Surveying and ÖAW operate 15 permanent GPS stations (Fig. 2.13), further activities will be set in 2003. Detailed investigations like the check of seasonal variations of the coordinates of Hafelekar (Innsbruck) are in progress, the planned re-monitoring of Slovenian sites (after the earthquake 1998) is now included in WP 10.1 of *CERGOP-2/Environment*.

Fig. 2.13: The Austrian permanent array of GPS monitoring stations.

EU Action COST-716

We gave a valuable contribution to this action, which uses GPS products (zenith-delays) for real-time numerical weather forecast. The Austrian permanent GPS network delivers hourly data for that purpose; a water-vapor radiometer (on loan from UBW Munich) was in operation at FZG Graz during the first half of 2002. A work package of *CERGOP-2/Environment* is dedicated to study the influences of the troposphere on GPS height determination or, equivalently, to extract the delay information with pre-supposed fixed height for meteorological applications. *COST-716* will be terminated in June 2003 giving, as a result, an operable European GPS network for near real-time water vapor predictions.

2.3 Satellite Laser Ranging

Current Measurements

The main tasks in 2002 were

- to obtain a maximum number of measurements with ultimate accuracy,
- upgrading the station capabilities, and
- preparing for further major upgrades.

In the first task we were extremely successful: The SLR Station Graz (see Fig. 2.14) measured distances to more than 30 satellites during this year. In addition to those which are already in orbit since some time, additional new satellites are now successfully measured from Graz: *Envisat*, *Grace-A*, *Grace-B*, *Reflector*, *METEOR-3M*, *Jason-1*. Details of these satellites and their missions can be viewed at the home page of the International Laser ranging Service (http://ilrs.gsfc.nasa.gov/). *ADEOS-2* and *ICESAT* were launched in December 2002 and January 2003, respectively.

Fig. 2.14: SLR Station Graz at Lustbühel Observatory.

Already at the end of October 2002, we had measured more passes than in 2001. This performance became feasible mainly due to an extensive optimization of the tracking software.

For a number of satellites, we measured more Normal Points than any other SLR station worldwide (see Fig. 2.15).

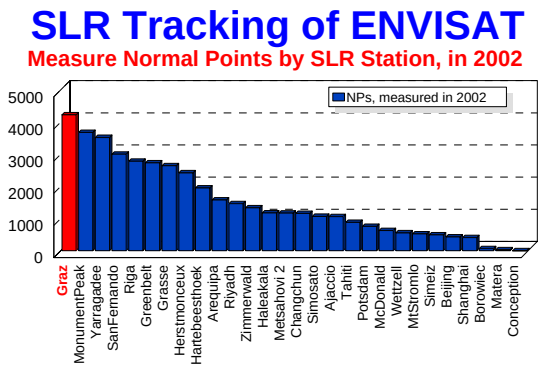

Fig. 2.15: SLR tracking of Envisat.

The accuracy of the measurements is also at a very high level. As an example, the achieved accuracy of *ERS-2* observations and calibration accuracy, as evaluated by *ILRS*, are shown in Fig. 2.16.

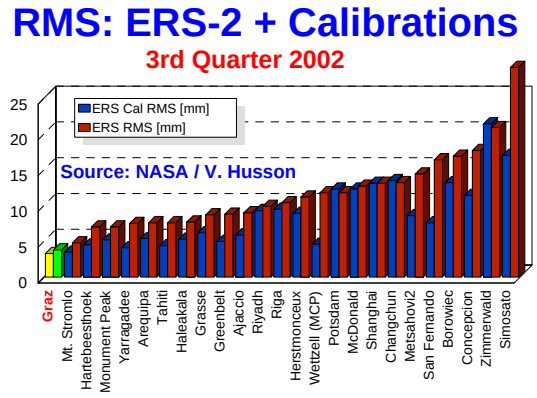

Fig. 2.16: ERS-2 RMS.

Other highlights of our tracking activities in 2002 are as follows:

- On October 1, 2002 SLR Graz collected the highest number of altimetry satellites' passes, ever measured during a 24 hours period (27); the second-best value was 21 passes.
- The measurements at SLR Graz are not only very accurate, but also very stable: We achieved the best long-term bias stability of all SLR stations worldwide.

The drawback of these results: Due to manpower limitations, we spent a major part of our time for ranging, keeping the ranging machine running, and looking for best possible absolute validity of our results. Besides the standard ranging and data processing tasks, this involves weekly and daily repairs of electronics, replacements of parts, handling some old laser parts, dealing with no-more-available spare parts, etc.

Hardware Developments

The new Range Gate Generator (RGG), as already described in the Annual Report 2001, was designed, built and implemented into the Graz SLR system. This device offers a resolution of < 500 ps, allows laser repetition rates of some kHz, and is fully programmable via PC and a standard 16-bit interface. It is implemented in FPGA technology (Field Programmable Gate Arrays), and therefore very flexible for future upgrades and add-ons.

This new RGG already now allows 10 Hz laser repetition rates for *all* satellites, including *ETALON*, *GLONASS*, *GPS* etc. This not only increases the data rate for these satellites – which we had to observe up to now with 5 Hz due to a time-of-flight of more than 100 ms – but also significantly improves the search, acquisition and tracking optimization of these high-altitude, single-photon-returns satellites. The RGG has been tested already with simulated laser repetition rates of up to 200 Hz, where up to 30 laser pulses are in flight simultaneously, and is intended as another major step towards kHz laser ranging.

Software Developments

In preparation for a possible – and highly desirable – upgrade of SLR Graz with a kHz la-

ser, a new real-time tracking and ranging program was developed and tested. It allows for completely free running laser pulses, with laser repetition rates from 10 Hz up to kHz ranges. Tests have been carried out very successfully on a standard PC environment with repetition rates of up to 70 Hz. Computer hardware replacement allowed already a 200 Hz Laser simulation. At kHz repetition rates, more than 100 shots are in flight simultaneously to and from *LAGEOS*, and even more from high orbit satellites. This new software has to handle all start and stop pulses, to associate the emission and detection events correctly, to set the RGG accordingly, etc.

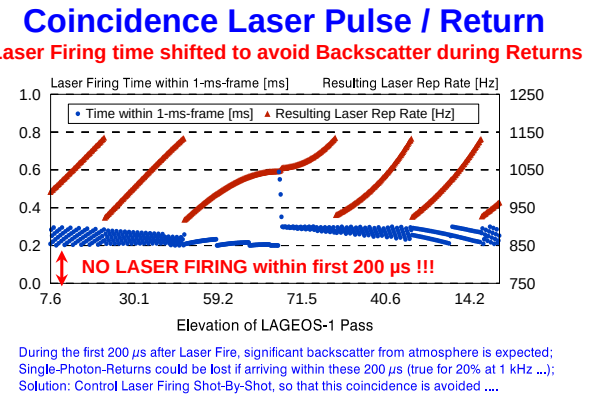

Fig. 2.17: Coincidence problem start/stop pulses.

Another problem with kHz laser ranging is the possible coincidence between laser start pulses and expected returns (Fig. 2.17). During the first 200 µs after the laser start, significant backscatter photons are impinging on the detector. If any return photon – and we do expect mainly single photons due to low laser energy – of an earlier laser shot arrives within these 200 µs, the detector might be blocked already by the noise. With a 1 kHz laser, this situation arises for 20 % of all shots. To avoid this situation, we investigated different methods. A promising approach is to shift the laser repetition rate on a shot-by-shot basis in a proper way, so that it never fires when a return is expected within the next 200 µs.

For better and faster acquisition of difficult targets (LEOs – Low Earth Orbiters, like *Champ*, *Grace, GOCE* etc.) a set of programs was designed and written, which collects – in intervals of 1 hour – all recently measured passes from all SLR stations via ftp, uses these results to calculate their measured time bias, and supplies a table with the most recent time biases of these satellites to the observer. This allows good assumptions of time biases to be expected, helping to acquire these satellites much faster.

Another approach was chosen by the EUROLAS group: Using these most recent passes, a server in Bern tries to predict the expected actual time biases of all satellites, applying also the predicted drag, and thus giving another estimation of the actual time bias value. The Graz programs transfer these results in regular intervals or on request, and display this time bias table for the observer.

The general Mount- and Telescope Control Software has also been significantly improved. In the previous versions, the telescope had to move always back to a zero-azimuth position to avoid ambiguity problems (maximum azimuth rotation is ±270°) when switching between passes. Now it commands the telescope directly to the starting position of the next pass, while taking into account all ambiguities, mechanical rotation limits, optimization of travel distances, etc.

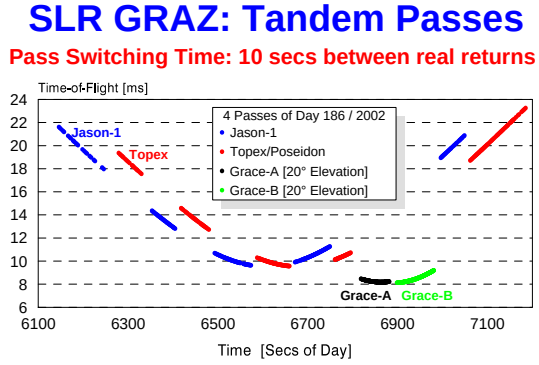

Fig. 2.18: Pass switching between 2 pairs of tandem sats.

With *Topex/Poseidon* and *Jason-1*, and then with *Grace-A* and *Grace-B*, we have now two pairs of "tandem" satellites (Fig. 2.18). All real-time programs have now been enhanced to allow fast switching between those tandem satellites. The usual time between last return of the one and first return of the other tandem satellite has been reduced to about 10 seconds. This allows quite frequent switches, even between low and fast flying satellites, like both *Grace* satellites. This system again allowed a significant increase of tracked passes.

Since 1995, a scientific pressure sensor was used to read atmospheric pressure with 0.1 hPa accuracy. Due to operational constraints, this sensor was never re-calibrated, but was compared in regular intervals via internet readings of instruments of the nearby Graz airport, but with a limiting resolution of 1.0 hPa only. Since a few months, this resolution is now 0.1 hPa. During summer, we compared it with a similar, calibrated sensor of the Herstmonceux (U.K.) SLR station, revealing an offset of 0.55 hPa. This triggered the installation of a second Meteo Device, in order to have an independent and accurate control of the air pressure values. The range bias due to the 0.55 hPa averages to about 2 mm.

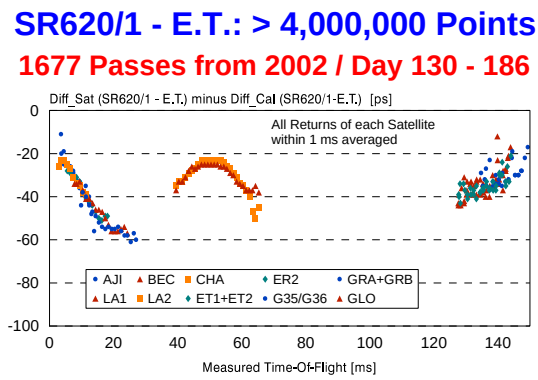

Fig. 2.19: Non-linearity of SR620 time interval counter.

During 2 months in spring 2002 we measured all passes not only with our Event Timer (E.T.), but also with 3 of our Time Interval (TI) Counters (2 x Stanford SR620, HP5370A). Storing all single shot values for each counter, gave more than 4 million values to check the TI counter linearity against the E.T. From the results it is obvious that the SR620 counters have significant non-linearity (Fig. 2.19), but also that this behavior is rather stable with time, regardless of internal counter calibrations etc.

2.4 Gravitomagnetism

Since in the weak field and slow velocity limit the gravitational field equations reduce to a set of Maxwell-type equations, gravitational phenomena in the solar system are expected to be similar to those known from electrodynamics. In particular, a mass current should produce a gravitomagnetic field in analogy to the magnetic field caused by electric currents. Therefore, the mass currents associated with the rotation of the Earth will produce a dipolar gravitomagnetic field, which in turn will perturb the orbits of satellites circling the Earth. Hence gravitomagnetic effects as predicted by general relativity can in principle be tested by the accurate determination of the orbits of near Earth satellites.

A number of gravitomagnetic observables, which are both sensitive to the direction of motion and expressible in terms of standard Keplerian elements, have been investigated. In particular, for two satellites along identical but opposite orbits the difference in the precession rate of the perigees is affected by gravitomagnetic perturbations, but is not influenced by the secular even zonal perturbations due to the nonsphericity of the Earth. Moreover, a choice of the orbital inclination of 63.4° (the so-called frozen perigee configuration) would make many of the periods of the time varying perturbations affecting the non-relativistic perigee motion reasonably short.

Another physical quantity suitable to study gravitomagnetic phenomena is the sidereal period of a satellite. Since the motion of a test particle about a rotating source is slower

when moving in the same direction as the rotation of the central body and faster in the opposite direction, the difference in the sidereal periods of two counter-revolving satellites reveals a gravitomagnetic signature which could in principle be detected with accurate orbital determination techniques. In order to observe this so-called gravitomagnetic clock effect, the orbit of the satellites must be known to the centimeter level over a time span of several years (Fig. 2.20). Preliminary error analysis suggests that the most critical orbital parameter for the time shift might be the orbital inclination and that equatorial orbits should be given preference over more inclined ones.

Although the clock effect will be masked by many gravitational and non-gravitational perturbations, its measurement seems to become possible with regard to the great experience gained in the *LAGEOS-LAGEOS II* Lense-Thirring experiment.

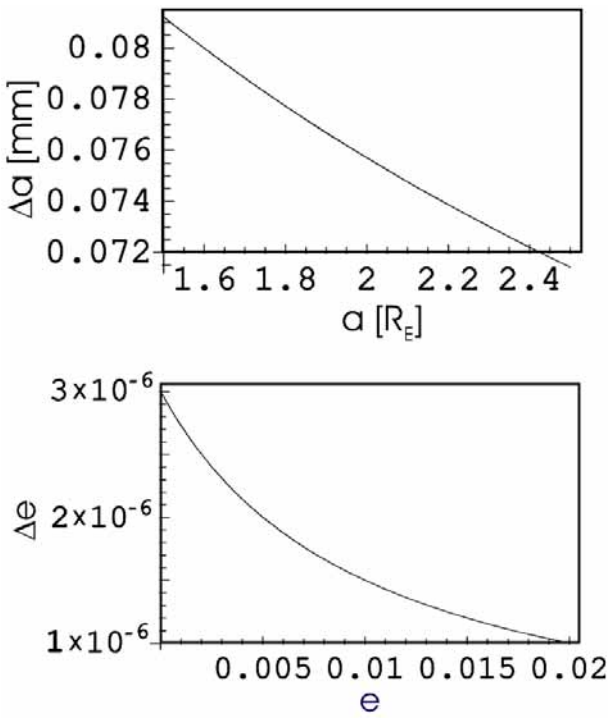

Fig. 2.20: Maximum tolerable error Δa and Δe in the semimajor axis a and eccentricity e per revolution for a nominal orbit of a=12000 km, e=0.01 and orbital inclination i=63.4°; in the upper panel a is given in Earth radii.

3 Near-Earth Space

The physics of the Earth's space environment is dominated by the interaction between the solar wind and the terrestrial magnetic field. The structures that are created in this interaction are: the bow shock, in which the supersonic solar wind is decelerated; a transition layer called the magnetosheath; the magnetopause, which is the boundary of the magnetosphere and the magnetosphere with its tail where the magnetic field from the Earth's dipole is dominating, and the ionosphere. In principle all these structures are magnetoplasmas, i.e., electrically charged particles (ions and electrons), where electric and magnetic fields dominate the physical processes.

3.1 Missions

In near-Earth space IWF is deeply involved in the *Cluster* mission, which now yields a wealth of new and exciting data. Corresponding data evaluation and analysis has been performed as outlined below in detail. In addition to *Cluster* also *Interball* data have been investigated.

DoubleStar

Within the *DoubleStar Project (DSP)*, two satellites to study the Earth's magnetosphere on near-equatorial and polar orbits, respectively, shall be launched in 2003/2004. *DSP* is a joint effort by China and ESA. More than half of the *DSP* payload will be provided by European PIs. IWF participates in this mission with two experiments, *DSP-ASPOC* to control the electric potential of the equatorial spacecraft, and *DSP-FGM* to measure the magnetic field on both satellites. IWF is also Co-Investigator for the PEACE and HIA experiment and will set up a European data distribution center for the mission. Further information on the history and objectives of this mission can be found in the Annual Report 2001 and on the IWF website.

After the formal kick-off of the project the activities to (re-)design and to build the instruments entered an intensive phase. Engineering Models (EMs) of the instruments, largely inherited from the *Cluster* mission, were refurbished and successfully integrated with a prototype of the spacecraft systems.

Flux-Gate Magnetometer (FGM): Unlike most of the other European instruments for *DSP*, *FGM* has been re-designed to accommodate the ITAR (International Traffic in Arms Regulations) requirements and will be built from scratch. The EM model has been verified successfully through the pre-integration test in September 2002. Two identical magnetometers with two sensors each will be built for the two spacecraft. The flight model delivery is envisaged in September 2003.

Active Spacecraft Potential Control (ASPOC): Lessons learned from *Cluster*, changed boundary conditions in the new mission and last, but not least ITAR have driven some modifications of the on-board software and hardware. The ion emitters have been optimized for this mission, and a prototype emitter has undergone first tests. Whereas the electrical interfaces between *ASPOC* and the spacecraft have been successfully verified at the EM (Fig. 3.1), the mechanical and thermal compatibility is to be tested using a structural-thermal unit of *ASPOC*, which has been

manufactured and delivered to China for vibration and thermal balance tests. The manufacturing of the Flight Model is on track for a delivery in the middle of 2003, following a last adjustment of the design based on the experience with the EM.

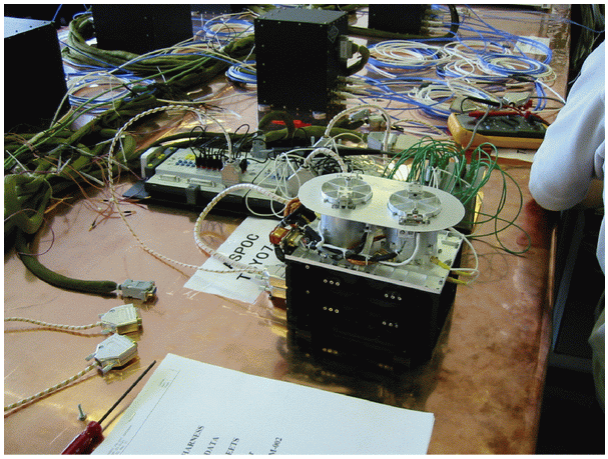

Fig. 3.1: ASPOC Engineering Model during the pre-integration tests.

European DoubleStar Data Distribution System (EDDS): As part of its commitments for *DoubleStar*, IWF took responsibility for the implementation of a Data Distribution System as a service for the European investigators. The center is to collect raw science data from the mission and to provide an interface for convenient data retrieval, with some similarities to the *Cluster* data facilities. The architecture and the interfaces of the EDDS have been defined.

3.2 Physics

A fleet of spacecraft within the terrestrial magnetosphere and in the near-Earth interplanetary space, like *Cluster*, *Geotail*, *AMPTE*, *Interball*, *Goes*, *Polar*, *ACE*, *Wind*, and others, only to mention the most important of them, provide us with an enormous amount of data representing the plasma and magnetic field behavior in this region. We developed various theoretical models describing physical processes, which are responsible for the formation of structures and phenomena in the near-Earth space. These are e.g., the evolution of the bow shock and the magnetosphere, the reconnection of magnetic field lines at the dayside magnetopause or in the nightside magnetotail and many others. In addition theoretical models are compared with spacecraft data.

Bow Shock

As a consequence of the interaction of the solar wind with the Earth's magnetosphere, a so-called bow shock forms standing off the obstacle. At this non-linear wave the physical parameters rapidly change. This has been successfully modeled taking into account the anisotropic nature of the plasma on either side of the shock. The approach is based on two plasma instabilities bounding the pressure anisotropy in the magnetosheath, namely the fire-hose and mirror instability. The variations across the shock are derived as functions of upstream parameters for various shock geometries and were further compared with spacecraft observations. It has to be noted that the two threshold conditions of the plasma instabilities are obtained in a kinetic approach using a bi-Maxwellian distribution function and thus limitations to the theory are implied.

Consequently, a more generalized distribution function has to be taken into account, the so-called kappa (κ) distribution, containing the loss cone index as well as the spectral parameter κ. In the limit $\kappa \rightarrow \infty$, this distribution transforms to the bi-Maxwellian one and thus a certain range of the spectral parameter gives additional information on the plasma, specifically on high-energy particle populations. This fact was applied to the bow shock and the modified threshold conditions of the fire-hose and that of the mirror instability are derived with the use of a kappa distribution function. Similarly to the approach as described above, the modified threshold conditions give a limiting range of stable solutions with regard to the pressure anisotropy down-

stream of the shock. For the sake of simplicity, the loss cone index was dropped in the analysis.

Fig. 3.2 shows the variation of the density across the shock as a function of the pressure anisotropy downstream of the discontinuity. The pressure anisotropy in the solar wind, λ_1, is chosen to be 0.5, the angle between the upstream magnetic field and the normal vector of the shock is assumed to be 45°, and the upstream Alfvén Mach number, M_A, is taken to be 5. The parameter A_s, i.e. the ratio of the upstream perpendicular pressure to the solar wind dynamic pressure, is considered to be 0.01. Additionally, the fire-hose and mirror criteria are computed for different values of the parameter κ raising up to the limit with respect to the bi-Maxwellian approach (blue lines in Fig. 3.2).

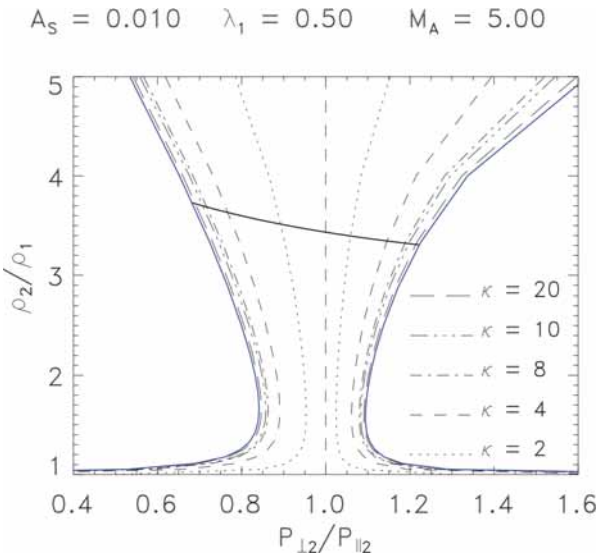

Fig. 3.2: Variation of the density across the shock as a function of the pressure anisotropy downstream of the discontinuity for different values of κ.

Magnetosheath

Experimental data show the solar wind plasma to be essentially anisotropic, especially in shocked regions, such as the magnetosheath. The anisotropy in a collisionless plasma originates from the independent evolution of the plasma temperatures in the directions parallel and perpendicular to the local magnetic field.

The disagreement of the different models with the experimentally deduced plasma anisotropy behavior is usually explained by proton scattering by a rather intensive wave turbulence in the magnetosheath. The fluctuations predominant in the magnetosheath are mirror-like and proton-cyclotron-like.

We estimated the value of the effective collision frequency from experimental data during various magnetosheath crossings of AMPTE/IRM. Three different regions characterized by different plasma turbulence modes and intensities could be distinguished. The first thin layer adjacent to the bow shock is characterized by rather intensive wave turbulence, most probably, of the ion-cyclotron mode. The second layer, occupying the largest part of the magnetosheath, is characterized by a gradual increase of the plasma anisotropy relaxation time in the midst of the magnetosheath and a subsequent decrease towards the magnetopause (Fig. 3.3). The predominant waves there seem to be mirror waves. The third region is the innermost magnetosheath layer adjacent to the magnetopause, with the predominant waves again the ion-cyclotron modes.

We found that the characteristic time of the proton temperature anisotropy relaxation distinctly depends on the intensity of mirror waves, which may be considered as an evidence for a significant role of these waves in the proton scattering. Besides, we could show that the sheath regions adjacent to the bow shock are characterized by intensive wave turbulence, most probably of the magnetosonic mode. It is supposed that this kind of turbulence is generated at the bow shock.

Due to the fact that these results have been obtained from an analysis based on a rather limited amount of data, the problem of wave turbulence and proton pitch-angle diffusion within the magnetosheath needs additional theoretical and experimental studies.

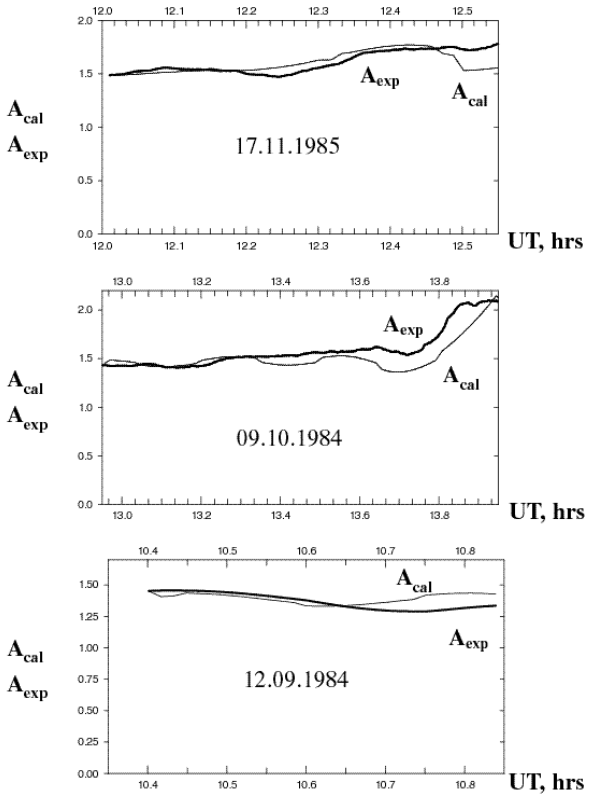

Fig. 3.3: Magnetosheath profiles of the observed running mean values of the proton temperature anisotropy (the thick solid line) and the calculated values for different days.

Magnetopause

Commonly, the location of the boundary of the terrestrial magnetic field, the so-called magnetopause, is defined at a distance where the planetary magnetic field pressure equals the dynamic pressure of the solar wind (neglecting the small contribution of the interplanetary magnetic field (IMF)). It emerges from the above that the primary source of magnetopause motion is a change in solar wind dynamic pressure. However, it has to be noted, that under special circumstances the magnetopause moves inwards even when the dynamic solar wind pressure remains unchanged. This phenomenon is called "erosion" and was already identified in the 1970s when magnetopause crossings made by OGO 5 spacecraft were investigated. Since a persistent southward orientation of the IMF is a prerequisite for magnetic reconnection to happen, a physical connection between the erosion and reconnection phenomenon was evident.

Thus, on the basis of former works on time-dependent reconnection, which have been carried out at IWF in collaboration with coworkers from the Institute of Physics in St. Petersburg, the Institute for Computational Modelling in Krasnoyarsk, Russia, and the Institute for Earth, Oceans, and Space of the University of New Hampshire, USA, we developed a new theoretical model, which describes the motion of the magnetopause after reconnection was initiated at the sub-solar magnetopause. Even more, within this model also an earthward displacement of the bow shock can be calculated.

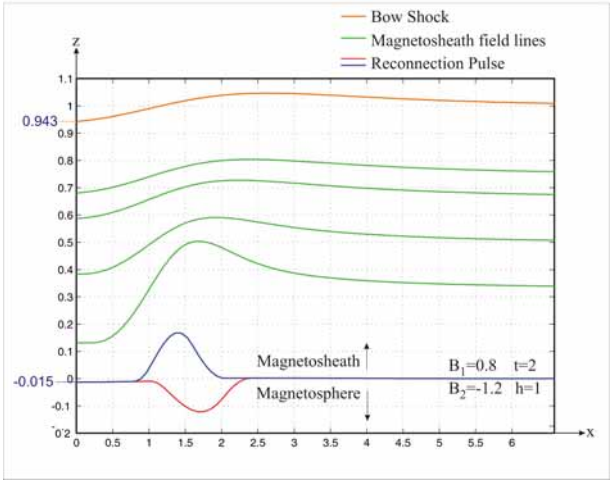

Fig. 3.4: Erosion of the magnetopause (blue line) and the bow shock (orange line). The blue and the red line show a reconnection pulse formed of two slow shocks, which are travelling along the magnetopause to the Cusp. Green lines show disturbances in the magnetosheath.

Fig. 3.4 shows the numerical results of our calculations. The zeroth level on the z-axis marks the magnetopause – below is the magnetosphere and above the magnetosheath, which ends at the bow shock at height h=1. The blue and red lines show the shape of two slow shocks emanating from point (0,0), where reconnection was initiated. At the left hand side of this reconnection pulse we can discover a shift of the current sheet of -0.015. Taking into account the scaling parameters, B_0=50 nT and T_0=100 s, we get for the

v_{A0}=500 km/s and for the characteristic scale length, L_0=8 R_E. Thus, this means that the magnetopause moves of about 0.1 R_E after the first reconnection pulse. Green lines show disturbances in the magnetosheath resulting in a shift of the bow shock of -0.057, which gives a local bow shock motion of ~ 0.4 R_E (orange line). Thus, the bow shock cannot be a smooth structure, in contrary, small bulges should be observed in the shape of the bow shock.

Magnetotail

At IWF, one of the main research areas in analyzing and interpreting spacecraft data, such as *Geotail*, *Equator-S*, and *Cluster*, is the study of the dynamics of the Earth's magnetotail, with special interest in the transport processes.

The *Cluster* quartet of satellites allows, for the first time, to separate spatial and temporal variations in arbitrary geometry measurements of space plasma parameters. This is of particular importance in a highly variable and dynamic region like the Earth's magnetotail and provides completely new insight into magnetotail dynamics. Further new understanding comes from new and improved instrumentation.

The *Cluster* spacecraft were launched in summer 2000 and put into a polar orbit and experienced the first tail passage from July to October 2001. The orbit of the *Cluster* quartet is almost fixed in the inertial frame, so that they pass the magnetotail from the dawn side flank to the dusk side flank as the Earth's magnetosphere revolves around the Earth once in a year in the inertial frame centered in the Earth. Of particular interest is the orientation and shape of the *Cluster* tetrahedron when it traverses the plasma sheet at its apogee from north to south at a radial distance of about 20 R_E. Fig. 3.5 shows the typical tetrahedron configuration during current sheet traversals: of particular importance for the current sheet studies will be that spacecraft (s/c) 3 leads the other s/c by about 1500 km on their north-to-south orbit.

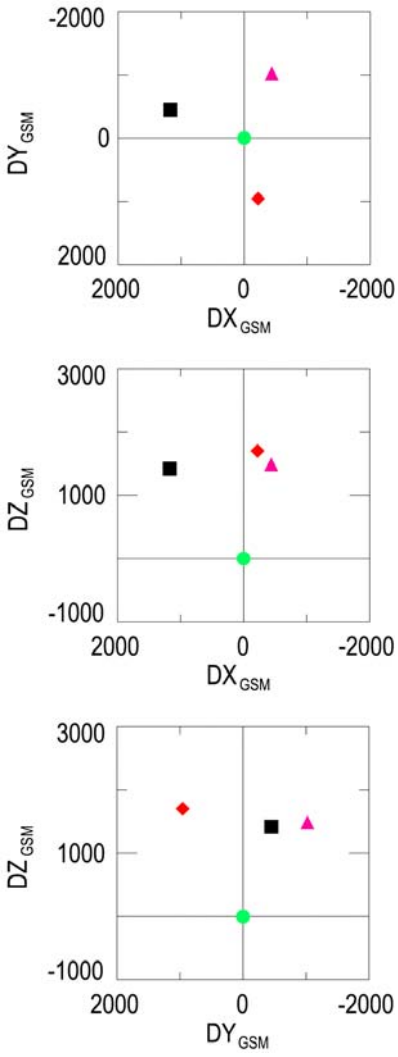

Fig. 3.5: Typical orientation of the Cluster tetrahedron during plasma sheet traversals in 2001.

Tail Lobe Convection: The interplanetary magnetic field (IMF) interacts with the Earth's dayside magnetic field through magnetic reconnection. The solar wind drags the reconnected field lines from the dayside to the night side, stretches the field lines, and stores the energy in the form of magnetic tension. The stored energy is released when the open magnetic field lines reconnect again to form closed field lines, which return toward the Earth. The convection in the lobe is tightly connected to dayside reconnection. The plasma density in the near-Earth lobe is typically lower than 0.01/cc, which makes the observations of lobe convection by particle

detectors difficult. Yet, by using the *Electron Drift Instrument (EDI)* the averaged near-Earth tail lobe convection and its relationship to IMF polarity can be studied.

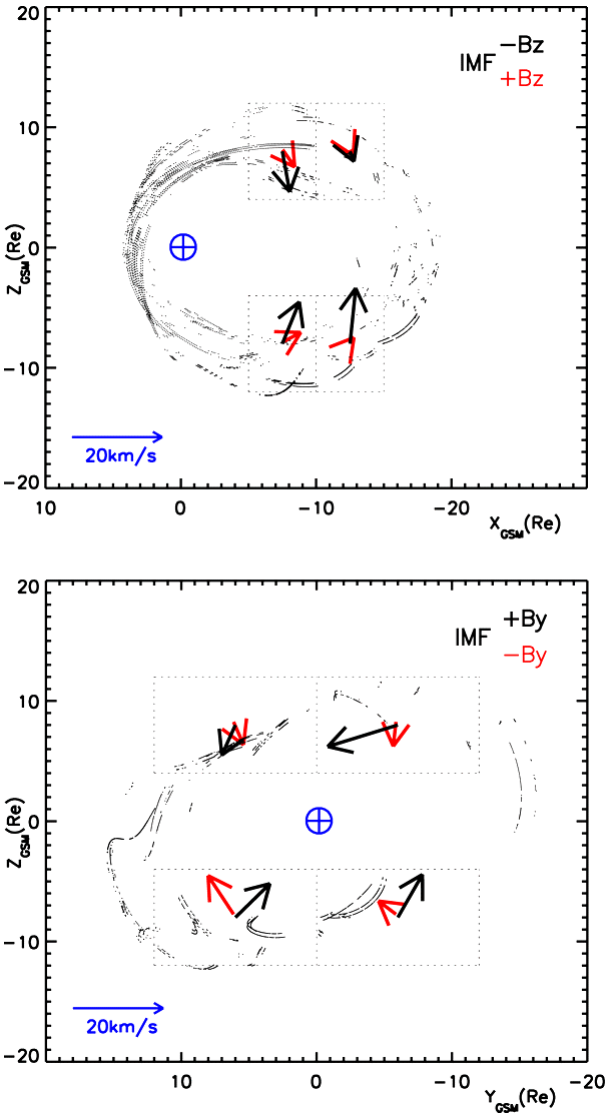

Fig. 3.6: Average lobe convection for different IMF clock angles (dusk is toward positive Y_{GSM}).

Fig. 3.6 is based on *EDI* data from July to October 2001 from three *Cluster* spacecraft (on s/c 4 *EDI* is not operated) and shows average tail lobe convection for 90-deg IMF clock angle sectors centered on $\pm B_Z$ and $\pm B_Y$. One can draw the following conclusions from this figure: First, the vectors point toward the neutral sheet in both panels. Second, the flow direction in the Y-Z plane changes between $+B_Y$ and $-B_Y$ conditions. For $+B_Y$, the vectors in all four quadrants have a counterclockwise component in this Y-Z plane, while for $-B_Y$ a clockwise component appears (that the vector in the northern dawn quadrant in the $-B_Y$ case has a different sense may be caused by the small amount of data for that state/bin). Third, as expected, the velocity becomes larger for IMF $-B_Z$, because for this IMF polarity dayside reconnection occurs most efficiently.

The most notable point is the difference of the velocity in the Y-Z plane under $\pm B_Y$ conditions. For $+B_Y$, field lines, which reconnect with the geomagnetic field in the dayside region and are subsequently transported to the night side by the solar wind, have a duskward velocity component in the northern and a dawnward component in the southern lobe. This will make a counterclockwise rotation of the convection in the night side. The opposite is true for $-B_Y$.

Current Sheet Thinning: On August 12, 2001 *Cluster* observed a fast flow event in the plasma sheet associated with a small substorm intensification at 18:38 UT. *Cluster*, located in the plasma sheet, experienced significant thinning of the current sheet associated with a high-speed Earthward flow of 900 km/s. The upper two panels of Fig. 3.7 show the ion velocity from s/c 1, 3, and 4 and the magnetic field data from the four spacecraft.

The flow and field disturbance can be divided into three intervals, delineated by the dashed lines. (1) During the first interval, when the flow starts to develop, the field traces for each s/c are quite different and so are the flow traces. The flow at s/c 3 is more developed compared to that at s/c 1 or 4. Since s/c 3 was located southward and closer to the central plasma sheet, the difference suggests that the flow is more developed near the neutral sheet. (2) During the second interval, on the other hand, the three traces of the flows are more similar, although the satellites are located at quite different places relative to the neutral sheet, i.e., north and south of the neutral sheet. Hence high-speed flow seems

spread throughout the plasma sheet. (3) During the third interval, the three satellites in the northern hemisphere, which are located nearly at the same distance from the neutral sheet, differed significantly in the magnetic field traces. This indicates an enhancement in the local current density at the three northern spacecraft regions. On the other hand, the flow traces are similar to that of interval (2).

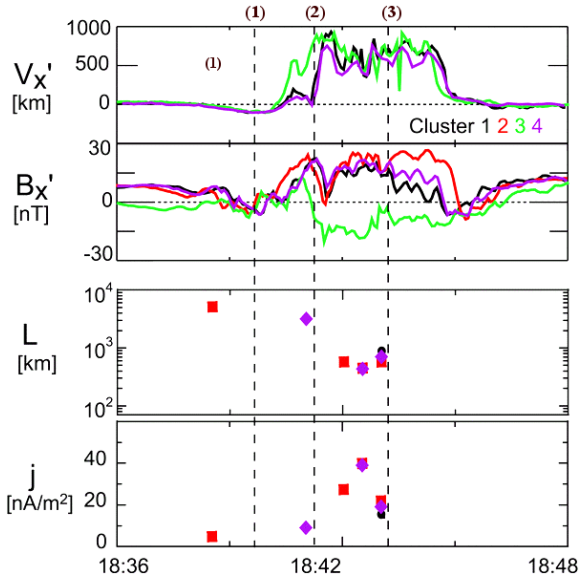

Fig. 3.7: Sunward component of ion velocity and magnetic field (data) and current sheet half width and current density (model).

The magnetic field data was fitted to the Harris current sheet to examine quantitatively how the current sheet is structured during the flow interval. In a Harris sheet the magnetic field is represented by $B_X(z)=B_L\tanh\{(z-z_0)/L\}$ where B_L is the lobe field outside the current sheet, z_0 is the location of the neutral sheet and L is the half-thickness of the current sheet. Simultaneous measurements from three spacecraft allow to estimate the three parameters and to compare the estimated model B_X at the location of the fourth spacecraft with the actual data to check the validity of the estimation. The bottom two panels of Fig. 3.7 show the result of the Harris sheet estimation for several sequences before and during the flow interval together with the averaged data. Results shown are mostly concentrated during interval (2). Nonetheless, it can be seen how the current sheet structure changes during the flow event. Before the onset of the flow, the spatial scale of the current sheet is 5000 km. After southward excursion of the current sheet, during interval (2), the scale reduces to 500 km, which is comparable to the ion inertial length. The maximum current density predicted from the Harris sheet model increases from 5÷10 to 20÷40 nA/m².

Bifurcated Current Sheets: The 1500 km separation of the *Cluster* spacecraft during the 2001 tail passages was not well suited to study the internal structure of the current sheet. However, at times, the current sheet underwent large-scale flapping motions with north-south velocities of up to 100 km/s. Since the current density profile did not change during these up-and-down motions, comparison of the difference in the magnetic fields measured by the southernmost and the northern spacecraft triad allowed the determination of the current density profile. On two different days, the tail current sheet clearly did not resemble a Harris sheet, but rather exhibited a double-peaked, bifurcated structure, with a pair of current sheets separated by a layer of weak quasi-uniform magnetic field in the center of the plasma sheet.

The first example was observed on August 29, 2001, during the recovery phase of an isolated substorm. Starting at 10:55:30 UT, *Cluster* detects a sudden expansion or flapping motion of the current sheet caused by a wave-like transient passing the *Cluster* tetrahedron. A multi-point timing analysis yields that the wave propagates toward dusk with a velocity of about 200 km/s and has a characteristic period near 90 s. The average normal (north-south) velocity of the current sheet motion is 60 km/s. The wavelength of the transient wave is about of 3 R_E, and the amplitude near 0.5 R_E. The wave travels toward dusk.

The observation of current sheet bifurcation is shown by a detailed analysis of the interval

around 11:01 UT (upper panel of Fig. 3.8). At the beginning of the interval all four spacecraft measure the same weak (about 2.5 nT) magnetic field. The same situation holds about a minute later: all four *Cluster* spacecraft observe a very weak (about 0.5 nT) magnetic field. Therefore, at these instances *Cluster* is located in an extended layer of very weak uniform magnetic field in the vicinity of the neutral sheet. In the center of this interval the traces of s/c 3 and the northern group (s/c 1, 2, 4) are different: s/c 3 stays in a weak field region (about 1 nT), while the northern group measures 6÷8 nT. The average vertical gradient of the magnetic field within the northern group of spacecraft is 9 nT/10^3 km, which corresponds to a current density of 7 nA/m^2. The lower panel of Fig. 3.8 illustrates the bifurcated current sheet model, superimposed on a wavy flapping motion (kink mode). The current sheet forms a wave structure, while its thickness remains relatively constant. The characteristic scale of the weak uniform field layer is of the order of the spacecraft separation, 2000 km.

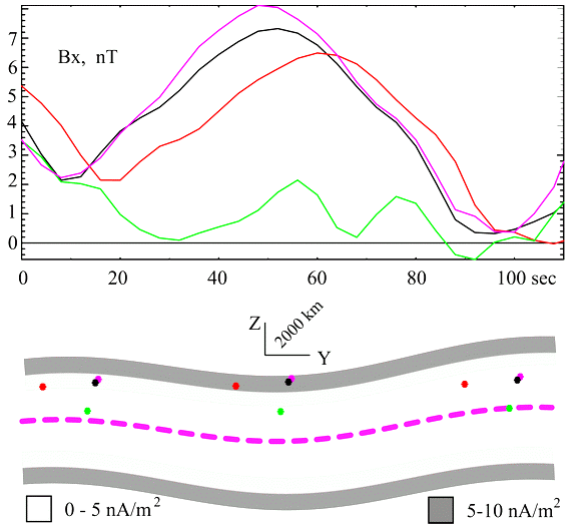

Fig. 3.8: A possible interpretation of the Cluster/Flux-Gate Magnetometer (FGM) measurements around 11:01 UT (upper panel): Current sheet bifurcation associated with a kink-type flapping oscillation.

A different event, observed on September 26, 2001, also clearly exhibits kink mode flapping and current sheet traversal. The wave travels again toward dusk, but in this case has larger amplitude, near 1 R_E. Using the difference ΔB_X= of the X-components measured by s/c 1 and 3 and the s/c separation ΔZ yields the current density $\Delta B_X/\mu_0 \Delta Z \cos\Phi$, where Φ is the angle between Z-axis and tilted (due to the kink mode) current sheet normal. As a label of position in the current sheet where this current density has to be assigned, the B_X component value in the mid point, that is $<B_X>=0.5(B_{X3}+B_{X1})$, is used.

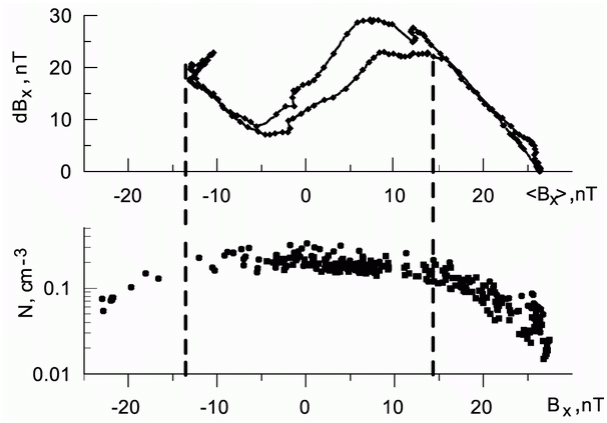

Fig. 3.9: Distribution of ion density and magnetic field difference for oscillation B versus B_X during two current sheet traversals.

A hodogram (at the top of Fig. 3.9) of ΔB_X versus $<B_X>$ during two complete current sheet traversals displays a systematic behavior, with a deep local minimum in the central part (where B_X~0) and the maximum ΔB_X at $|B_X|$~10÷15 nT. This bifurcated current structure was nearly stable for the next 15 minutes. The ΔB_X value at the current maximum of about 25 nT yields ~12 nA/m^2 (vertical separation about 1500 km), which is the lower limit for the current density in the maximum region. The bifurcated current peaks at $|B_X|$~0.5 B_L (lobe field B_L~27 nT) and has a deep (a factor 2÷3 lower than the peak value) broad valley in the central part of the current sheet. Note that the plasma density (lower panel) shows the typical flat profile between ±0.5 B_L and then drops off toward the lobe.

Further Studies: Further studies have obtained very interesting characteristics of the current sheet in terms of (1) extreme orientation of

the current sheet and (2) wave and turbulence characteristics.

(1) Based on analysis using the four point measurements a number of cases were found when the orientation of the current sheet extremely deviated from the average configuration. It was found that a twisted and warped current sheet superposed on oscillations can even tilt the current sheet orientation more that 90 degree so that a reversed current sheet orientation can occur. Such a vertical current sheet was also observed during a period of northward IMF and interpreted as being formed due to high-latitude reconnection.

(2) In another study on large scale current sheet oscillations, it was found that these oscillations can be modeled as a magnetoacoustic eigenmode of the current sheet, with a damping rate related to the thickness of the current sheet. In addition to these large-scale oscillations, persistent compressional waves in the 30÷60 mHz band were observed. The latter waves show clear dependence on substorm activity and/or fast flows. Magnetic field fluctuations were further examined using a multifractal-based algorithm. It was found that the intermittent fluctuations in the magnetic field during fast flow and current sheet oscillation events show a clear indication of cross-scale energy flow.

Spacecraft Charging

The *Cluster* payloads include instruments for active spacecraft potential control (*ASPOC*) developed under the leadership of IWF (see the Annual Report 2001 and the IWF website for details), with the objective to minimize the disturbances of low-energy plasma measurements caused by high spacecraft potentials, which often reach several tens of volts positive in the Earth's magnetosphere and may severely affect both electron and ion measurements at low energies. Spacecraft potential control ensures effective, complete measurements of the ambient plasma, which is particularly important for comparative, multi-spacecraft studies.

ASPOC emits an Indium ion beam of 5 to 50 µA (typically 10 µA) and 6 to 9 keV. This current adds to the plasma electron current and helps to set an upper limit to the spacecraft potential when the plasma is too tenuous to support currents of the order of the photoelectron current originating at the spacecraft surface.

The spacecraft potential measured by the double-probe experiment EFW in 2001 have been analyzed, and an example is given in Fig. 3.10, showing (in red) a histogram of spacecraft potential on *Cluster* 3 for all times when *ASPOC* was active. The potential is at or below 7 V, whereas the black curve, showing of simultaneous data on the uncontrolled spacecraft 1, includes a significant fraction of potentials up to 50 V, mainly measured in the lobes. The similarity of the histograms below 5 V – mainly data in the solar wind region – where the ion beam only marginally affects the charge equilibrium, confirms that both spacecraft 1 and spacecraft 3 typically saw the same plasma environment at nominal inter-spacecraft distances between 600 and 2000 km.

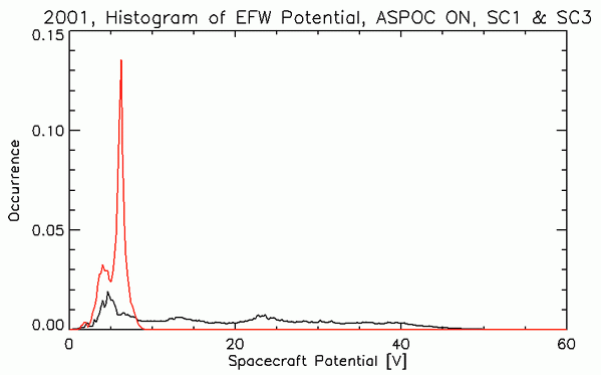

Fig. 3.10: Histogram of spacecraft potential on Cluster 1 and 3 in 2001, during ASPOC operations on Cluster 3.

Terrestrial Radio Emissions

Within the terrestrial magnetosphere various types of non-thermal radio emissions are generated providing evidence of wave-particle

interactions. After having analyzed the Auroral Kilometric Radiation (AKR) as observed by *Interball/POLRAD* it turned out to be of essential importance to validate the reception properties of the antenna system in order to yield reliable results. Corresponding investigations have been performed (see 5.2 Radio Antennas).

Plasmaspheric fine structures observed by the Cluster WBD experiment: In collaboration with the University of Iowa, Department of Astronomy (Prof. Gurnett) we investigated the radio emissions generated in the Earth's plasmasphere. We used the data observed by the wideband plasma experiment (WBD) on board of the *Cluster* satellites, in the frequency range between 1 and 20 kHz. Special emphasis was laid on the spectral features of the triggered very low frequency (VLF) emissions, which appear as narrowband and fine structures with distinctive shapes as shown in Fig. 3.11. First results concentrated on the quasi-periodic (QP) and the fine structures. The origin of the QP structures seems to be related to the ultra-low frequency (ULF) emissions, which are generated during the motion of the magnetopause towards the Earth. The EM fine structures observed in the Earth's plasmasphere, however, were found to have similar spectral features as in the case of emissions within the Jovian magnetosphere.

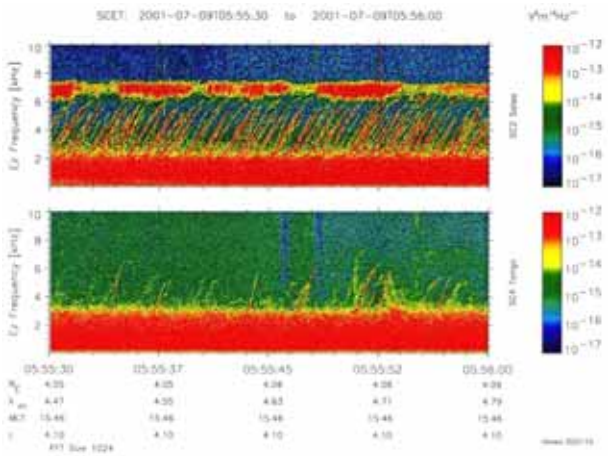

Fig. 3.11: Radio signatures of plasmaspheric structures observed by the WBD experiment aboard the Cluster satellites.

Ionosphere

The modeling work on the lower ionosphere, which in 2001 had concentrated on the disturbed, auroral regions, was complemented by a model of the neutral atmosphere at high latitudes, based on experimental data. The new reference atmosphere models the transitions winter-spring and summer-autumn more accurately than CIRA-86, and it will provide a firm basis for the ion-chemical model, which is under development.

4 Solar System

In continuation of previous studies IWF is engaged in many missions, experiments and corresponding data analysis of a multitude of solar system phenomena. The physics of the Sun as central star with an expanding atmosphere, the so-called solar wind, its interaction with solar system bodies (magnetized/unmagnetized, planets, comets), and various kinds of planetary atmosphere/surface/subsurface interaction phenomena are under detailed investigation.

4.1 Sun

Specific parts of the complex dynamics within the low solar corona have been modeled and simulated by a magnetohydrodynamic approach, as outlined below. Additionally, the Sun was also observed and investigated as emitter of radio waves, generated over a wide radial range along coronal structures, which are heavily influenced by energetic particle beams and shock structures.

Solar Orbiter

Solar Orbiter is a mission to the Sun, which is still in the planning phase. The spacecraft shall surround the Sun with a perihelion between 0.2 and 0.3 AU. Utilizing this very good observation condition for solar radio emissions, a *Radio and Plasma Wave Analyzer (RPW)* will be incorporated in the spacecraft instrumentation. After a feasibility study, which analyzed the kind of antennas and receivers that could be used to meet scientific objectives under certain observation restrictions, preliminary wire grid constructions were made in 2002. These wire grids will be finished when definite spacecraft configuration layouts will be available. Then these grids can be used for numerical simulations of the *RPW* antennas and their reception properties.

Physics

Particle beams in solar magnetic flux tubes: We have studied the magnetohydrodynamic response of a plasma in the low solar atmosphere to a changing current system of a flaring magnetic tube, which contains a beam of fast non-thermal electrons. The local disturbances of a current system within a magnetic tube are estimated using the classical idea of a return current. According to this idea, after injection of a beam, the total current density in a magnetic tube, which includes as well the current density of the beam j_b, should not change compared to the current density in the tube before the injection. In order to keep constant the total current density $j=j'+j_b$, the current density of the magnetic tube j' in fact changes. This change is due to a return current $j_{r.c.}=-j_b$, which compensates the current density of the injected beam of fast electrons. Various types of magnetic tube response onto injection of a beam of energetic electrons have been studied using the dynamic models developed in previous investigations.

Solar magnetic loops: Effects of electromagnetic inductive interactions in groups of slowly growing current-carrying loops have been investigated. Each loop is considered as an equivalent electric circuit with variable resistance and inductive coefficients. These parameters depend on the geometry of the loop, its position with respect to neighboring loops,

as well as on the plasma temperature and density in the magnetic tube. By means of such a model the process of generation of currents and temperature change in coronal loops moving relative to each other, and their dynamic interaction were analyzed. There are three main results of this analysis. First, the possibility of a relatively quick development of a significant longitudinal current in a rising and initially current-free magnetic loop is demonstrated. Second, the processes of fast, flare-like, plasma temperature increase in inductively connected growing loops with high enough currents, ~10^{10}÷10^{11} A, as well as run-away electrons acceleration in the loops by inductive electric fields are modeled. And third, based on the analysis of a ponderomotoric interaction of current-carrying magnetic loops, conditions for their oscillations or a fast change of the loops inclination, possibly resulting in their coalescence and magnetic reconnection, have been investigated. The observational information about the 3D structure of coronal loops and their global dynamics (rising, twisting, oscillation) is crucial for the considered models, and we expect that the data from the NASA *STEREO* mission, planned for launch in 2005, will appear as a good test for verification of the models.

Solar decametric emission: Solar decametric observations have regularly been performed at the Lustbühel radio station in Graz, Austria, (http://www.radiotelescope-graz.oeaw.ac.at) since September 2000. A logarithmic-periodic (log-per) antenna connected to a digital spectro-polarimeter (DSP) and a multichannel receiver (MC) provided dynamic spectra of the solar coronal radio emission in the frequency range from 30 MHz to 50 MHz. The Lustbühel radio station is part of the European network, which includes Kharkov radio telescope UTR-2 (Ukraine), the Tremsdorf radio telescope close to Potsdam (AIP Potsdam, Germany) and the Nançay Decametric Array (Observatoire de Paris-Meudon and Nançay, France). The combined efforts lead to simultaneous high-resolution observations of the low frequency radiation (down to 15 MHz) emitted by the solar corona.

The solar radio data from October 2000 until January 2001 of the DSP of the Lustbühel radio station (Graz, Austria) have been statistically analyzed. A catalogue containing relevant parameters (duration, bandwidth, intensity) of the emissions, selected according to their spectral features was established, which provides information on separating man-made interference and instrumental effects from natural radio source signatures. Four main events of solar activity have been further analyzed and compared, estimations of burst evolutions (e.g. drift rate) showed different characteristics of solar type III bursts (see Fig. 5.3).

Fig. 4.1: Crossed log-per antenna for the observation of solar radio bursts at Lustbühel Observatory.

Within the frame of the INTAS project "New frontiers of decameter radio astronomy" IWF planned and performed during June-November 2002 in cooperation with the Radioastronomy Institute Kharkov the solar radio measurement campaign C4 using the world-largest decameter antenna array UTR-2. Even after having passed the maximum of solar activity in the year 2000, high activity in radio emission has been observed during this campaign indicating a second solar maximum. Detailed studies on type II solar radio bursts connected to strong shock events have been initiated.

4.2 Mercury

Mercury is the planet nearest to the Sun. It is a significantly dense planet, which suggests a large iron core and possesses a weak global magnetic field. Until now only one space probe, *Mariner 10,* has done measurements around Mercury during three flybys. The planned ESA mission *BepiColombo* to Mercury will explore the planet in detail and over a longer period of time in the coming decade – with Austrian participation.

BepiColombo

BepiColombo is a satellite mission to Mercury. It is new and special in several ways. Not only is it the first joint European-Japanese satellite project, in which both the European Space Agency ESA and the Japanese Institute for Space and Astronautical Science (ISAS) are participating, it is also the first time that two orbiters are flying to this innermost planet.

Although the final selection of the experiments will be made in 2003 only, it is almost definite that IWF will participate in several of them.

Within the scope of the European-Japanese *MERMAG Consortium*, IWF will participate in proposals for magnetometers on both spacecraft. IWF will likely be in charge of the *MERMAG-M* magnetometer on the Japanese-built Magnetospheric Orbiter. IWF will also participate within the *NPA Consortium* (Neutral Particle Analyzer) on the proposed *MAIA* experiment (Mercury Apparatus for Ions and Atoms) on board of ESA's Mercury Planetary Orbiter.

Physics

Mercury exosphere: A Monte-Carlo model of Mercury's exosphere density was developed to study if the proposed *MAIA* instrument on board of ESA's *BepiColombo* Mercury Planetary Orbiter (MPO) will be able to detect and identify the exospheric composition along the MPO orbit. We study the exospheric densities by using a Monte-Carlo technique, which has the advantage that different particle release processes from Mercury's surface can be modeled. Our model follows the trajectories of each particle by numerical integration until the particle hits Mercury's surface again or escapes from the calculation domain. From many of these trajectories bulk parameters of the exospheric gas are derived, e.g. particle densities for various atomic and molecular species (Fig. 4.2). Our study suggests that *MAIA* should be able to detect at least at MPO's periherm all particle species, which are released from the surface.

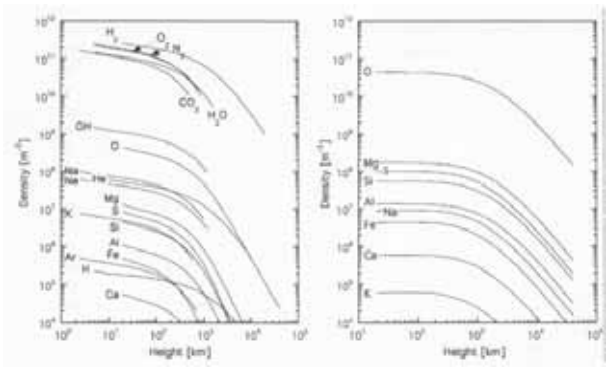

Fig. 4.2: Calculated exosphere densities for micrometeoritic impact vaporization (left panel) and surface sputtering (right panel).

Efficiency of particle surface release processes: In a second step we studied the efficiency of several particle surface release processes by calculating stopping cross sections, surface sputter yields (Fig. 4.3), and source rates for particle sputtering and Photon Stimulated Desorption (PSD). A solar UV model was used to yield the surface UV irradiance at any time and place over a Mercury year. Seasonal and diurnal variations are calculated and PSD fluxes along Mercury's orbit were evaluated. We found that a solar UV "hotspot" is created towards perihelion, with significant average PSD particle release rates and an Na flux of about $3.0 \times 10^6\,cm^{-2}s^{-1}$. The average source rates for Na particles released by PSD are about $10^{24}\,s^{-1}$. For surface particle sput-

tering we used in the calculation of the stopping cross section the "Universal Potential" because this fits well the laboratory data for atomic collisions.

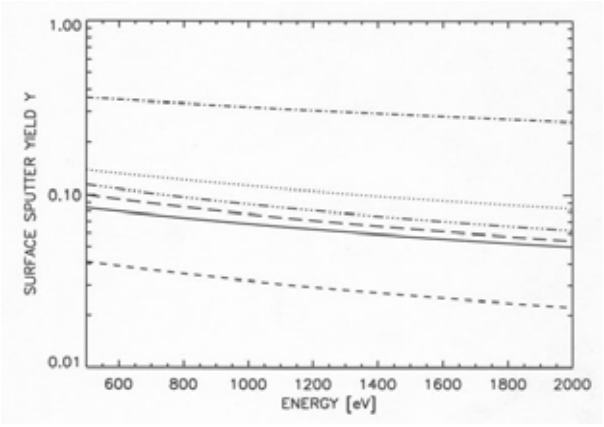

Fig. 4.3: Sputter yields for Na (dashed-dotted line, sputter agents N^+, binding energy 2 eV; dotted line H^+ sputter agents, binding energy 1.2 eV; solid line H^+ sputter agents, binding energy 2 eV), O (dashed line), K (long-dashed line) and Ca (dashed-dotted-dotted line) atoms as function of energy and incident solar wind H^+ particles.

For the estimation of the surface sputtering source rates a modified Tsyganenko T96 model was used for the calculation of the geometry of the magnetic field that could characterize Mercury and its response to the variations of the impinging solar wind and of the interplanetary magnetic field. The precipitating particle flux and energy was evaluated as a function of the open field line position, according to different solar wind conditions. It is possible to derive an open field line area where a typical value is about 2.8×10^{16} cm^2. By taking this area we get average surface sputter rates for Na of about 4.5×10^{21} s^{-1} $\div6.0\times10^{22}$ s^{-1} and for O of about 2.8×10^{23} s^{-1} $\div4.4\times10^{24}$ s^{-1}. The results depend strongly on various parameters like binding energies, solar wind density, magnetic field direction, open field lines and variability and Mercury's regolith composition. All of these parameters at present can only be determined within a given range due to the lack of experimental data. Our results suggest that the average source rates for the exosphere from solar particle and radiation induced surface processes during quiet solar conditions are about in the same order as particles, which are released from the surface by micrometeoroid vaporization.

4.3 Venus

Venus, like other planets in the solar system, is under the influence of a continuous flow of charged particles from the Sun, the solar wind. However, lacking of an intrinsic magnetic field makes Venus a unique object to study the interaction between the solar wind and the planetary body. Venus has a dense atmosphere, but no magnetic field, thus the solar wind interacts directly with the upper atmosphere. The absence of a planetary magnetic field leads to important differences between Venus' and Earth's atmospheric escape and energy deposition processes.

Previous missions, *Venera* and *Pioneer* orbiters, found that the current induced by the solar wind electric field (in the frame of Venus) forms a magnetic barrier that deflects most of the solar wind flow around the planet and leads to the formation of the bow shock. The ionosphere is terminated on the dayside, developing rapid anti-sunward convection and tail rays. However, the short lifetime of the *Venera* orbiters, and insufficient temporal resolution of the *Pioneer* plasma instrument did not allow to study the mass exchange between the solar wind and the upper atmosphere of Venus and energy deposition to the upper atmosphere in sufficient detail.

Venus Express

Venus Express (Fig. 4.4) is an ESA mission to Venus with the re-use of *Mars Express* spacecraft platform. IWF takes the lead on one of the core payload instruments, the magnetometer. The magnetometer aboard *Venus Express* will conduct the following studies:

1. Provide the magnetic field data for any combined field, particle and wave studies

such as lightning and planetary ion pickup processes;

2. Map with high time resolution the magnetic properties in the magnetosheath, magnetic barrier, the ionosphere, and the magnetotail. Identify the plasma boundaries between the various plasma regions;
3. Study of the solar wind interaction with the Venus atmosphere.

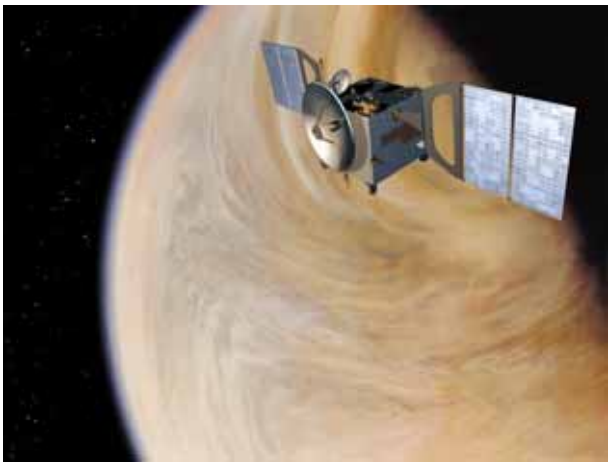

Fig. 4.4: Venus Express orbiting Venus.

Physics

Solar wind interaction: The solar wind interaction with Venus leads to an ionopause separating the ionosphere and the solar wind plasma. Even though Venus is unmagnetized, the solar wind flow around the ionopause is strongly affected by the interplanetary magnetic field (IMF). This effect becomes stronger as the ionopause is approached, giving rise to a magnetic barrier, characterized by an increased magnetic pressure and a low plasma beta. The effect of the magnetic barrier also intensifies, when the Alfvén Mach number upstream of the bow shock decreases. The equilibrium of the subsolar ionopause is provided by a pressure balance, namely, the ionosphere plasma pressure is equal to the solar wind dynamic pressure. The plasma pressure has a specific non-monotonic behavior from the bow shock towards the ionosphere: first it decreases to a minimum value in the magnetic barrier and then it increases again to a large value corresponding to that at the ionosphere. This is the case when the interchange instability has to grow up. This instability is similar in nature to the Rayleigh-Taylor instability in classical hydrodynamics, where the magnetic stress plays the role of an effective gravitational force. The interchange instability modes grow up when the magnetic tension acts in a direction of the gradient of the plasma pressure in the layer.

The ionopause with the magnetic barrier of Venus is shown to be an unstable structure with respect to the interchange instability.

Fig. 4.5 shows the distribution of the total pressure as a function of the x, y coordinates: x is the distance along the subsolar line with origin at the center of the planet, and y is the distance along the ionopause in the direction perpendicular to the magnetic field. These coordinates are normalized to the curvature radius of the ionopause.

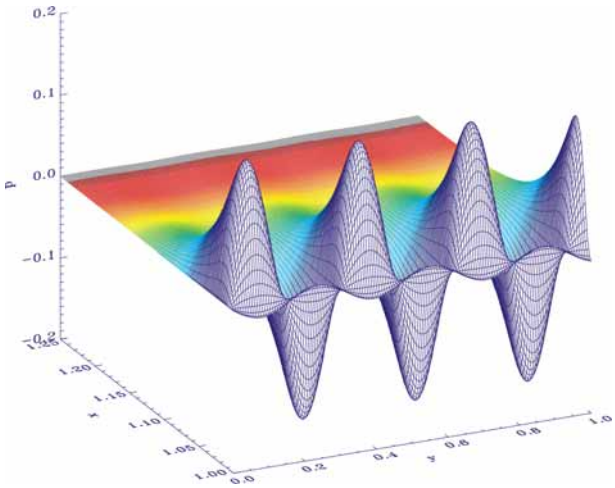

Fig. 4.5: Distribution of the total pressure perturbations versus the x (subsolar line) and y (along the ionopause, perpendicular to the magnetic field) coordinates.

From Fig. 4.5 one can see that the perturbations are mainly localized within the magnetic barrier. They do not disturb the magnetosheath region adjacent to the bow shock.

The physical reason for this instability is that the plasma pressure increases across the ionopause from the magnetic barrier towards the ionosphere. A steady-state ideal MHD

solution with mass loading is used as a background for the instability analysis. In the MHD treatment, a growth rate of the interchange instability is calculated as a function of the wave number, curvature radius and the ionospheric ion density. For an increasing wave number, the instability growth rate increases monotonically until saturation. The perturbations with smaller length scales are more unstable. In particular, for a length scale of about 100 km, the growth time of the instability is less than the time scale of the magnetic barrier formation. The perturbations of the magnetic field and plasma parameters related to the interchange instability are mainly localized inside the magnetic barrier. The interchange instability of the ionopause enables the penetration of magnetic flux tubes from the magnetosheath into the ionosphere of Venus.

Energetic Neutral Atoms (ENAs): Due to the interaction of the solar wind with the upper atmosphere of Venus, ENAs can be produced via electron impact, charge exchange or photoionization. When an atmospheric constituent becomes ionized, it is accelerated by the induced electric field and eventually transformed back by charge exchange into a neutral particle, thus forming an ENA.

Another source of energetic hydrogen atoms is the solar wind, since they can also be produced directly from the solar wind via charge exchange.

Since the production of ENAs is an additional mechanism for the erosion of a planetary atmosphere, the distribution of energetic hydrogen and oxygen atoms at Venus has been simulated in view of the evolution of the Venusian atmosphere.

Fig. 4.6 shows an example of both the flux and the energy of energetic O atoms through a sphere centered at Venus and with a radius of 3 planetary radii. Here, 0° latitude corresponds to the magnetic equator defined by the direction of the interplanetary magnetic field and the electric field points into the direction of increasing latitude values, i.e. into the northern hemisphere. Because of their large gyro radii, the O^+ ions are mainly accelerated upward into the direction of the electric field.

In comparison with Mars, the particles are more energetic at Venus, while their flux is higher at Mars since the Martian neutral corona is more extended with respect to the planetary dimensions than at Venus.

First observations of the ENA distribution near Venus will be obtained by the neutral mass spectrometer aboard *Venus Express,* which will then also allow a closer comparison between experimental and theorectical results.

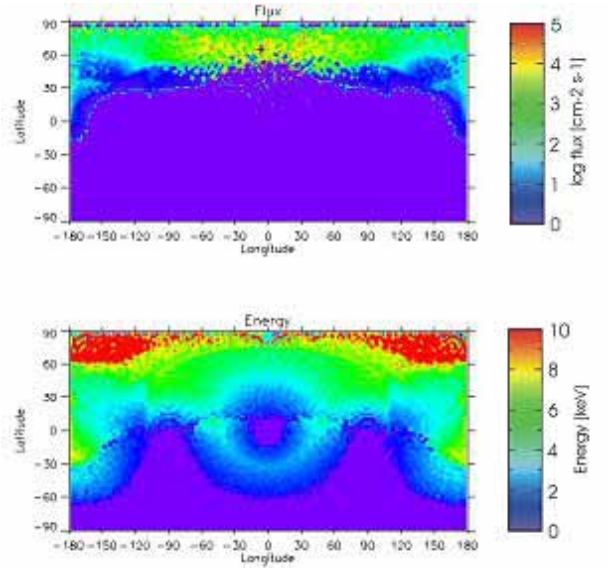

Fig. 4.6: Flux and energy distribution of energetic oxygen atoms for solar maximum on a sphere centered at Venus and with a radius of 3 planetary radii. The interplanetary magnetic field is assumed perpendicular to the solar wind and the electric field points in the upward direction.

Planetary atmospheres: Isotopic fractionation by gravitational escape processes: Present natural "data bases" for abundances of the isotopic compositions of noble gases, carbon and nitrogen inventories can be found in the Sun, the solar wind, meteorites and the planetary atmospheres and crustal reservoirs. Mass distributions in the various volatile reservoirs

provide boundary conditions, which must be satisfied in modeling the history of the present atmospheres. Such boundary conditions are constraints posed by comparison of isotopic ratios in primordial volatile sources with the isotopic pattern, which was found on the planets and their satellites.

Observations from space missions and Earth-based spectroscopic telescope observations of Venus, Mars and Saturn's satellite Titan show that the atmospheric evolution of these planetary bodies to their present states was affected by processes capable of fractionating their elements and isotopes. The isotope ratios of D/H in the atmospheres of Venus and Mars indicate evidence for their planetary water inventories. Venus' H_2O content may have been at least 0.3 % of a terrestrial ocean. Analysis of the D/H ratio on Mars imply that a global H_2O ocean with a depth of < 30 m was lost since the end of hydrodynamic escape.

We used a Monte Carlo model for the simulation of the time evolution of the $^{15}N^{14}N$ isotope anomalies in the atmospheres of Mars and Titan. These simulations show that the Martian atmosphere was at least ≥ 20 times denser than at present and that the mass of Titan's early atmosphere was about 30 times greater than its present value. A detailed study of gravitational fractionation of isotopes in planetary atmospheres furthermore indicates a much higher solar wind mass flux of the early Sun during the first half billion years. Studies are under preparation, which investigate if such a strong solar wind and solar EUV (extreme ultraviolet) fluxes, which are 100 times higher, could have been responsible for the D/H isotope fractionation in Venus' atmosphere.

4.4 Mars

The planet Mars continued to be in the focus of research activities in 2002. New investigations concerning a possible participation in ESA's planned *ExoMars* mission have been started. Model calculations concerning the behavior of ice melting probes that might be developed in the foreseeable future to explore the vertical structure of the Mars polar caps have been performed. The theoretical studies concerning the UV and particle fluxes and their influence on atmospheric loss mechanisms have been continued and extended.

NetLander

The main goal of the *NetLander* mission is to set up a meteorological and seismic network at the surface of Mars, using 4 identical landers. The launch of the mission has been postponed from 2007 to 2009.

SPICE: The main activity associated with the *NetLander/SPICE* experiment was the development of a new penetrometry test stand (see Chapter 5.3). First prototypes for the *SPICE* tips with integrated load cells were designed and built.

The second main activity, performed in cooperation with ETH Zürich, were seismic measurements with a standard STS2 seismometer mounted on the *SPICE* tips equipped with the foreseen load cells. It turned out that the load cells had a rather strong influence on the seismic measurements. These results lead to a redesign of the construction insofar as the load cells will now be mounted at the rear end of the legs instead of the tips. Further tests with the new design are in preparation.

Physics

Evolution of the Martian Water Inventory: We studied the evolution of the Martian atmosphere escape and atmosphere-surface-interaction processes with regard to its water inventory which is influenced by thermal atmospheric loss processes of H, H_2, non-thermal atmospheric loss processes of H^+, H_2^+, O, O^+, CO_2, O_2^+ and chemical weathering of oxygen with the surface soil (Fig. 4.7).

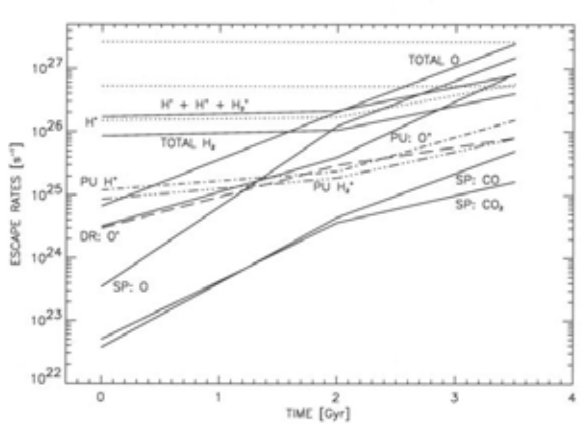

*Fig. 4.7: Thermal and non-thermal loss processes of hydrogen and oxygen from the present to 3.5 Gyr ago (PU: ion pick up, SP: atmosphere sputtering, DR: dissociative recombination, * thermal escape). The dotted lines at the top of the plot show an area where escape rates are comparable to hydrodynamic escape.*

Since the evolution of thermal and non-thermal escape processes such as exospheric loss of oxygen via dissociative recombination, atmospheric sputtering and ion pick up depend on the history of the intensity of the solar EUV radiation and the solar wind density we used actual data from the observation of solar proxies with different ages for reconstructing the Sun's history of the spectral evolution from X-rays to EUV, from the present to 3.5 Gyr ago. The high X-ray activity and the fast rotation of the young solar-like stars indicate a much higher solar wind for the young Sun. We used a correlation between mass loss and X-ray surface flux for a power law relation, which indicates a solar wind up to 1000 times more massive in the distant past. A gas dynamic test particle model which involves the motion in the interplanetary electric and magnetic field for the estimation of the pick up ion loss rates (found to be the most efficient non-thermal loss process of the Martian atmosphere) was used together with newly calculated atmospheric sputter yields and exospheric loss rates.

Our study suggests a total loss of water from Mars since 3.5 Gyr ago of an amount, which is equivalent to a depth of a global ocean of about 17 m. From the evolution of the D/H ratio in the Martian atmosphere and SNC meteorites we estimated a depth of a water reservoir of about 27 m 3.5 Gyr ago if the water originated from comets and about 20 m by using the terrestrial seawater D/H standard. Our results suggests that much more H_2O, necessary for the explanation of geological surface features, should have been lost from Mars before 3.5 Gyr via hydrodynamic escape caused by the early active Sun, or liquid CO_2 may have been involved in the formation of certain geological features in the Martian past.

Further, we found in our evaluation of the water loss to space that the total escape processes of oxygen to space from present Mars cannot maintain the sum of thermal and non-thermal atmospheric loss rates of hydrogen in the ratio of 2:1. At present the ratio is about 25:1. Our result suggests that atmospheric escape to space can therefore not be the only sink for oxygen on Mars since the desirable ratio of 2:1 of H:O loss rates should be established.

Atmosphere-surface-interaction: We studied atmosphere-surface-interaction processes where oxygen is incorporated from the atmosphere into the Martian surface by chemical processes, which oxidize the soil. Based on our results on the evolution of the Martian water inventory a global surface sink of about 2×10^{42} oxygen particles into the Martian soil over geologic time-scales must be assumed. Due to intense oxidation of inorganic matter this may lead to the formation of considerable amounts of sulfates and ferric oxides on Mars (Fig. 4.8).

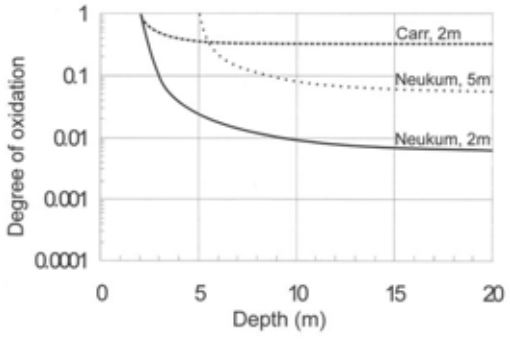

Fig. 4.8: Degree of oxidation with depth for Carr and Neukum crater-rate datasets.

Our results show that the present Martian atmosphere reacts strongly with the soil, resulting in combination with UV surface fluxes in the production of adsorbed oxygen ions and biologically hostile radical products and have important implications for subsurface radar sounding techniques and for the toxicology of the surface soil.

4.5 Jupiter

One of the most intriguing solar system phenomena is the Jupiter-Io interaction leading to specific physical processes, as there are active volcanism, shock pulses along the Io flux tube and triggered non-thermal radio emission. These processes are of specific interest to us, thus both experimental and theoretical investigations have continuously been performed.

Cassini Jupiter Flyby

During the Jupiter flyby phase in December 2000, several roll maneuvers of the *Cassini* spacecraft were done to calibrate the three *RPWS* (Radio and Plasma Wave Science) antennas using components of the non-thermal radio emissions of Jupiter, the broad-band kilometric (bKOM) and the hectometric (HOM) emission, respectively. In collaboration with the scientific leading team at University of Iowa, Iowa City (USA) and French colleagues (Observatoire de Paris-Meudon), the theoretical approach is based on singular value decomposition technique (SVD) which enables the estimation of the electric direction of each antenna element independently. Using auto- and cross-correlation measurements of the three antennas and several strong restrictions to the data sets, i.e., a) circularly polarization of the observed electromagnetic waves, b) difference between the calculated direction of the radio signals and Jupiter's position is less than 5 degrees, c) frequency range, f, is chosen to be 575 kHz $\leq$ f $\leq$ 1.2 MHz, d) high parameter resolution for both, the co-latitude and azimuth of each electric monopole, the effective length vectors are finally calculated for the u/v monopoles under the SVD approach. As a result one gets the co-latitude (θ) and the azimuth angle (Φ) of the u and v electric monopoles. Specifically, the direction of the u antenna is $\theta(\sigma)$: 106.38° (1.08°) and $\Phi(\sigma)$: 15.52° (1.65°) whereas the direction of the v antenna is derived as $\theta(\sigma)$: 107.58° (1.39°) and $\Phi(\sigma)$: 163.07° (1.58°), where the numbers in brackets give the standard deviation. It has to be noted that the w electric monopole cannot unambiguously be determined within the SVD approach.

Jupiter Radio Observations

Polarization studies at decametric wavelengths: The multichannel receiver at Graz, Lustbühel Observatory, is connected to two logarithmic periodic antennas (east and west side of the main building). Their polarization planes are oriented orthogonally against each other and they cover a frequency range from 13 to 32 MHz, i.e. in the decameter (DAM) wavelength range.

The multichannel receiver is now ready to run in four different observation modes including the polarimetric mode (time resolution 16 ms). In the single signal mode, time resolution of 4 ms is possible (Fig. 4.9).

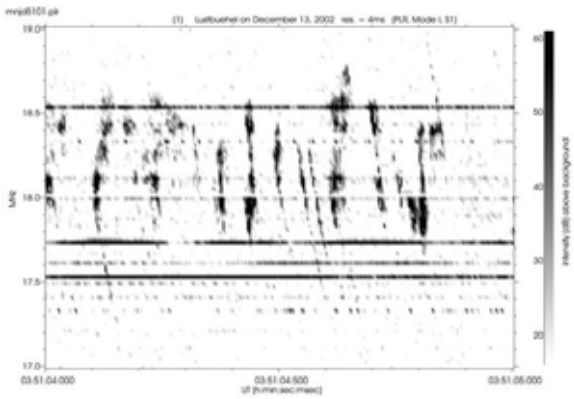

Fig. 4.9: Jupiter millisecond radio bursts observed at Lustbühel Observatory, Dec. 13, 2002. The bursts in this dynamic spectrum are under polarimetric investigation.

The polarization mode is specifically adjusted to measure the state of polarization of ex-

tremely short radio burst phenomena. For Jupiter millisecond radio bursts this property enables the determination of radio source conditions. Observations have been performed in combination with the world-largest decameter array at Kharkov (Ukraine), which is most sensitive to DAM radio emission but still unable to provide polarization information. Since this is still an open question with regard to millisecond radio bursts, further observations and studies are necessary.

Modulation Lanes: During the INTAS C2 measurement campaign (February–May, 2000) Jovian radio emission was simultaneously recorded by DSP receivers in Kharkov (Ukraine) and in Nançay (France).

Spectral resolution was possible down to 2 ms and 12.5 kHz. Both stations were simultaneously (time synchronized by GPS) operating in defined sequences alternatively with medium and high time resolution. The present analysis concentrates on Jovian decametric radio phenomena, in particular on simultaneously observed modulation lanes and S-burst features.

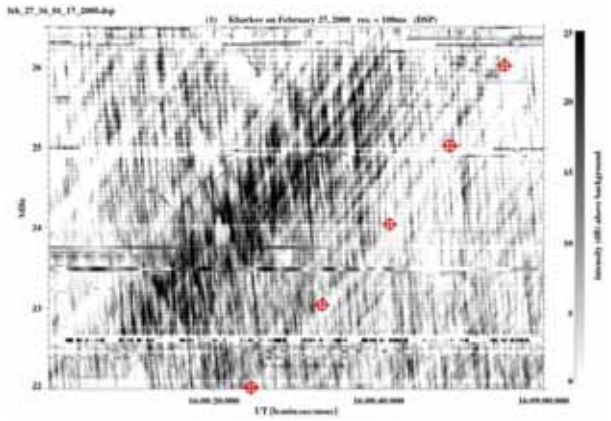

Fig. 4.10: Zoom into a Jovian L-burst, recorded on February 27, 2000, when the Jovian radio source "Io-B" was active. The striped pattern of modulation lanes is the dominant feature.

Geometrical source conditions can be derived from the shape of these modulation lanes: the lead angle α of the active field line (i.e. the angle between the position of Io and the field line carrying the source) or the cone half-angle β of the emission cone. Five red spots in Fig. 4.10 mark the edge of one modulation lane reaching from 22 MHz up to 26 MHz, thus a lead angle in the range of $40° < \alpha < 50°$ can be deduced.

Hectometric "caustic-like" pattern: As observed by the *Wind*/*WAVES* experiment in the frequency range from 1 to 7 MHz, i.e. in the hectometer (HOM) wavelength range, the analysis on a "caustic-like" pattern in the beam associated to the Jovian hectometric emission was performed for the period 1996 through 2000, with changing Jovicentric declination. There exists a selective effect where only part of the hectometric beams (HOM) could be observed at the Earth's orbit by the satellite *Wind*. We show that the origin of the "caustic-like" pattern is related to the geometric observation conditions between Sun, Jupiter and the Earth.

Fig. 4.11 shows the occurrence of the "caustic-like" pattern versus the central meridian longitude (CML) and the Jovicentric declination. The origin of the "caustic-like" pattern seems to be directly related to physical conditions occurring in the Io-torus during some specific periods of time.

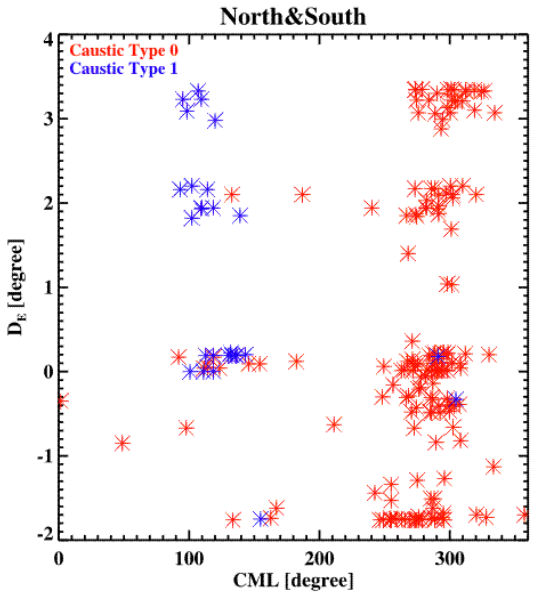

Fig. 4.11: "Caustic-like" pattern occurrence versus the central meridian longitude (CML) and the Jovicentric declination (D_E).

Sounding of the Jovian magnetosphere activity using hectometric and kilometric radio emission: We analyzed the variation of the Jovian radio emission in the frequency range between 10 kHz and 6 MHz by combining *Galileo* and *Wind* observations. Special emphasis was laid on emissions observed during the second *Galileo's* orbit, which corresponds to the period from August 31 to October 23, 1996. For a given period of time, the central meridian longitudes associated to the observer (*Wind* or *Galileo* spacecraft) were evidently different. This opportunity enabled us to compare the variation of the hectometric radiation as observed by the two satellites, *Wind* on the dayside and *Galileo* on the nightside of Jupiter.

We show that periodic intermittent enhancements of hectometric emission during long (several days) or short (few hours) intervals are quasi-simultaneously recorded by both spacecraft. Such Jovian "sub-storms" seem to affect also lower frequencies and in particular the Jovian kilometric radiation. The spectral boundaries of the HOM and KOM (kilometric) emission during these particular phases and their inter-correlations have been analyzed in detail.

Io-Jupiter Interaction

Many energetic phenomena near the ionosphere of Jupiter, including non-thermal radio emission and aurora, are triggered by the orbital motion of the satellite Io. From the theoretical point of view, the moon Io can be considered as a source of disturbances, which are guided along the magnetic field thereby transporting energy from Io towards the surface of Jupiter.

Within the frame of MHD, there are two different modes of wave propagation providing a possible theoretical background for the description of this energy transport, i.e., the Alfvén and the slow magnetosonic wave. It is well known that in contrast to the Alfvén wave, which is propagating strictly along the direction of the magnetic field, a slow mode wave shows a deviation from the ambient magnetic field. This deviation is determined by the dispersion equation for the slow mode wave. With the help of this dispersion equation we present a theoretical study of the spatial and temporal evolution of an initial pressure disturbance in a homogeneous and constant background magnetic field. The main factor determining the amount of the deviation is the so-called plasma beta, i.e., the ratio of magnetic to thermal energy. We obtain that for a low beta plasma, as it is the case near Io due to the strong Jovian magnetic field, the disturbance propagates more or less strictly along the magnetic field.

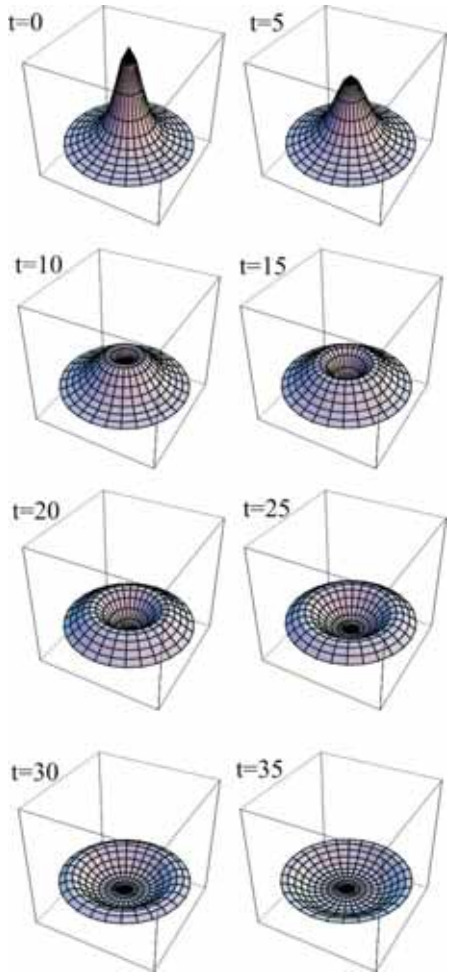

Fig. 4.12: Evolution of a pressure pulse along the magnetic field.

In Fig. 4.12 the evolution of a pressure disturbance is shown for successive times scaled to l_0/c_S and for a plasma beta of 0.5 for a clear

view of the occurring effects. For the presentation of the solution a coordinate system is chosen co-moving with the pressure disturbance in order to focus on the behavior perpendicular to the magnetic field.

4.6 Titan

Titan, the Earth-like moon of Saturn, will be investigated by the joint NASA/ESA mission *Cassini/Huygens*. The planetary probe *Huygens* will descend to Titan's surface in January 2005 (Fig. 4.13) and the *Cassini Orbiter* will investigate the Saturnian System for several years.

Fig. 4.13: Huygens probe descending to Titan's surface.

IWF developed modules of the *Huygens* Atmospheric Structure Instrument *(HASI)* and the Aerosol Collector and Pyrolyser *(ACP)* and participates in the *Huygens* Gas Chromatograph and Mass Spectrometer *(GCMS)* and the *Cassini* Radio and Plasma Wave Science Experiment *(RPWS)*, too. In order to prepare for the data analysis several physical models of the atmosphere/ionosphere and surface are under development at IWF.

Physics

Schumann resonances at Titan: The so-called Schumann resonances are characteristic properties of electromagnetic waves in a cavity formed by the conducting surface and the ionosphere. At Earth they occur in the extreme low frequency range with the fundamental mode at about 8 Hz. They are triggered by lightning phenomena. The measurements of the Schumann resonances is one method to detect lightning activity on Titan, which is predicted be several models.

The *Huygens Atmospheric Structure Instrument (HASI)* aboard the *Huygens* probe is capable to detect low frequency electric fields in the frequency range up to 100 Hz (Schumann mode). We investigated theoretically the propagation of low-frequency electromagnetic waves in the atmosphere/ionosphere of Titan. First we used two concentric shells (surface, ionosphere) with a uniform conductivity as a representation of the ionospheric waveguide. The results of calculations applied on the terrestrial case reveal that the resonance frequencies are 30 % too high in comparison to the experimentally measured frequencies. Additionally, the use of a numerical method provided the opportunity to include realistic electrical conductivity profiles of the atmosphere. The Transmission Line Method yielded satisfactory results for the resonance curves.

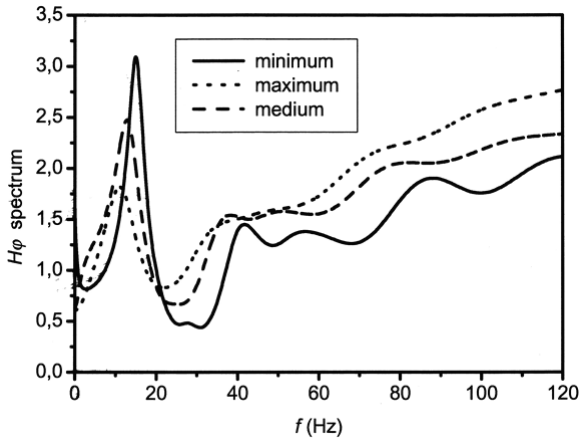

Fig. 4.14: Titan Schumann resonance spectra for different typical atmospheric conductivity profiles.

The main difference of the lower atmosphere of Titan with regard to the Earth's cavity is its higher conductivity. Our Titan results are

based on models of the neutral and ion atmospheric chemistry. Due to the geometric properties of the cavity the resonances are expected to be a factor of 2.5 higher than on Earth. We calculated the Titan Schumann spectrum and found it much broader than that for Earth (Fig. 4.14). Taking into account the uncertainty of the conductivity profile the higher resonances can also almost disappear for very high conductivity levels.

The simulations will be continued and improved in order to have an appropriate tool for the analysis of the *Huygens* 2005 descent data.

Lightning on Titan: The search for lightning on Saturn's satellite Titan is one of the scientific targets of the *Cassini/Huygens* mission. Although *Voyager 1* did not detect any radio emissions attributed to lightning during its flyby in November 1980, one cannot generally rule out their existence because of low flash rates or ionospheric radiation blockade. The thundercloud model in Titan's troposphere, which was discussed in the Annual Report 2001, favors the existence of lightning and predicts the charge densities as a function of altitude for simulated clouds charged by electron attachment or collisional charging. A study was performed by replacing the horizontally homogenous charge densities of the model by homogenously charged spheres, and electrostatic energy considerations were made for various stages of a possible lightning stroke: In the initial stage the thundercloud is approximated by two spherical charges at certain heights. The intermediate stage is the situation just before the return stroke, when a certain amount of charge is distributed along the so-called leader channel, and in the final stage all this leader charge is neutralized in the return stroke process. The energy of the system in the leader stage behaves in an interesting way and has a minimum, which corresponds to a certain leader charge, which will preferentially be lowered in the following return stroke process. It was also found that the energy in the return stroke stage mainly depends on the length of the channel and the amount of lowered charge. For a simulated Titan monopolar cloud charged by electron attachment cloud-to-ground lightning strokes lowering 30 C (Coulomb) of charge and dissipating energies around 10^{10} J (Joule) were calculated. For the modeled bipolar clouds charged by collisional charging these values are a few C of lowered charge and about 10^{8} J of dissipated energy, which are quite similar to typical Earth values.

Titan atmosphere chemistry simulation: Using the available Titan atmospheric data, simulations are currently under preparation, which will be done with a program called ASPEN. This program works with all acknowledged thermodynamic models. The choice of the right thermodynamic model depends on the number of the expected phases, the polarity of the substances, and their interaction. To get as close as possible realistic results we support our theoretical studies with laboratory experiments by means of a chemical reactor where we can simulate Titan’s atmospheric conditions also close to its surface. The experimental set up and the experiments, which are carried out in the reactor, are currently developed.

4.7 Comets

Comets are considered to have their origin in cool and distant regions of our solar system at very early stages of its evolution. Thus, cometary matter might have preserved some original signatures of the materials at that time. The scientific interest in comets is characterized by their dual role as messengers from the beginnings of the solar system and as relatively unexplored, "exotic" small bodies. So far, our current knowledge is based on the cometary missions to comet Halley in the late 1980's, which were not more than a quick snapshot of a cometary nucleus.

Rosetta

ESA took a lead in closing some of the knowledge gaps by assigning a cornerstone mission to the exploration of a comet in all detail by measurements in-situ. This mission, labeled *Rosetta*, will monitor the evolution of a comet during its approach nearer to the Sun over a long period of time from an Orbiter. In addition, a Lander will be dropped on the surface of the nucleus. Due to problems with the Ariane-5 rocket, the launch, which was foreseen for January 2003, was postponed. Scientists believe that *Rosetta* can no longer reach its original target, comet P/Wirtanen. *Rosetta's* new flight path and the comet on which it will land have not yet been determined.

IWF participates in a number of experiments in this key ESA mission. It is leading the investigation of dust particles collected in the coma by means of an atomic force microscope. This instrument *MIDAS* on the *Rosetta Orbiter* is to investigate the structure, flux and magnetic properties of the grains. IWF also contributes to the mass spectrometer *COSIMA* and to the magnetometer *RPC-MAG* on the Orbiter.

The Lander instrumentation has contributions by IWF to the *MUPUS* and *ROMAP* experiments and to the development of the *Rosetta Lander* anchoring system. *MUPUS* consists of a group of sensors to measure the thermal and mechanical properties of layers near the surface. *ROMAP* is a magnetometer to investigate the magnetic field during the descent to the surface and of possible variations after the landing.

MIDAS

The dust emitted from the nucleus when solar irradiation becomes strong enough to sublimate the ices is not only creating an essential part of the spectacular coma; it also carries important information on the nucleus. The instrument *MIDAS* (Micro-Imaging Dust Analysis System) on board of the *Rosetta Orbiter* will allow to investigate the texture of individual grains and statistical features of the dust flux by means of atomic force microscopy. The instrument has been developed under the leadership of IWF (see the Annual Report 2001 and the IWF website for details).

The *MIDAS* Flight Model had been completed and integrated on the *Rosetta Orbiter* in September, 2001. Since then it has remained on the spacecraft and accompanied it during the long series of system level tests in 2002, starting with the thermal vacuum test in the new facility at ESTEC (Fig. 4.15).

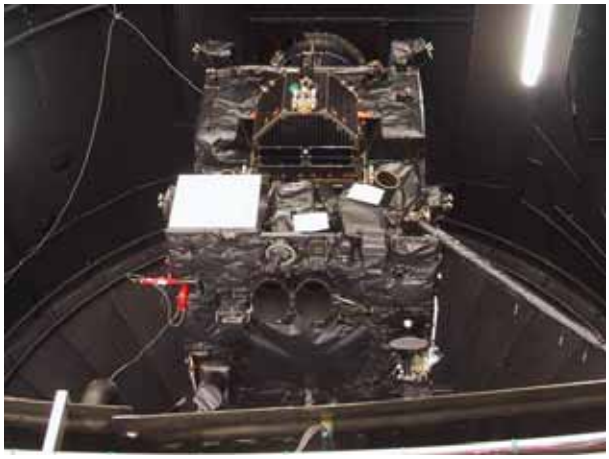

Fig. 4.15: The Rosetta spacecraft being mounted inside the thermal vacuum facility at ESTEC.

The environmental and functional system tests continued until August with acoustic and vibration tests, electromagnetic compatibility test, and system validation tests. All tests were performed at ESTEC. Based on results collected during the tests and on further experience gained by operating the Qualification Model of the instrument at IWF, the flight software was upgraded including new modules for on-board processing of the collected images of cometary dust particles. The final flight software was uploaded to the instrument and verified in August, just before the transport of the spacecraft to the Kourou launch site. Another abbreviated functional test and a system validation test were per-

formed in Kourou. *MIDAS*, as all payload, participated in these tests. The data could eventually be retrieved both at the ESA flight control center in Darmstadt, Germany (ESOC) and at IWF, using the *Rosetta* Data Disposition System.

In parallel to the flight model activities, the experimental program on the ground continued. A spare unit of the instrument, to be used for investigations on cometary analogue materials throughout the next decade, has been completed. This unit will also serve as a test bed for procedures to be executed on the flight unit later on. For this unit, parts of the Engineering Model (EM) had to be refurbished. As the latter is to be kept at ESOC for command verification purposes, the parts removed form the EM had to be replaced by functionally equivalent elements, and a copy of the final flight software had to be installed.

The accompanying ground investigation program based on atomic force microscopy until and during the near-nucleus operations phase (2012 to 2013) requires a significant number of spare sensors for the AFM, which are very susceptible to mishandling in the laboratory and also show degradation after extensive use. Sensors for additional 40 scanner heads have been received and inspected, and the assembly of the heads has started.

COSIMA

The acronym *COSIMA* stands for Cometary Secondary Mass Spectrometer, an instrument on board the *Rosetta Orbiter* dedicated to the chemical and isotopic analysis of dust grains collected in the coma. The work principle is that of secondary ion mass spectrometry (SIMS), when a primary ion beam of high energy is focused to a small spot on the target where it releases molecules out of the target material and ionizes a fraction of 0.1 to 10%. In the case of *COSIMA*, a primary beam of Indium ions at 10 keV is applied. The small spot size of ca. 10 µm radius allows to spatially resolve chemical features on larger single particles. The secondary ions extracted from the target are fed into a time-of-flight mass spectrometer with a large mass range.

The development of the instrument is performed by an international collaboration chaired by the Max-Planck-Institut für extraterrestrische Physik (MPE) in Garching, Germany. IWF provides electronics for the primary ion beam system, consisting of high voltage and heater supplies for the ion sources.

In 2002, the manufacturing of the flight model electronics was completed. After testing and calibration the hardware was delivered to the PI institute for integration into the instrument. After a series of tests the instrument was finally integrated into the *Rosetta* spacecraft in July 2002.

MUPUS

In 2002 both the *MUPUS* penetrator and the *Rosetta Lander* anchors have been delivered to ESA, shipped to the Kourou launch site and mounted at the lander. All FM tests have been successfully so far. Some calibration tests with the ground reference models are still to be done.

ROMAP

The experiment *ROMAP* (Rosetta Lander Magnetometer and Plasma Monitor) aboard the *Rosetta Lander* is a multi-sensor experiment. A fluxgate magnetometer (TU Braunschweig) investigates the magnetic field, ion and electron rates are detected by means of an electrostatic analyzer (KFKI Budapest / MPAe Lindau) and the ambient pressure is measured by Pirani and Pennings sensors. The different sensors and their accompanying electronics are controlled by the *ROMAP* Controller developed at IWF, which includes the instrument's telemetry interface.

In parallel to *ROMAP*, plasma parameters are measured by the *Rosetta Orbiter*. This makes it possible to investigate the comet / solar wind interaction (generation of the coma and the plasma tail) as function of the distance from the Sun at two different points.

The following tasks have been performed in the year 2002:

- Several integration tests with the Flight Model 2 at MPAe Lindau and at the Kourou launch site
- Production and assembling of a Flight Reference Model
- GSE software improvements
- Design of a data conversion module for data visualization at the *Rosetta Lander* Data Center.

RPC-MAG

The fluxgate magnetometer *RPC-MAG* is one of the five instruments included in the *Rosetta Plasma Consortium (RPC*, Fig. 4.16). It is designed to measure the magnetic environment of a comet and to determine its magnetic property. During the two years period of *Rosetta* orbiting around the comet, the comet tail will be observed in detail for the first time.

Fig. 4.16: External view of the RPC-0 Box.

The lead institution of the *RPC-MAG* consortium is the Institut für Geophysik und Meteorologie of TU Braunschweig. The analogue-to-digital converter of the magnetometer is built by IWF.

In 2002, the Graz team has participated in various tests and calibrations. For the *Rosetta Orbiter*, the determination and compensation of the magnetic stray field are very important. IWF has developed a special GSE software and made tests together with TU Braunschweig. After a series of tests at ESTEC, *RPC* was finally integrated into the *Rosetta* spacecraft and transported with the spacecraft to French Guyana in September 2002.

4.8 Solar Wind

The particles emanating from the Sun, the so-called solar wind, consist of protons, helium, and other particles, including electrons. Processes on the Sun, like coronal holes, solar flares and sunspots cause temporal and spatial disturbances in the solar wind and a sequence of fast and slow plasma streams. This results in the interactions of shock fronts.

Instabilities

Various kinds of waves and instabilities exist in space plasmas. We study in particular the Kelvin-Helmholtz instability at the magnetopause, the interchange instability, and the growth rate of mirror modes in the terrestrial magnetosheath. Both instabilities are of interest for studying phenomena at planet Venus and therefore important for the upcoming space mission *Venus Express*.

Non-thermal particles

Numerous in-situ observations indicate clearly the presence of non-thermal electron and ion structures as ubiquitous and persistent feature of most space plasma environments. The three detected dominant deviations from multi-temperature Maxwellians are suprathermal particle populations, loss-cone

structures and, provided by recent high-resolution data analysis, gyrophase-bunched electron and ion distributions at plasma boundary layers.

After clarifying the occurrence of specific non-thermal features in various space plasma environments, different generation mechanisms of energetic particles can be deduced and studied in view of coronal/solar wind and magnetospheric conditions. Wave-particle interaction based on a Fokker-Planck approach demonstrates how Landau interaction ultimately leads to kappa-distributions, favored in astrophysical plasma modeling. In turn, it can be shown that these distributions are theoretically a consequence of non-extensive thermo-statistics, thus can be considered as plasma equilibrium state. Moreover, magnetic field gradients can act as catalyst for the generation of energetic particle populations up to relativistic energy due to synergetic effects in a multi-stage acceleration process relevant, for instance, for solar flare conditions.

With regard to further studies of wave-particle interaction processes and instability analysis a class of highly general analytical representations of velocity space distributions was developed, shown to model accurately observed complicated situations ranging from multi-component, two-temperature high energy tail structures and loss-cone features to non-gyrotropic distributions, where Maxwellians are recovered as special case.

Multi-component solar wind models from non-extensive entropy environments: Most astrophysical plasmas are observed to have velocity distribution functions exhibiting non-Maxwellian suprathermal tails where the high-energy particle populations are accurately represented by the family of kappa-distributions. Since these distributions turn out as equilibrium state within the framework of pseudo-additive entropy, non-extensive thermo-statistics have been considered as ideal basis for the development of highly accurate solar wind velocity space distributions and used to formulate a theoretical foundation of multi-component solar wind models.

Growth rates of mirror and ion-cyclotron modes for suprathermal-, loss-cone, ring and non-gyrotropic velocity space distributions: In view of equilibrium conditions magnetic fluctuations were recognized in a large variety of space plasmas by increasingly high resolution in-situ observations as mirror wave mode structures. Similar as for the ion-cyclotron instability, a typical requirement for the excitation of mirror modes is a dominant perpendicular pressure in a high beta plasma environment. It was demonstrated from a realistic kinetic analysis how details of the velocity space distributions are of considerable significance for the mirror instability threshold.

Magnetic Clouds

Magnetic clouds belong to the phenomena of Coronal Mass Ejections (CME) and can be determined by several characteristics. They are different from the surrounding solar wind and have (1) an enhanced field strength, (2) a large and smooth rotation of the magnetic field vector, (3) lower proton temperature and (4) low plasma-beta. After their release at the Sun they move away and since they are generally moving faster than the normal solar wind they often drive a shock front. While their propagation outward they are expanding which is often finished when they reach 1 AU.

For corresponding studies observations from the *Wind* spacecraft at 1 AU, and *HELIOS 1 & 2* spacecraft, positioned at 0.3÷1.0 AU, were used.

The developed model regards the magnetic cloud to be locally a cylinder with a force-free magnetic field configuration, and it is based on a least-square fit to the x-, y-, and z-

components. Since *HELIOS* observations were made at different radial distances from the Sun, changes of the cylindrical diameter, the maximum magnetic field strength, and changes of the orientation with radial distance were examined.

Usual magnetic clouds are driving a shock front, and the relation of the stand-off distance of the shock with the maximum field strength of the magnetic cloud were determined. As a result we state that with an additional magnetic field the stand-off distance increases, which can clearly be seen in the observations.

An example of a magnetic cloud observed by the *HELIOS 1* spacecraft at 0.84 AU is shown in Fig. 4.17. The thick red lines in the B_x, B_y and B_z panels is an estimated fit to these magnetic cloud's magnetic field components.

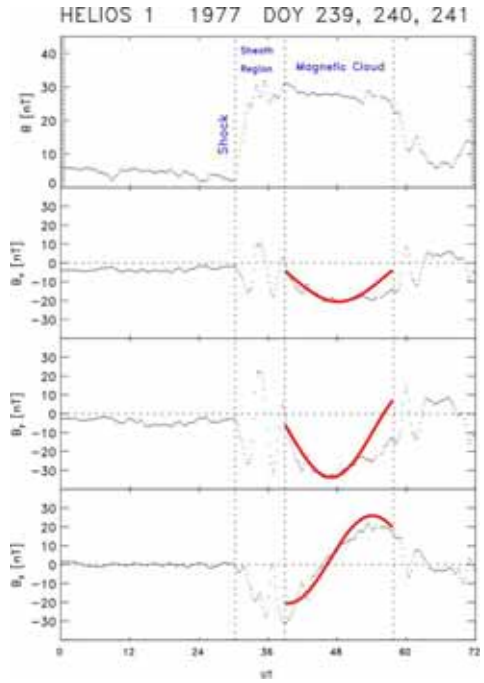

Fig. 4.17: From top to bottom: The total magnetic field strength with the components in x-, y- and z-direction (12 minute averages in GSE coordinate system). Red lines show an estimated fit to the magnetic field components.

5 Laboratory Experiments

The vast experience of IWF in the development and building of instruments for space missions and subsequent data analysis enables the institute to perform experiments in IWF laboratories, to develop software and to provide calibration tools for radio antennas.

5.1 Magnetic Cleanliness

The *Multi-Magnetometer-Sensing* (MMS) study was completed at the close up meeting held at IWF in October 2002. The main topics of this meeting were the final review of the s/c development software tool POLYMAG, discussions about first POLYMAG design results for the *Venus Express* mission and the follow-on project *MAGLAB*. The start of *MAGLAB*, planned as cooperation between ESA (The Netherlands), IGM (Germany) and IWF, was postponed to the middle of 2003. IWF was invited to work on this new international *MAGLAB* project and a decision about participation will be taken at the beginning of 2003.

The main tasks of the *MMS* activities in 2002 were the maintenance of the POLYMAG software, the completion of the technical reports and the first application of the software package for the s/c mission *Venus Express*. During extensive tests and study procedures several software modifications were implemented. All technical reports have been revised and delivered to ESA/ESTEC. In more detail, the POLYMAG software package was used to determine an optimum geometrical configuration of boom and magnetic field sensors for the planned *Venus Express* mission.

The insights and results of this first application showed that the POLYMAG s/c design tool constitutes a valuable support for optimizing real magnetic field measurements on s/c.

5.2 Radio Antennas

One main competence of IWF is the capability to determine the reception properties of radio antenna systems of spacecraft as well as of ground-based radio telescopes, by various means and tools. Following the already performed investigations on the *Cassini RPWS* antenna system, which yielded remarkable coinciding results by means of rheometry, wire-grid numerical calculations and in-flight calibration, recent studies concentrated on the determination of the effective antenna vectors of the *Interball POLRAD* and the *Mars Express MARSIS* antenna systems.

The POLRAD experiment on Interball 2: The joint Austrian-Russian project "Rheometry analysis of the antenna system of the *POLRAD* experiment aboard the *Interball 2* satellite *(AURORAL PROBE)*" aims for the rheometric determination of the reception properties of the *POLRAD* antennas. The rheometry technique is based on electrolytic tank measurements, using a down-scaled spacecraft model with the *POLRAD* antennas (Fig. 5.1). The measurement series performed in 2002 showed that the electrically effective antenna axes of four antennas are tilted by about 6 degrees from their respective nominal (mechanical) axes towards the -X (symmetry) axis. The results will be used for improved evaluation of *POLRAD* AKR data, in particular the

study of radio wave polarization and calibration techniques. Furthermore, it provides an estimation of the influence of the non-operational element (antenna arm) of the *POLRAD* antenna system.

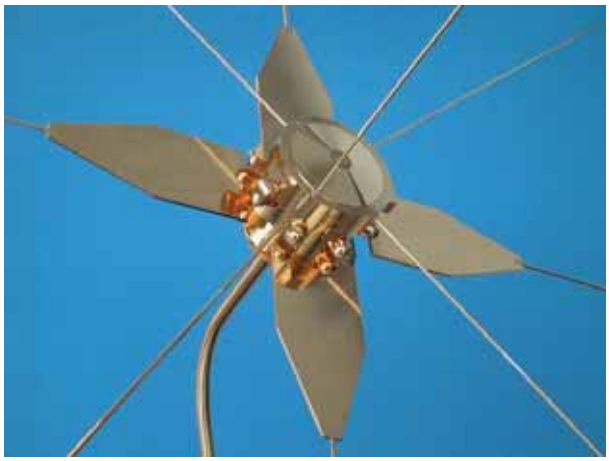

Fig. 5.1: Interball 2/POLRAD rheometry model, scale 1:30.

MARSIS antennas aboard Mars Express: The *MARSIS* (Mars Advanced Radar for Subsurface and Ionosphere Sounding) experiment aboard *Mars Express* is a ground penetrating radar for the investigation of the Martian surface and subsurface structure, especially to map underground water and ice, which is thought to be essential in the search for microbial life on Mars. The *MARSIS* antenna system consists of a primary dipole for transmission and reception of radar pulses, and a secondary receiving monopole for the cancellation of surface clutter echoes. The exact knowledge of the null-axis (axis of minimum sensitivity) of the monopole is decisive for the sounding technique. As the effective axis of the monopole is significantly perturbed by the spacecraft body, the determination of the offset of the axis from the nominal direction is crucial.

In the year 2002 we performed preliminary numerical simulations to determine the reception properties of the clutter monopole, especially its effective axis. The calculations are based on a wire grid model representing those features of the *Mars Express* spacecraft which are most important with regard to the antenna properties: the central body, solar panels, dipole arms and the monopole antenna (Fig. 5.2). First results show the enormous influence of the solar panels and the primary dipole antenna. In particular, the monopole radiation pattern is very sensitive to the termination impedances of the dipole. It was found that a realistic description of the reception properties of the clutter antenna could only be accomplished by taking into account the impedance matching network of the dipole in the modeling. This is planned for future simulations, including improvements of the wire grid design.

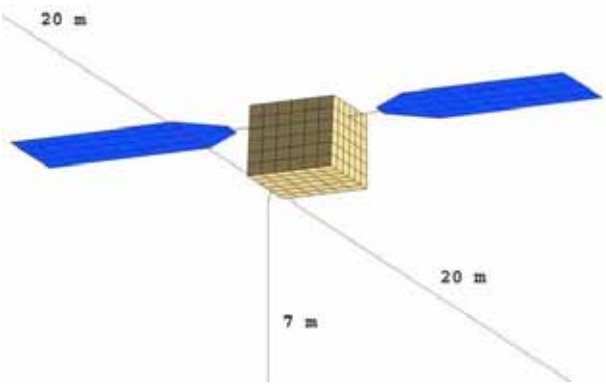

Fig. 5.2: Wire grid for numerical simulation of MARSIS antennas aboard Mars Express. The monopole antenna is 7 m long, the dipole consists of two 20 m elements, and the size of the central body is approx. (1.65x1.7x1.4) m.

Radio emission visualization by Spectrum Analyzer (SA): The Anritsu MS2661C is a modern spectrum analyzer for observations of solar and Jovian decametric radio emissions at the Lustbühel radio station. It is a swept frequency analyzer, which measures the input signal at a number of frequency channels in a serial way by analyzing one channel after another. A time-frequency representation can be obtained by sweeping in a certain time from the start to the stop frequency by means of a tunable band pass filter (with a certain resolution bandwidth), whose center frequency is periodically deplaced.

For the visualization of the observed radio emissions by means of a so-called dynamic spectrum (i.e. a signal intensity plot versus the frequency and the time) it was necessary to implement a computer control, which can

display such a spectrum and save the corresponding data. LabView was used as a programming tool to implement such a remote computer control.

Fig. 5.3 shows solar bursts recorded with the SA at August 21, 2002, with the start time 11:48:48.14 UT. Two type III bursts can be identified with a lower frequency limit of about 27 MHz, and the more intense one has a time duration of about 50 seconds. The vertical streaks in the spectrum are caused by lightning from a nearby thunderstorm.

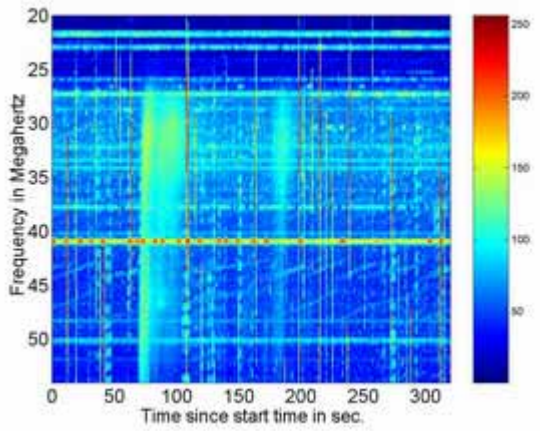

Fig. 5.3: Solar radio bursts recorded with the Anritsu MS2661C spectrum analyzer at Lustbühel Observatory.

5.3 Space Simulation

Solid State Greenhouse Effect

As a new project (funded by FWF) the investigation of the solid-state greenhouse effect in planetary ices has been started in mid 2002. Its goal is to reach a better understanding of the energy conversion processes in cometary near surface layers and in other planetary ice layers, like the poles of Mars and the icy satellites in the solar system. Two main activities have been commenced:

- Development of a thermal model describing the heat transfer in optically transparent ices, and
- Build-up of an irradiation system (solar simulator), which is combined with our existing cryogenic vacuum chamber. The solar simulator is currently being installed. A result of one of the model calculations, showing the typical subsurface temperature maximum inside an irradiated transparent ice layer, is given in Fig. 5.4.

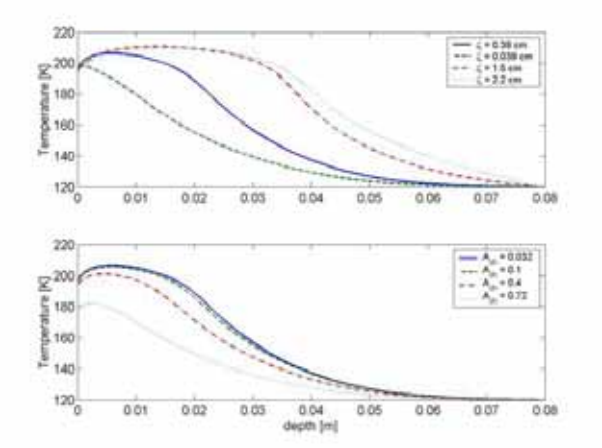

Fig. 5.4: Temperature distribution in an irradiated transparent ice layer, as calculated by a thermal model. The upper panel shows temperature profiles for different absorption scale lengths, while the lower panel shows the effect of varying the albedo.

Exobiology

EXPOSE/Phage and Uracil Response (PUR): Theoretical studies and laboratory experiments for the *PUR* experiment, which is selected for the first mission of ESA's EXPOSE space exposure facility at the ISS, have been performed. The main goal of the studies is to examine and quantify the effect of specific space parameters such as VUV, UV radiation, dehydration effects, non-oxidative environments etc. related to space vacuum conditions on nucleic acid models. We used Uracil thin layers in the ground-based experiments as a part of the living RNA as a model of UV damage in a biological system. A new improved method for the evaluation of the fine optical changes in Uracil due to UV irradiation was developed using the second derivatives of the absorption spectra allowing the optimization of the signal-noise ratio. Short-term tests of vacuum and temperature stability of the sandwich samples were performed under

simulated space vacuum condition in the space simulation chamber at IWF Graz and DLR Cologne. Our experiments show that dimerization caused by the UV exposure of a Hg germicidal lamp can effectively be reverted by the use of a lamp with shorter wavelength components emitting radiation also below 200 nm. We could demonstrate experimentally, for the case of a Uracil thin-layer that the photo-reaction process of the nucleotides can be both, dimerization and the reverse process: monomerization (Fig. 5.5). These results are important for the study of solar UV exposure on early organisms in the terrestrial environment more than 2 Gyr ago where Earth had no UV protecting ozone layer and in the search for live on Mars since we can show that biological harmful effects can also be reduced by shorter wavelength UV radiation, which is important for reducing DNA damages provoked by wavelengths longer than about 240 nm.

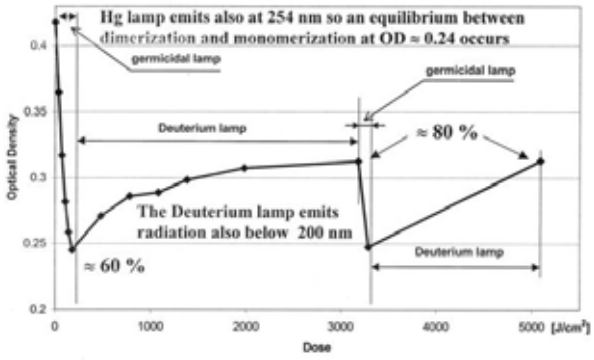

Fig. 5.5: Decrease of the optical density of a Uracil layer due to dimerization by the exposure with a germicidal lamp. A follow-up exposure of the same Uracil layer with a short wavelength Deuterium lamp shows a strong reversion in monomers.

Experiments on Extremeophiles under Martian Conditions: Experiments of halobacterial cells under simulated Martian conditions were also carried out at the IWF space simulation facility. Halobacteria are considered suitable model organisms for exploring the possibility of long-term survival of microorganisms on Mars. First results showed a reduction of viable cells.

Response on Organisms in the Martian Environment (ROME): Due to our participation in the ESA Topical Team ROME, seasonal and diurnal variations in Martian surface UV irradiation with particular emphasis placed on the interpretation in a biological context of the data were studied. A solar UV model was used to yield the surface solar UV irradiance at Martian latitude at any time and place over a Martian year. Seasonal and diurnal variations are calculated, and biological effective dose rates evaluated. The biological interpretation of the solar UV dose rates is performed by determining the DNA damage effects upon Uracil and Phage T7, which are used as examples for biological UV dosimeters. Our studies show that a solar UV "hotspot" is created towards perihelion in the southern hemisphere, with significant damaging effect upon these species. The results are used now for landing site discussions of future Mars landers whose focus is the search for microbial life.

Penetrometry Test Stand

A new penetrometry test stand with the primary purpose to be used for tests within the *NetLander/SPICE* experiment has been installed at the IWF laboratory. This device allows to perform controlled material strength tests over a wide range of cohesive strengths. Its operation is controlled by a LABVIEW program, which performs both the data acquisition and secures the sensitive load cells against damage by overload. Two load cells are incorporated: one covering a range up to 2000 N, allowing penetration tests with hard materials (e.g. consolidated soils or ice crusts), acting also as monitor for the test stand and one with a range of 25 N in compression, corresponding to the range relevant for the *SPICE* experiment. An example of such a measurement, showing the resistance force of a conical tip penetrating into Mars analog soil, is shown in Fig. 5.6.

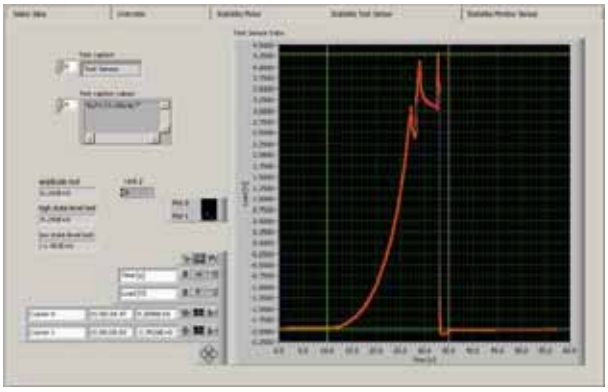

Fig. 5.6: A typical data set measured by the new penetrometry device. It can be seen that the insertion force exponentially increases with depth.

Vacuum Chamber

For functional tests and calibration of space instruments, including future electron beam experiments, a large vacuum chamber with manipulators and sensors is necessary. A suitable chamber, which had been used for similar purposes, has been received from MPE Garching/Germany. The refurbishment of this chamber has started by adding thermal isolation (Fig. 5.7), the renewal of flanges as necessary, and the replacement of some mechanisms. A new set of vacuum pumps and a new control system will complete this facility, which will allow IWF to proceed with its long-term plans for space instrumentation.

Fig. 5.7: Vacuum chamber with thermal isolation.

Temperature Test Facility

During space missions, scientific sensors mounted outside of the spacecraft are usually exposed to extreme temperature conditions. This is in particular true for spacecraft of the upcoming ESA missions to Venus (*Venus Express*, launch 2005) and Mercury (*BepiColombo*, launch 2010).

For this reason a special temperature test facility (Fig. 5.8) for magnetic field sensors was constructed at the Magnetometer Laboratory. It enables all basic test and calibration measurements (offset, scale factor, transfer function …) for especially low-range magnetic field sensors over an extended temperature range (−170 °C through +200 °C). The test facility consists of a three layer magnetic shielding set, the temperature control equipment and a calibration coil for magnetic field stimuli.

Fig. 5.8: Temperature test facility for magnetic field sensors.

5.4 COROT

In co-operation with the Institute for Astronomy, University of Vienna, IWF contributes to the French space telescope *COROT* (Convection, Rotation and Planetary Transit). The scientific goal is the investigation of dynamic

processes in the interior of stars and the search and survey of extrasolar planets. In both cases, astroseismology and exoplanetology, the variation of the brightness of stars is the key parameter. The determination of these variations is done by high precision photometry, with a resolution better than 10 ppm. In astroseismology, the amplitude and frequency of brightness variations is used to derive the oscillation mode and furthermore to determine the physical and chemical processes in the interior. Variations in the brightness can be caused by bypassing planets too; therefore, this effect is used to identify extrasolar planets. To distinguish variation due to oscillations from bypassing planets, spectral analysis in the red and blue zone is performed. In astroseismology, only a few targets are observed, while in exoplanetology the data of 6000 stars are processed simultaneously.

IWF develops the so-called extractor (Boîtiers Extracteur, BEX) a computer system with dedicated pre-processors for the selection and classification of image data. The in-house developed pre-processors allow the identification of pixels, which are part of pre-defined image areas, up to a data rate of 200 kpixel. The essential technology is hardware supported data mining under the constraints for real-time operation. In addition to the development and assembly of the space-qualified hard- and software as well as the ground support equipment, IWF will participate in the integration and test campaign.

The pre-defined image areas are irregular patterns, which compensate the non-linearity of the optics. The processor load is directly depending on the position of the pre-defined areas; therefore, clustering shall be avoided. The so-called look-up table generator program supports the placement, creates the look-up table and estimates the needed system performance.

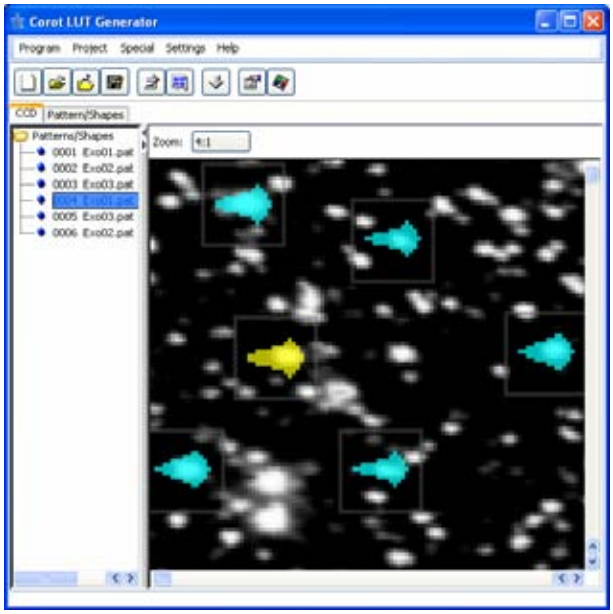

Fig. 5.9: Screen shot of the look-up table generator program.

The design activities dedicated to the hardware are almost finished and the design was presented during the Preliminary Design Review. Presently the laboratory model is assembled and the electrical tests will be finished by the end of 2002.

6 Publications & Talks

6.1 Refereed Articles

Arshoukova, I.L., N.V. Erkaev, H.K. Biernat: Instability of the magnetopause with a finite curvature radius and velocity shear, *Int. J. Geomag. Aeron.*, **3**, 27-34 (2002)

Arshoukova, I.L., N.V. Erkaev, H.K. Biernat: Magnetohydrodynamic instabilities of a high magnetic shear layer with a finite curvature radius, *Physics of Plasmas*, **9**, 401-408 (2002)

Baumjohann, W., R. Schödel, R. Nakamura: Bursts of fast magnetotail transport, *Adv. Space Res.*, **30**, 2241-2246 (2002)

Baumjohann, W.: Modes of convection in the magnetotail, *Physics of Plasmas*, **9**, 3665-3667 (2002)

Biernat, H.K., C.J. Farrugia, G.R. Lawrence, V.S. Semenov, D.F. Vogl, M.T. Kiendl, R.P. Rijnbeek, N.V. Erkaev: Flux transfer events at the magnetopause: Data aspects and theoretical approaches, *Recent Research Developments in Plasmas*, **2**, 1-17 (2002)

Biernat, H.K., S. Mühlbachler, V.S. Semenov, N.V. Erkaev, D.F. Vogl, V.V. Ivanova: Petscheck shocks of reconnection for anisotropic pressure, *Adv. Space Res.*, **29**, 1069-1074 (2002)

Bonev, T., K. Jockers, E. Petrova, M. Delva, G. Borisov, A. Ivanova: The dust in Comet C/1999 S4 (LINEAR) during its disintegration: Narrow-band images, color maps, and dynamical models, *Icarus*, **160**, 419-436 (2002)

Bouhram, M., N. Dubouloz, M. Hamelin, S.A. Grigoriev, M. Malingre, K. Torkar, M.V. Veselov, Y. Galperin, J. Hanasz, S. Perraut, R. Schreiber, L.V. Zinin: Electrostatic interaction between Interball-2 and the ambient plasma. 1. Determination of the spacecraft potential from current calculations, *Ann. Geophys.*, **20**, 1-12 (2002)

Dunlop, M.W., E.A. Lucek, L.M. Kistler, P. Cargill, A. Balogh, W. Baumjohann: Equator-S observations of ion cyclotron waves outside the dawnside magnetopause, *J. Geophys. Res.*, **107**, 10.1029/2001JA900170 (2002)

Dyadechkin, S.A., V.S. Semenov, H.K. Biernat: Accretion of magnetized plasma on a gravitational center, *Int. J. Geomag. Aeron.*, **3**, 77-86 (2002)

Erkaev, N.V., V.A. Shaidurov, V.S. Semenov, H.K. Biernat: Effects of MHD slow shocks propagating along magnetic flux tubes in a dipole magnetic field, *Nonlin. Proc. Geophys*, **9**, 163-172 (2002)

Erkaev, N.V., V.S. Semenov, H.K. Biernat: Rate of unsteady reconnection in an incompressible plasma, *Adv. Space Res.*, **29**, 1075-1080 (2002)

Erkaev, N.V., V.S. Semenov, H.K. Biernat: Two-dimensional MHD model of the reconnection diffusion region, *Nonlin. Proc. Geophys.*, **9**, 131-138 (2002)

Erkaev, N.V., V.S. Semenov, V.A Shaidurov, D. Langmayr, H.K. Biernat, H.O. Rucker: Investigation of MHD slow shocks propagating along the Io flux tube, *Int. J. Geomag. Aeron.*, **3**, 67-76 (2002)

Friedrich, M., K.M. Torkar, M. Harrich, R. Pilgram, S. Kirkwood: On merging empirical models for the lower ionosphere of auroral and non-auroral latitudes, *Adv. Space Res.*, **29**, 929-935 (2002)

Friedrich, M., M. Harrich, K.M. Torkar, P. Stauning: Quantitative measurements with wide-beam riometers, *J. Atmos. Solar-Terr. Phys.*, **64**, 359-365 (2002)

Friedrich, M., M. Posch, S. Kirkwood, K. Stebel, K. Torkar: A novel, high resolution temperature sensor for balloon applications, *Adv. Space Res.*, **30**, 1365-1369 (2002)

Gurnett, D.A., W.S. Kurth, G.B. Hospodarsky, A.M. Persoon, P. Zarka, A. Lecacheux, S.J. Bolton, M.D. Desch, W.M. Farrell, M.L. Kaiser, H.-P. Ladreiter, H.O. Rucker, P. Galopeau, P. Louarn, D.T. Young, W.R. Pryor, M.K. Dougherty: Control of Jupiter's radio emission and aurorae by the solar wind, *Nature*, **415**, 985-987 (2002)

Iorio, L., H.I.M. Lichtenegger, B. Mashhoon: An alternative derivation of the gravitomagnetic clock effect, *Class. Quantum Grav.*, **19**, 39–49 (2002)

Khodachenko, M., V. Zaitsev: Formation of Intensive Magnetic Flux Tubes in a Converging Flow of Partially Ionized Solar Photospheric Plasma, *Astrophys. Space Sci.*, **279**, 389–410 (2002)

Kitaev, A.V., H.K. Biernat: On the effect of geomagnetic field diffusion at the magnetopause, *Planet. Space Sci.*, **50**, 811–816 (2002)

Klimov, S.I., V.A. Grushin, Y.V. Lissakov, M.N. Nozdrachev, A.A Petrukovich, E.A. Grachev, O.R. Grigoryan, D.S. Lysakov, K. Schwingenschuh, H.U. Auster, K–H. Fornacon, J. Rustenbach, V.E. Korepanov, J. Juchniewicz, Y.V. Afanasjev, K. Kudela: Interball–1 and MIR orbital station coordinated magnetic field and energetic particles measurements, *Adv. Space Res.*, **30**, 1847–1853 (2002)

Kömle, N.I., G. Kargl, K. Seiferlin, W. Marczewski: Measuring thermo–mechanical properties of cometary surfaces, *Earth, Moon and Planets*, **90**, 269–282 (2002)

Kubyshkina, M.V., V.A. Sergeev, S.V. Dubyagin, S. Wing, P.T. Newell, W. Baumjohann, A.T.Y. Lui: Constructing the magnetospheric model including pressure measurements, *J. Geophys. Res.*, **107**, 10.1029/2001JA900167 (2002)

Leubner, M.P., N. Schupfer: A universal mirror wave–mode threshold condition for non–thermal space plasma environments, *Nonlin. Proc. Geophys.*, **9**, 75 (2002)

Leubner, M.P.: A non–extensive entropy approach to kappa–distributions, *Astrophys. Space Sci.*, **282**, 573 (2002)

Lichtenegger, H.I.M., H. Lammer, W. Stumptner: Energetic neutral atoms at Mars III: Flux and energy distributions of planetary energetic H atoms, *J. Geophys. Res.*, **107**, 10.1029/2001JA000322 (2002)

Lopez–Moreno, J.J., G.J. Molina–Cuberos, M. Hamelin, V.J.G. Brown, F. Ferri, R. Grard, I. Jernej, J.M. Jeronimo, G.W. Leppelmeier, T. Makinen, R. Rodrigo, L. Sabau, K. Schwingenschuh, H. Svedhem, J. Zarnecki, M. Fulchignoni: The Comas Sola mission to test the HUYGENS/HASI instrument on board a stratospheric balloon, *Adv. Space Res.*, **30**, 1359–1364 (2002)

Molina–Cuberos, G.J., H.I.M. Lichtenegger, K. Schwingenschuh, J.J. Lopez–Moreno, R. Rodrigo: Ion–neutral chemistry model of the lower ionosphere of Mars, *J. Geophys. Res.*, **107**, 10.1029/2000JE001447 (2002)

Moukis, C.G., L.M. Kistler, W. Baumjohann, E.J. Lund, A. Korth, B. Klecker, E. Möbius, M.A. Popecki, J.A. Savaud, H. Reme, A.M. DiLellis, M. McCarthy, C.W. Carlson: Equator–S observations of He+ energization by EMIC waves in the dawnside equatorial magnetosphere, *Geophys. Res. Lett.*, **29**, 10.1029/2001GL013899 (2002)

Mühlbachler, S., C.J. Farrugia, H.K. Biernat, D.F. Vogl, V.S. Semenov, P. Aber, J.M. Quinn, N.V. Erkaev, G.W. Ogilvie, R.P. Lepping, S. Konkubun, T. Mukai: Effects of solar wind dynamic pressure and magnetosonic Mach number on the bow shock and the possible occurence of erosion: October 18–19, 1995, *Int. J. Geomag. Aeron.*, **3**, 5–18 (2002)

Mühlbachler, S., H.K. Biernat, V.S. Semenov, C.J. Farrugia, D.F. Vogl, N.V. Erkaev: Magnetic field line reconnection in the frame of anisotropic MHD, *Adv. Space Res.*, **29**, 1113–1118 (2002)

Nakamura, R., J.B. Blake, S.R. Elkington, D.N. Baker, W. Baumjohann, B. Klecker: Relationship between ULF waves and radiation belt electrons during the March 10, 1998, storm, *Adv. Space Res.*, **30**, 2163–2168 (2002)

Nakamura, R., W. Baumjohann, A. Runov, M. Volwerk, T.L. Zhang, B. Klecker, Y. Bogdanova, A. Roux, A. Balogh, H. Réme, J.A. Sauvaud, H.U. Frey: Fast flow during current sheet thinning, *Geophys. Res. Lett.*, **29**, 10.1029/2002GL016200 (2002)

Nakamura, R., W. Baumjohann, B. Klecker, Y. Bogdanova, A. Balogh, H. Reme, J.M. Bosqued, I. Dandouras, J.A. Sauvaud, K.–H. Glaßmeier, L. Kistler, C. Mouikis, T.L. Zhang, H. Eichelberger, A. Runov, R. Nakamura: Motion of the dipolarization front during a flow burst event observed by Cluster, *Geophys. Res. Lett.*, **29**, 10.1029/2002GL015763 (2002)

Neagu, E., J.E. Borovsky, M.F. Thomsen, S.P. Gary, W. Baumjohann, R.A. Treumann: Statistical survey of magnetic field and ion velocity fluctuations in the near–Earth plasma sheet: Active Magnetospheric Particle Trace Explorers/Ion Release Module (AMPTE/IRM) measurements, *J. Geophys. Res.*, **107**, 10.1029/2001JA000318 (2002)

Nikutowski, B., J. Büchner, A. Otto, L.M. Kistler, A. Korth, C. Moukis, G. Haerendel, W. Baumjohann: Equator-S observation of reconnection coupled to surface waves, *Adv. Space Res.*, **29**, 1129-1134 (2002)

Oka, M., T. Terasawa, H. Noda, Y. Saito, T. Mukai: Acceleration of interstellar helium pickup ions at the Earth's bow shock: GEOTAIL observation, *Geophys. Res. Lett.*, **29**, 10.1029/2001GL014150 (2002)

Oka, M., T. Terasawa, H. Noda, Y. Saito, T. Mukai: 'Torus' distribution of interstellar helium pickup ions: Direct observation, *Geophys. Res. Lett.*, **29**, 10.1029/2002GL015111 (2002)

Patel, M.R., A. Bercés, C. Kolb, H. Lammer, P. Rettberg, J.C. Zarnecki, F. Selsis: Seasonal and diurnal variations in Martian surface UV irradiation: Biological and chemical implications for the Martian regolith, *Int. J. Astrobiol.*, **1/3**, 1-7 (2002)

Pudovkin, M.I., S.A. Zaitseva, B.P. Besser, W. Baumjohann, C.-V. Meister, A.L. Maulini: Proton pitch angle diffusion rate and wave turbulence characteristics in the magnetosheath plasma, *J. Geophys. Res.*, **107**, 1402, 10.1029/2001JA009149 (2002)

Pudovkin, M.I., S.A. Zaitseva, V.V. Lebedeva, A.A. Samsonov, B.P. Besser, C.-V. Meister, W. Baumjohann: MHD-modelling of the magnetosheath, *Planet. Space Sci.*, **50**, 473-488 (2002)

Pudovkin, M.I., S.A. Zaitseva, V.V. Lebedeva, A.A. Samsonov, B.P. Besser, C.-V. Meister: Some problems of magnetosheath physics, *Int. J. Geomag. Aeron.*, **3**, 93-107 (2002)

Romstedt, J., A. Jäckel, W. Klöck, K. Nakamura, H. Arends, K. Torkar, W. Riedler: In situ imaging of µm and sub-µm-sized grains in a cometary environment by atomic force microscopy, *Planet. Space Sci.*, **50 (3)**, 347-352 (2002)

Runov, A.V., M.I. Pudovkin, B.P. Besser: MHD model of plasma sheet evolution in an external electric field: Plasma sheet - fast magnetosonic wave interaction, *Int. J. Geomag. Aeron.*, **3**, 131-139 (2002)

Schödel, R., K. Dierschke, W. Baumjohann, R. Nakamura, T. Mukai: The storm time central plasma sheet, *Ann. Geophys.*, **20**, 1737-1741 (2002)

Semenov, V.S., D.B. Korovinski, H.K. Biernat: Euler potentials for the MHD Kamchatnov-Hopf soliton solution, *Nonlin. Proc. Geophys.*, **9**, 131-138 (2002)

Semenov, V.S., O.B. Alexandrova, N.V. Erkaev, S. Mühlbachler, H.K. Biernat: A simple model of magnetopause erosion as a consequence of pile-up process and bursty reconnection, *Int. J. Geomag. Aeron.*, **3**, 109-116 (2002)

Semenov, V.S., S.A. Dyadechkin, I.B. Ivanov, H.K. Biernat: Energy confinement for a relativistic magnetic flux tube in the ergosphere of a Kerr black hole, *Physica Scripta*, **65**, 13-24 (2002)

Zhang, T.L., W. Baumjohann, R. Nakamura, A. Balogh, K.-H. Glaßmeier: A wavy twisted neutral sheet observed by Cluster, *Geophys. Res. Lett.*, **29**, 10.1029/2002GL015544 (2002)

Zhang, T.L., H. Zhao, G. Le, C.T. Russell, K. Schwingenschuh, W. Magnes, W. Riedler, G.C. Zhou, D.J. Wang, Z.X. Liu, Y.F. Gao, K.Y. Tang, K. Yumoto: Polarization characteristics of dayside Pi2 pulsation on June 14, 1998, *Adv. Space Res.*, **30**, 2339-2343 (2002)

6.2 Proceedings and Book Chapters

Alexeev, I.V., V.S. Semenov, N.V. Erkaev, R.P. Rijnbeek, H.K. Biernat: Rate of Petschek-type magnetic reconnection. In: *Proc. 4th Int. Conf. „Problems of Geocosmos“*, Eds. V.S. Semenov et al., Univ. of St. Petersburg, 34-36 (2002)

Arshoukova, I.L., N.V. Erkaev, H.K. Biernat: Magnetohydrodynamic instability of thin curved layers with smooth variations of the tangential magnetic field. In: *Proc. 4th Int. Conf. „Problems of Geocosmos“*, Eds. V.S. Semenov et al., Univ. of St. Petersburg, 38-41 (2002)

Arsov, K., T. Badura, E. Höck, R. Pail, M. Rothacher, D. Svehla: Effect of temporal variations on high-low SST observations. In: *From Eötvös to Milligal+, ESA Study, Final Report*, Ed. H. Sünkel, TU Graz, 217-319 (2002)

Becker, M., E. Cristea, M. Figurski, L. Gerhatova, G. Grenerczy, J. Hefty, A. Kenyeres, T. Liwosz, G. Stangl: Central European intraplate velocities from CEGRN campaigns. In: *Reports on Geodesy*

No. 1 (61), 2002, Ed. Institute of Geodesy and Geodetic Astronomy, Warsaw University of Technology, 83–92 (2002)

Bérces, A., G. Kovávs, Gy. Rontó, T. Kerékgyártó, H. Lammer, G. Kargl, N.I. Kömle: Uracil dosimeter in simulated extraterrestrial conditions. In: *Proc. 2nd European Workshop on Exo/Astrobiology*, Ed. H. Sawaya-Lacoste, ESA SP-518, 431–432 (2002)

Besser, B.P., K. Schwingenschuh, I. Jernej, H.-U. Eichelberger, H.I.M. Lichtenegger, M. Fulchignoni: Schumann resonances as indicators for lightning on Titan. In: *Proc. 2nd European Workshop on Exo/Astrobiology*, Ed. H. Sawaya-Lacoste, ESA SP-518, 341–344 (2002)

Biernat, H. K., V. S. Semenov, N. V. Erkaev, R. Nakamura, W. Baumjohann, S. Mühlbachler, C. J. Farrugia, D. F. Vogl: Some signatures of magnetic field line reconnection. In: *VIII Int. Symp. on Atmospheric and Oceans Optics: Atmospheric Physics*, Eds. G.A. Zherebetsov et al., International Society for Optics, Washington, 498–506 (2002)

Biernat, H.K., N.V. Erkaev, T. Penz, D.F. Vogl, S. Mühlbacher, H. Lammer, S.C. Manrubia, F. Selsis: Magnetic field reversals on Earth: Possible implications for the biosphere. In: *Proc. 2nd European Workshop on Exo/Astrobiology*, Ed. H. Sawaya-Lacoste, ESA SP-518, 433–434 (2002)

Biernat, H.K., S. Mühlbachler, C.J. Farrugia, R. Nakamura, V.S. Semenov, N.V. Erkaev, W. Baumjohann, D.F. Vogl, D. Langmayr: Reconnection associated discontinuities – Isotropic versus anisotropic plasma conditions. In: *Proc. 4th Int. Conf. „Problems of Geocosmos"*, Eds. V.S. Semenov et al., Univ. of St. Petersburg, 42–49 (2002)

Cockell, C.S., P. Rettberg, G. Horneck, M.R. Patel, H. Lammer, C. Cordoboa-Jabonero: Ultraviolet protection in micro-habitats – lessons from the terrestrial poles applied to Mars. In: *Proc. 2nd European Workshop on Exo/Astrobiology*, Ed. H. Sawaya-Lacoste, ESA SP-518, 215–218 (2002)

Delva, M., H. Feldhofer, K. Schwingenschuh, K. Mehlem: A new multiple sensor magnetic compatibility technique for magnetic field measurements in space. In: *EMC Europe 2002 – Int. Symp. on Electromagnetic Compatibility*, Ed. EMC Europe 2002, AEI, Milan, 523–528 (2002)

Denissenko, V.V., A.V. Mezentsev, S.S. Zamai, H.K. Biernat: The modification due to the movement of ionospheric medium. In: *Proc. 4th Int. Conf. „Problems of Geocosmos"*, Eds. V.S. Semenov et al., Univ. of St. Petersburg, 164–167 (2002)

Ellery, A., A. Ball, C.S. Cockell, P. Coste, D. Dickensheets, H.G.M. Edwards, H. Hu, C. Kolb, H. Lammer, R. Lorenz, G. McKee, L. Richter, A. Winfield, C. Welch: Robotic Astrobiology – the need for sub-surface penetration of Mars. In: *Proc. 2nd European Workshop on Exo/Astrobiology*, Ed. H. Sawaya-Lacoste, ESA SP-518, 313–318 (2002)

Erkaev, N.V., H.K. Biernat, C.J. Farrugia: Magnetic barrier variations caused by reconnection pulses. In: *Proc. 4th Int. Conf. „Problems of Geocosmos"*, Eds. V.S. Semenov et al., Univ. of St. Petersburg, 54–57 (2002)

Fekete, A., K. Módos, M. Hegedüs, Gy. Rontó, G. Kovács, A. Bérces, G. Kargl, N.I. Kömle, H. Lammer: Study of the effect of simulated space environment on nucleoprotein and DNA thin films. In: *Proc. 2nd European Workshop on Exo/Astrobiology*, Ed. H. Sawaya-Lacoste, ESA SP-518, 67–70 (2002)

Fischer, G., T. Tokano, W. Macher, H. Lammer, H.O. Rucker: Energy dissipation of possible Titan lightning strokes as production mechanism for prebiotic molecules. In: *Proc. 2nd European Workshop on Exo/Astrobiology*, Ed. H. Sawaya-Lacoste, ESA SP-518, 511–512 (2002)

Gibbs, P., F. Koidl, G. Kirchner: Comparisons of a single SR620 timer against a variety of timers from the Eurolas network. In: *Proc. 13th Int. Workshop on Laser Ranging*, NASA/GSFC online: http://cddisa.gsfc.nasa.gov/lw13/docs/papers/time_gibbs_1m.pdf, Washington D.C., (2002)

Jernej, I., Ö. Aydogar, B.P. Besser, P. Falkner, M. Fulchignoni, R. Grard, M. Hamelin, J.J. Lopez-Moreno, G.J. Molina-Cuberos, K. Schwingenschuh, R. Trautner: Possible Detection of Lightning at Titan by the Huygens Experiment HASI-PWA. In: *Proc. 2nd European Workshop on Exo/Astrobiology*, Ed. H. Sawaya-Lacoste, ESA SP-518, Noordwijk, 517–518 (2002)

Kaufmann, E., N.I. Kömle, G. Kargl: Experimental and theoretical investigation of the solid-state greenhouse effect. In: *Proc. 2nd European Workshop on Exo/Astrobiology*, Ed. H. Sawaya-Lacoste, ESA SP-518, 87–90 (2002)

Kirchner, G., F. Koidl: Kilohertz Laser Ranging at Graz: Our Plans. In: *Proc. 13th Int. Workshop on Laser Ranging*, NASA/GSFC online: http://cddisa.gsfc.nasa.gov/lw13/docs/papers/tech_kirchner_1m.pdf, Washington D.C., (2002)

Kolb, C., H. Lammer, H.S. Voraberger, A. Bizzarri, A. Del Bianco: Spectroscopic determination of the chemical environment in the Martian regolith. In: *Proc. 2nd European Workshop on Exo/Astrobiology*, Ed. H. Sawaya-Lacoste, ESA SP-518, 465-466 (2002)

Kolb, C., H. Lammer, R. Abart, A. Ellery, H.G.M. Edwards, C.S. Cockell, M.R. Patel: The Martian oxygen surface sink and its implications for the oxidant extinction depth. In: *Proc. 2nd European Workshop on Exo/Astrobiology*, Ed. H. Sawaya-Lacoste, ESA SP-518, 181-184 (2002)

Kolb, C., R. Abart, B. Sauseng: Adsorption-experiments under Martian conditions by means of in-situ Thermo-Gravimetry, DRIFT-spectroscopy and MS in the laboratory. In: *Proc. 2nd European Workshop on Exo/Astrobiology*, Ed. H. Sawaya-Lacoste, ESA SP-518, 467-468 (2002)

Kömle, N.I., G. Kargl, M.B. Steller: Melting probes as a means to explore planetary glaciers and ice caps.. In: *Proc. 2nd European Workshop on Exo/Astrobiology*, Ed. H. Sawaya-Lacoste, ESA SP-518, 305-308 (2002)

Lammer, H., A. Hickel, M.G. Tehrany, A. Hanslmeier, I. Ribas, E.F. Guinan: Simulating the early solar radiation environment: X-ray radiation damage experiments. In: *Proc. 2nd European Workshop on Exo/Astrobiology*, Ed. H. Sawaya-Lacoste, ESA SP-518, 469-470 (2002)

Lammer, H., A. Hosseinmardi, H.I.M. Lichtenegger, C. Kolb, S.J. Bauer: The evolution of the Martian water inventory. In: *Proc. 2nd European Workshop on Exo/Astrobiology*, Ed. H. Sawaya-Lacoste, ESA SP-518, 531-532 (2002)

Lammer, H., F. Selsis, G.J. Molina-Cuberos, W. Stumptner, F. Selsis, T. Kerékgyártó, A. Bérces, Gy. Rontó: Was the ancient Martian surface sterilized by radiation? In: *The Evolving Sun and its Influence on Planetary Environments*, Eds. B. Montesinos et al., Astronomical Society of the Pacific, San Francisco, 151-163 (2002)

Lammer, H., H.I.M. Lichtenegger, C. Kolb, I. Ribas, E.F. Guinan, S.J. Bauer: The Martian atmospheric oxygen surface sink: A source for super-radicals. In: *Proc. 2nd European Workshop on Exo-/Astrobiology*, Ed. H. Sawaya-Lacoste, ESA SP-518, 177-180 (2002)

Lammer, H., P. Wurz, I.L. ten Kate, R. Ruiterkamp: Sputtering of surface matter from Europa. In: *Proc. 2nd European Workshop on Exo/Astrobiology*, Ed. H. Sawaya-Lacoste, ESA SP-518, 533-534 (2002)

Lammer, H., W. Stumptner, G.J. Molina-Cuberos, L.M. Lara, M.G. Tehrany: From atmospheric isotope anomalies to a new perspective on early solar activity. In: *The Evolving Sun and its Influence on Planetary Environments*, Eds. B. Montesinos et al., Astronomical Society of the Pacific, San Fransisco, 249-261 (2002)

Langmayr, D., N.V. Erkaev, V.S. Semenov, V.A Shaidurov, H.K. Biernat, H.O. Rucker, D.F. Vogl, S. Mühlbachler: Electric potential difference due to MHD slow shocks propagating along the Io flux tube. In: *VIII Int. Symp. on Atmospheric and Oceans Optics: Atmospheric Physics*, Eds. G.A. Zherebetsov et al., The International Society for Optics, Washington, 507-512 (2002)

Langmayr, D., P. Zarka, N.V. Erkaev, V.S. Semenov, H.K. Biernat, H.O. Rucker: Theoretical models describing the energy transport along the Io flux tube and the data point of view. In: *Proc. 4th Int. Conf. „Problems of Geocosmos"*, Eds. V.S. Semenov et al., Univ. of St. Petersburg, 154-157 (2002)

Leitner, M., C.J. Farrugia, H.K. Biernat: Stand-off distance of interplanetary magnetic clouds detected by WIND. In: *Proc. 4th Int. Conf. „Problems of Geocosmos"*, Eds. V.S. Semenov et al., Univ. of St. Petersburg, 12-15 (2002)

Leubner, M.P.: On the origin of discrete cosmic structure scales. In: *Proc. 9th Marcel Grossmann Meeting on Recent Developments in General Relativity, Gravitation and Relativistic Field Theories*, Eds. V.G. Gurzadyan et al., World Scientific, Singapore, 2011-2012 (2002)

Leubner, M. P.: Dark matter distribution from gravitational entropy evolution. In: *Dark Matter in Astro- and Particle Physics*, Eds. H.V. Klapdor-Kleibgrothaus et al., Springer, Heidelberg, 312-321 (2002)

Leuko, S., G. Weidler, C. Radax, N.I. Kömle, G. Kargl, H. Stan-Lotter: Examining the physico-

chemical resistance of halobacteria with the LIVE-DEAD kit, following exposure to simulated martian atmospheric conditions and heat. In: *Proc. 2nd European Workshop on Exo/Astrobiology*, Ed. H. Sawaya-Lacoste, ESA SP-518, 473-474 (2002)

Macher, W., G. Fischer, H.O. Rucker, H. Lammer, C. Kolb, B. Schraußer, G. Kargl: Analysis of sounding antennas of the Mars Express MARSIS experiment. In: *Proc. 2nd European Workshop on Exo/Astrobiology*, Ed. H. Sawaya-Lacoste, ESA SP-518, 539-540 (2002)

Molina-Cuberos, G.J., J.A. Morente, J. Portí, K. Schwingenschuh, B.P. Besser, H.I.M. Lichtenegger, H.-U. Eichelberger, A. Salinas: A study of planetary ionospheric cavity using the TLM numerical method: Schumann resonances. In: *Proc. 10th Int. IGTE Symp. on Numerical Field Calculation in Electrical Engineering*, TU Graz, 89-93 (2002)

Mühlbachler, S., C.J. Farrugia, H.K. Biernat, R.B. Torbert, V.S. Semenov: Geostationary magnetic field signatures of erosion: WIND-GEOS observations. In: *SOLSPA 2001*, Ed. H. Sawaya-Lacoste, ESA SP-477, 459-462 (2002)

Mühlbachler, S., C.J. Farrugia, H.K. Biernat, V.S. Semenov, N.V. Erkaev, R.B. Torbert, D.F. Vogl, D. Langmayr: Studies of dayside magnetopause erosion on geostationary orbit using WIND and GEOS data (1996-1999). In: *VIII Int. Symp. on Atmospheric and Oceans Optics: Atmospheric Physics*, Eds. G.A. Zherebetsov et al., The International Society for Optics, Washington, 523-531 (2002)

Mühlbachler, S., C.J. Farrugia, H.K. Biernat, V.S. Semenov, R.B. Torbert, D.F. Vogl, D. Langmayr: The geostationary field as a function of dynamic pressure under northward IMF conditions. In: *Proc. 4th Int. Conf. „Problems of Geocosmos"*, Eds. V.S. Semenov et al., Univ. of St. Petersburg, 75-78 (2002)

Nakamura, R., W. Baumjohann, H. Noda, G. Paschmann, B. Klecker, P. Puhl-Quinn, J. Quinn, R. Torbert, A. Balogh, H. Reme, H.U. Frey, C.J. Owen, A.N. Fazakerly, J.P. Dewhurst: Substorm expansion onsets observed by Cluster. In: *Proc. 6th Int. Conf. on Substorms*, Ed. R.M. Winglee, University of Washington, Seattle, 55-62 (2002)

Nykyri, K., A. Otto, J. Büchner, B. Nikutowski, W. Baumjohann, L. Kistler, C. Mouikis: Equator-S observations of boundary signatures: FTE's or Kelvin-Helmholtz waves? In: *Earth's Low-latitude Boundary Layer*, Eds. P.T. Newell et al., AGU, Washington, 205-210 (2002)

Pany, T., P. Pesec, G. Stangl: Network Monitoring at the OLG Analysis Centre. In: *EUREF Publication No. 10*, Verlag des Bundesamtes für Kartographie und Geodäsie, Frankfurt/M, 125-129 (2002)

Pastorek, L., Z. Vörös: Nonlinear analysis of solar cycle variability. In: *Proc. 10th European Solar Physics Meeting*, Ed. A. Wilson, ESA SP-506, 197-200 (2002)

Patel, M.R., J.C. Zarnecki, H. Lammer, C. Kolb, F. Selsis: The Variation of Ultraviolet Irradiance at the Martian Surface. In: *Proc. 2nd European Workshop on Exo/Astrobiology*, Ed. H. Sawaya-Lacoste, ESA SP-518, 161-164 (2002)

Povoden, G., H. Lammer, G. Grampp, F. Stelzer: Experiments and simulation models for the study of prebiotic chemistry in Titan's atmosphere. In: *Proc. 2nd European Workshop on Exo/Astrobiology*, Ed. H. Sawaya-Lacoste, ESA SP-518, 549-550 (2002)

Pudovkin, M.I., S.A. Zaitseva, B.P. Besser: Magnetosheath current system and the magnetopause erosion. In: *Proc. 4th Int. Conf. „Problems of Geocosmos"*, Eds. V.S. Semenov et al., Univ. of St. Petersburg, 81-89 (2002)

Rontó, Gy., A. Bérces, A. Fekete, T. Kerékgyártó, H. Lammer, G. Kargl, N.I. Kömle: Biological samples on the ISS-EXPOSE facility for the ROSE/PUR experiment. In: *Proc. 2nd European Workshop on Exo/Astrobiology*, Ed. H. Sawaya-Lacoste, ESA SP-518, 63-66 (2002)

Rucker, H.O.: Radioastronomical Aspects in the search for Extrasolar Planets. In: *Proc. 2nd European Workshop on Exo/Astrobiology*, Ed. H. Sawaya-Lacoste, ESA SP-518, 421-426 (2002)

Schmieder, B., B. Vincent, W. Baumjohann, T. Ono, S. Basu, L. Lean: Climate and weather of the sun earth system: CAWSES, SCOSTEP'S program for 2003-2008. In: *SOLSPA 2001*, Ed. H. Sawaya-Lacoste, ESA SP-477, 59-62 (2002)

Schwingenschuh, K., H.I.M. Lichtenegger, M. Menvielle, M. Hamelin, W. Magnes, I. Jernej, H.-U. Eichelberger, C. Kolb, H. Lammer, G. Musmann, W. Zambelli, G.J. Molina-Cuberos: Investigations of Water on Mars Using Netlander Electric and

Magnetic Experiments. In: *Proc. 2nd European Workshop on Exo/Astrobiology*, Ed. H. Sawaya-Lacoste, ESA SP-518, 559-560 (2002)

Selsis, F., H. Lammer, I. Ribas, E.F. Guinan, H.I.M. Lichtenegger, L. Lara, M.G. Tehrany, A. Hanslmeier: Radiation and particle exposure of the Martian paleoatmosphere: Implications for the loss of water. In: *Proc. 2nd European Workshop on Exo/Astrobiology*, Ed. H. Sawaya-Lacoste, ESA SP-518, 553-554 (2002)

Stangl, G.: Creating a common CEGRN solution: The rules behind. In: *Reports on Geodesy*, Ed. Institute of Geodesy and Geodetic Astronomy, Warsaw University of Technology, Warsaw, 23-26 (2002)

Steller, M.B., J. Heihsler, H. Ottacher: From Stars to Habitable Planets, the Austrian Contribution to the COROT Mission. In: *Proc. 2nd European Workshop on Exo/Astrobiology*, Ed. H. Sawaya-Lacoste, ESA SP-518, 561-562 (2002)

Visser P.N.A.M., R. Rummel, G. Balmino, H. Sünkel, J. Johannessen, M. Aguirre, P.L. Woodworth, C. LeProvost, C.C. Tscherning, R. Sabadini: The European Earth Explorer Mission GOCE: Impact for the Geosciences. In: *Ice Sheets, Sea Level and the Dynamic Earth,* Eds. J.X. Mitrovica et al., AGU, Washington, 95-107 (2002)

Vogl, D.F., D. Langmayr, N.V. Erkaev, H.K. Biernat, S. Mühlbachler: The anisotropic jump equations for a perpendicular fast shock in a kappa distributed medium. In: *Proc. 4th Int. Conf. „Problems of Geocosmos"*, Eds. V.S. Semenov et al., Univ. of St. Petersburg, 103-107 (2002)

Vogl, D.F., N.V. Erkaev, H.K. Biernat, H.O. Rucker, S. Mühlbachler, D. Langmayr: The analysis of an inclined shock including pressure anisotropy. In: *VIII Int. Symp. on Atmospheric and Oceans Optics: Atmospheric Physics*, Eds. G.A. Zherebetsov et al., The International Society for Optics, Washington, 513-522 (2002)

Weidler, G., S. Leuko, C. Radax, G. Kargl, N.I. Kömle, H. Stan-Lotter: Viability and DNA damage of halobacteria under physical stress condition, including a simulated martian atmosphere. In: *Proc. 2nd European Workshop on Exo/Astrobiology*, Ed. H. Sawaya-Lacoste, ESA SP-518, 491-492 (2002)

Zhang, Z., Y. Fumin, G. Kirchner, F. Koidl: Automated Operational Software at Shanghai SLR Station. In: *Proc. 13th Int. Workshop on Laser Ranging*, NASA/GSFC online: http://cddisa.gsfc.nasa.gov/lw13/docs/papers/auto_zhang_1m.pdf, Washington D.C., (2002)

6.3 Books

Semenov, V.S., A.M. Lyatskaya, M.V. Kubyshkina, H.K. Biernat (Eds.): *Proc. 4th Int. Conf. "Problems of Geocosmos"*, Univ. of St. Petersburg, 368+viii pages (2002)

6.4 Other Publications

Angelopoulos, V., C.W. Carlson, G.T. Delory, R.P. Lin, S. Mende, F.S. Mozer, G.K. Parks, T.D. Phan, M.A. Temerin, K.K. Khurana, X. Li, M.G. Kivelson, A.T.Y. Lui, J. Raeder, D. Sibeck, C.T. Russell, R.E. Ergun, U. Auster, K.-H. Glaßmeier, W. Baumjohann, A. Roux, R. Nakamura, E. Donovan, K. Schwingenschuh, P. Escoubet, J. Büchner, H. Laakso, O. Le-Contel, M. Fujimoto, C.J. Jacquey, I. Voronkov, D. LeQueau, V. Sergeev, J. Samson, H.J. Singer: THEMIS: Time History of Events and Macroscale Interactions during Substorms, Phase A Study Report to NASA, 132 pages (2002)

Arsov, K., et al.: From Eötvös to Milligal+, WP4: Effect of Temporal Variations on High-Low SST Observations, Final Report, 92 pages (2002)

Besser, B.P.: Franz Ulinski, an Almost Forgotten Early Pioneer of Rocketry, Techn. Paper IAC-02-IAA.2.1.04, 5 pages (2002)

Delva, M., H. Feldhofer, K. Schwingenschuh: MMS Technical Report - Phase II, Workpackages 4-7, MMS-IWF-TR004/7, 132 pages (2002)

Eichelberger, H.-U., K. Schwingenschuh, Ö. Aydogar, W. Baumjohann: Sample Rate and Frequency Response Analysis of Rosetta RPC-MAG, IWF 2002/01, 53 pages (2002)

Feldhofer, H., M. Delva, W. Magnes, W. Koren, K. Schwingenschuh: MMS Technical Report - Phase III, Workpackages 8-9, MMS-IWF-TR-008; MMS-IWF-HW-TD-1-6, 141 pages (2002)

Feldhofer, H., M. Delva: MMS - POLYMAG Software User manual, MMS-IWF-UMAN-001, 162 pages (2002)

Feldhofer, H., M. Delva: MMS - POLYMAG Software Specification and Architectural Design Docu-

ment, MMS-IWF-SSAD-001, 112 pages (2002)

Fischer, G.: Remote Control of the Anritsu MS2661C Spectrum Analyzer, IWF 142, 25 pages (2002)

Stangl, A., M.Y. Boudjada, H.O. Rucker, W. Voller, G. Fischer: Catalogue of Solar decametric emissions observed by the Digital SpectroPolarimeter (DSP) from October 2000 to January 2001, IWF 125, 59 pages (2002)

Sünkel, H., et al.: *GOCE: Preparation for the Level 1 to Level 2 Data Processing*, ESA/ESTEC Contract No. 14986/01/NL/DC, Final Report, 270 pages, Graz (2002)

Sünkel, H., et al.: *From Eötvös to Milligal+*, ESA/ESTEC Contract No. 14287/00/NL/DC, Final Report, 319 pages, Graz (2002)

Sünkel, H.: *Advanced Mathematical Methods and Applications in Satellite Geodesy*, Lecture Note, 170 pages, University of Calgary (2002)

Taubenschuss, U., M.Y. Boudjada, H.O. Rucker, P.H.M. Galopeau: Study of the attenuation band patterns observed by WAVES experiment on board Wind satellite, IWF 139, 20 pages (2002)

Vogl, D.F., H.P. Ladreiter, P. Zarka, B. Cecconi, W.S. Kurth, W. Macher, H.O. Rucker, G. Fischer: Calibration of the Cassini RPWS antenna system: Roll maneuver on DOY 022, 2001, IWF 131, 185 pages (2002)

Vogl, D.F., H.P. Ladreiter, P. Zarka, B. Cecconi, W.S. Kurth, W. Macher, H.O. Rucker, G. Fischer: Calibration of the Cassini RPWS antenna system: Roll maneuver on DOY 027, 2001, IWF 132, 185 pages (2002)

Vogl, D.F., H.P. Ladreiter, P. Zarka, B. Cecconi, W.S. Kurth, W. Macher, H.O. Rucker, G. Fischer: Calibration of the Cassini RPWS antenna system: Roll maneuver on DOY 036, 2001, IWF 133, 185 pages (2002)

Vogl, D.F., H.P. Ladreiter, P. Zarka, B. Cecconi, W.S. Kurth, W. Macher, H.O. Rucker, G. Fischer: Calibration of the Cassini RPWS antenna system: Roll maneuver on DOY 037, 2001, IWF 134, 185 pages (2002)

6.5 Invited Talks

Baumjohann, W., R. Nakamura: What is Cluster telling us about substorms, *COSPAR Assembly*, Houston, Oct 2002.

Baumjohann, W.: Response of the magnetosphere, *ASA/ESA Summerschool*, Alpbach, Jul 2002.

Baumjohann, W.: Wissenschaftliche Weltraumforschung: Das Sonnensystem, *Alpbacher Technologiegespräche 2002*, Alpbach, Aug 2002.

Nakamura, R., et al.: Space Weather and Cluster observations, *EGS Meeting*, Nice, Apr 2002.

Nakamura, R., et al.: Substorm expansion onsets observed by Cluster, *6th Int. Conf.on Substorms (ICS-6)*, Seattle, Mar 2002.

Nakamura, R., et al.: Plasma sheet expansion observed by Cluster and Geotail, *COSPAR Colloquium "Frontiers of magnetospheric plasma physics"*, Sagamihara, Jul 2002.

Rucker, H.O.: Planetare Radiostrahlung, *66. Physikertagung der Deutschen Physikalischen Gesellschaft*, Leipzig, Mar 2002.

Rucker, H.O.: Planetare Radiostrahlung - eine Möglichkeit zur Detektion von extrasolaren Planeten, Institut für Theoretische Physik, TU Braunschweig, Dec 2002.

Runov, A., R. Nakamura, W. Baumjohann, H. Noda, T.L. Zhang, M. Volverk, A. Balogh, G. Paschmann, J.M. Quinn, H. Reme, B. Klecker: Cluster magnetotail observations: Some first results, *4th Int. Conf. „Problems of Geocosmos"*, St. Petersburg, Jun 2002.

Sünkel, H.: Satelliten als Spione im Erdschwerefeld, PANGEO Austria – Erdwissenschaften in Österreich, Salzburg, Jun 2002.

Sünkel, H.: Erdbeobachtung, *Alpbacher Technologiegespräche 2002*, Alpbach, Aug 2002.

Sünkel, H.: Gravity Field Recovery from Space - Status and Perspectives of the Recent Gravity Field Missions, *VII Int. Congress on Earth Sciences*, Santiago, Oct 2002.

Volwerk, M., et al.: Dynamic Thin Current Sheets: FGM Observations by Cluster, *Maryland Workshop on Thin Current Sheets*, College Park, Apr 2002.

Volwerk, M., et al.: ULF Waves as a Diagnostic Tool: Results from Cluster, *AGU Fall Meeting 2002*, San Francisco, Dec 2002.

6.6 Oral Presentations

Baumjohann, W., et al.: Substorm expansion onsets observed by Cluster, *EGS Meeting*, Nice, Apr 2002.

Baumjohann, W., et al.: The CAWSES program, *EGS Meeting*, Nice, Apr 2002.

Baumjohann, W.: Space Physics at IWF, Tokyo University, Tokyo, Jun 2002.

Besser, B.P., K. Schwingenschuh, H.I.M. Lichtenegger, H.-U. Eichelberger, G.J. Molina-Cuberos, J.A. Morente, J. Portí, A. Salinas: Analytical and numerical investigations of Schumann resonances, *COSPAR Assembly*, Houston, Oct 2002.

Besser, B.P., K. Schwingenschuh, I. Jernej, H.-U. Eichelberger, H.I.M. Lichtenegger, M. Fulchignoni: Schumann resonances as indicators for lightning on Titan, *2nd European Workshop on Exo/Astrobiology*, Graz, Sep 2002.

Besser, B.P.: Franz Ulinski, an Almost Forgotten Early Pioneer of Rocketry, *IAF Congress*, Houston, Oct 2002.

Besser, B.P.: Friedrich Schmiedl - Raketenpionier und Wegbereiter der Weltraumforschung, MASTERMINDS, Graz, Dec 2002.

Cristea, E., G. Stangl: OLG Monitoring of the Balkan Mountains and the Eastern Mediterranean Area, *Symp. of the IAG Subcommission for Europe (EUREF)*, Ponta Delgada, Jun 2002.

Feldhofer, H., M. Delva: A new multiple sensor magnetic compatibility technique for magnetic field measurements in space, *EMC Europe 2002*, Sorrento, Sep 2002.

Kargl, G., N.I. Kömle, M. Thiel, M. Hlond, C. Kolb, H. Lell: Detection of small-scale structures with the MUPUS ANC-M sensor on the Rosetta Lander, *ACM (Asteroids, Comets, Meteors)*, Berlin, Aug 2002.

Kargl, G.: Facilities for planetary simulation experiments at the IWF in Graz, *2nd European Workshop on Exo/Astrobiology*, Graz, Sep 2002.

Kaufmann, E.: Experimental and theoretical investigation of the solid state greenhouse effect, *2nd European Workshop on Exo/Astrobiology*, Graz, Sep 2002.

Khodachenko, M., H.O. Rucker, G. Haerendel: Effects of inductive interaction in groups of solar current-carrying magnetic loops, *EGS Meeting*, Nice, Apr 2002.

Khodachenko, M., H.O. Rucker: Inductive interaction of longitudinal currents as a possible source for magnetic loops oscillations in solar active regions, *EGS Meeting*, Nice, Apr 2002.

Khodachenko, M.L.: Dynamic processes in groups of coronal current-carrying magnetic loops, University of Warwick, Dept. of Physics, Coventry, May 2002.

Khodachenko, M.L.: MHD effects triggered by beams of fast particles in magnetic tubes and their possible relation to plasma heating during solar flares, School of Math. & Statistics, Univ. of St. Andrews, May 2002.

Kirchner, G., F. Koidl: Kilohertz Laser Ranging at Graz: Our Plans, *13th Int. Workshop on Laser Ranging*, Washington D.C., Oct 2002.

Kirchner, G., F. Koidl: New Detection Package at Graz, *13th Int. Workshop on Laser Ranging*, Washington D.C., Oct 2002.

Kolb, C., H. Lammer, R. Abart, A. Ellery, H.G.M. Edwards, C.S. Cockell, M.R. Patel: The Martian oxygen surface sink and its implications for the oxidant extinction depth, *2nd European Workshop on Exo/Astrobiology*, Graz, Sep 2002.

Kolb, C., H. Lammer: Application of a planetary simulation chamber in context of UV-induced molecular adsorption and toxicological aspects on Mars, *Int. Workshop on Water in the Upper Martian Surface*, Potsdam, Apr 2002.

Kömle, N.I., G. Kargl, K. Seiferlin, T. Spohn: Measuring thermophysical properties of cometary surfaces: in situ methods, *IAU-Colloquium No. 186: Cometary Science after Hale-Bopp*, Puerto de la Cruz, Jan 2002.

Kömle, N.I.: Melting probes as a means to explore planetary glaciers and subsurface oceans, *2nd European Workshop on Exo/Astrobiology*, Graz, Sep 2002.

Lammer, H., H.I.M. Lichtenegger, C. Kolb, I. Ribas, E.F. Guinan, S.J. Bauer: The Martian atmospheric oxygen surface sink: A source for superradicals,

2nd European Workshop on Exo/Astrobiology, Graz, Sep 2002.

Lammer, H., H.I.M. Lichtenegger, C. Kolb: Loss of water from Mars, *Int. Workshop on Water in the Upper Martian Surface*, Potsdam, Apr 2002.

Lammer, H., H.I.M. Lichtenegger, C. Kolb: Loss of water from Mars: What can we expect from Mars Express and Nozomi?, *EGS Meeting,* Nice, Apr 2002.

Lammer, H., S.J. Bauer: Isotopic fractionation by gravitational escape, *Workshop Solar System History from Isotopic Volatile Signatures*, Bern, Jan 2002.

Lammer, H., W.W. Weiss, R. Dvorak: Upper exosphere temperature estimations on exosolar planets, *3th COROT Week*, Liege, Dec 2002.

Lammer, H.: Atmosphere-surface interaction on Mars, *EGS Meeting*, Nice, Apr 2002.

Lammer, H.: Ozone: from a life protecting gas on Earth to a biomarker on exosolar planets, Biophysics Research Group, Hungarian Academy of Sciences, Budapest, Oct 2002.

Lammer, H.: Radiation exposure experiments in space, Biophysics Research Group, Hungarian Academy of Sciences, Budapest, Jun 2002.

Lammer, H.: Stability estimations of exospheres on exosolar planets, Departament d'Astronomia i Meteorologia, Universitat de Barcelona, Dec 2002.

Lammer, H.: The early Sun: Implications for Mercury, Physics Department, University of Bern, Jul 2002.

Lammer, H.: The Martian oxygen surface sink and toxicological implications of the surface, Institute of Advanced Studies, Colloquium Budapest, Budapest, Jun 2002.

Lichtenegger, H.I.M., H. Lammer, D.F. Vogl, S.J. Bauer: Temperature effects of energetic neutral hydrogen on the Martian exosphere, *COSPAR Assembly*, Houston, Oct 2002.

Lichtenegger, H.I.M., L. Iorio, B. Mashhoon: The gravitomagnetic clock effect and its possible observation, *COSPAR Assembly*, Houston, Oct 2002.

Magnes, W., A. Valavanoglou, A. Frank, K. Schwingenschuh, D. Pierce, C.T. Russell: Design principles of a sigma-delta fluxgate magnetometer, *EGS Meeting*, Nice, Apr 2002.

Nakamura, R., et al.: Fast flows during substorm intensifications observed by Cluster, *EGS Meeting*, Nice, Apr 2002.

Pesec, P.: CERGOP-2, a Multi Purpose and Interdisciplinary Sensor Array for Environmental Research in Central Europe, *EGS Meeting*, Nice, Apr 2002.

Pesec, P.: CERGOP-2/Environment - its impact on EUREF, *Symp. of the IAG Subcommission for Europe (EUREF)*, Ponta Delgada, Jun 2002.

Pesec, P.: New Efforts of the CERGOP data-bank at Graz for CERGOP-2, *EGS Meeting*, Nice, Apr 2002.

Pesec, P.: The Role of Transponders in the GAVDOS Project, TUC Chania, Jan 2002.

Riedler, W., K. Torkar, H. Jeszenszky, J. Romstedt: Atomic force microscopy for cometary dust, *2nd European Workshop on Exo/Astrobiology*, Graz, Sep 2002.

Rucker, H.O.: Radioastronimocal aspects in the search for extrasolar planets, *2nd European Workshop on Exo/Astrobiology*, Graz, Sep 2002.

Rucker, H.O.: Simultane Messungen der Dekameter Radiostrahlung von Jupiter und der Sonne / Radioastronomische Aspekte bei extrasolaren Radioplaneten, AIP, Potsdam, Nov 2002.

Stangl, G., R. Weber, N. Höggerl, E. Fragner: EUREF-Campaign for the introduction of ETRS89 in Austria, *EUREF TWG*, Delft, Nov 2002.

Sünkel, H.: The Space Research Institute of the Austrian Academy of Sciences, Landesverteidigungsakademie, Vienna, Apr 2002.

Sünkel, H.: Die Erde lebt - die Erde bebt, Rotary Club, Liezen, Jun 2002.

Sünkel, H.: Die Satellitenmission GOCE der ESA - Eine Herausforderung an Mathematik, Numerik und Informatik, *SAG-BGÖ Benutzertreffen*, Semmering, Oct 2002.

Torkar, K., M. Fehringer, C.P. Escoubet, M. André, A. Pedersen, K.R. Svenes, P.M.E. Décréau: Analysis of Cluster spacecraft potential during active control, *COSPAR Assembly*, Houston, Oct 2002.

Vogl, D.F., D. Langmayr, H.K. Biernat, N.V. Erkaev, S. Mühlbachler: The anisotropic jump equations

for oblique fast shocks in a kappa distributed medium, *COSPAR Assembly*, Houston, Oct 2002.

Vogl, D.F.: The calibration of the Cassini RPWS antenna system, *COSPAR Assembly*, Houston, Oct 2002.

Vogl, D.F.: The perpendicular fast shock including pressure anisotropy and kappa distribution function, *EGS Meeting*, Nice, Apr 2002.

Volwerk, M., et al.: Compressional waves in the current sheet: A Cluster study, *AGU Fall Meeting 2002*, San Francisco, Dec 2002.

Vörös, Z., P. Kovacs, D. Jankovicova: Multifractal analysis of magnetospheric and solar wind data, *EGS Meeting*, Nice, Apr 2002.

Zhang, T.L.: The magnetotail current sheet observed by Cluster, CSSAR, Beijing, Oct 2002.

6.7 Posters

Arsov, K., R. Pail: Gravity field recovery from GOCE GPS-SST observations, *EGS Meeting*, Nice, Apr 2002.

Boudjada, M.Y., A. Stangl, S. Sawas, H.O. Rucker, G. Mann, A. Konovalenko, A. Lecacheux, W. Voller, V. Mostetschnig: Spectral and polarization analysis of the Solar decametric emissions, *EGS Meeting*, Nice, Apr 2002.

Boudjada, M.Y., J.S. Pickett, P. Decreau, H.O. Rucker, N. Cornilleau, K. Mursula: Quasi-periodic structures in the Earth's plasmasphere observed by WBD experiment on board the CLUSTER satellites, *COSPAR Assembly*, Houston, Oct 2002.

Boudjada, M.Y., P.H.M. Galopeau, H.O. Rucker: Jovian 'sub-storm' and its influence on the hectometric and kilometric emissions, *EGS Meeting*, Nice, Apr 2002.

Fischer, G., T. Tokano, W. Macher, H. Lammer, H.O. Rucker: Energy dissipation of possible Titan lightning strokes as production mechanism for prebiotic molecules, *2nd European Workshop on Exo/Astrobiology*, Graz, Sep 2002.

Fischer, G., T. Tokano, W. Macher, H. Lammer, H.O. Rucker: Energy dissipation of possible Titan lightning strokes, *Eurojove*, Lisbon, Jun 2002.

Höck, E.: The treatment of ocean tides in the context of the GOCE satellite mission, *EGS Meeting*, Nice, Apr 2002.

Jernej, I., Ö. Aydogar, B.P. Besser, P. Falkner, M. Fulchignoni, R. Grard, M. Hamelin, J.J. Lopez-Moreno, G.J. Molina-Cuberos, K. Schwingenschuh, R. Trautner: Possible Detection of Lightning at Titan by the Huygens Experiment HASI-PWA, *2nd European Workshop on Exo/Astrobiology*, Graz, Sep 2002.

Kargl, G.: Facilities for planetary simulation experiments at the IWF in Graz, *2nd European Workshop on Exo/Astrobiology*, Graz, Sep 2002.

Khodachenko, M., H.O. Rucker: MHD effects triggered by beams of fast particles in magnetic tubes and their possible manifestations in microwave and X-ray emissions from solar-flares, *Western Pacific Geophysics Meeting*, Wellington, Jul 2002.

Khodachenko, M., H.O. Rucker: On the inductive interaction of current-carrying magnetic loops in solar active regions, *STEREO Workshop*, Paris, Mar 2002.

Khodachenko, M., H.O. Rucker: Tests of the models of Coronal magnetic loops inductive interaction within the SECCHI on the STEREO mission and their relation to CME phenomena, *STEREO Workshop*, Paris, Mar 2002.

Kolb, C., H. Lammer, H.S. Voraberger, A. Bizzarri, A. Del Bianco: Spectroscopic determination of the chemical environment in the Martian regolith, *2nd European Workshop on Exo/Astrobiology*, Graz, Sep 2002.

Kolb, C., R. Abart, B. Sauseng: Adsorption-experiments under Martian conditions by means of in-situ Thermo-Gravimetry, *2nd European Workshop on Exo/Astrobiology*, Graz, Sep 2002.

Kolb, C., R. Abart, H. Lammer, G. Grampp, S. Landgraf, G. Povoden: Planetary multi-user simulation facilities, *EGS Meeting*, Nice, Apr 2002.

Lammer, H., A. Hickel, M.G. Tehrany, A. Hanslmeier, I. Ribas, E.F. Guinan: Simulating the early solar radiation environment: X-ray radiation damage experiments, *2nd European Workshop on Exo/Astrobiology*, Graz, Sep 2002.

Lammer, H., A. Hosseinmardi, H.I.M. Lichtenegger, C. Kolb, S.J. Bauer: The evolution of the Martian water inventory, *2nd European Workshop on Exo/Astrobiology*, Graz, Sep 2002.

Lammer, H., M.G. Tehrany, A. Hanslmeier, I. Ribas, E.F. Guinan, C. Kolb: Erosion and sublimation

effects on Mercury's surface: past and present, *EGS Meeting*, Nice, Apr 2002.

Lammer, H., P. Wurz, I.L. ten Kate, R. Ruiterkamp: Sputtering of surface matter from Europa, *2nd European Workshop on Exo/Astrobiology*, Graz, Sep 2002.

Lammer, H., P. Wurz, M.R. Patel, G.J. Molina-Cuberos, C. Kolb: Particle release processes and radiation environment on Mercury`s surface in view of ESA`s BepiColombo mission, *EGS Meeting*, Nice, Apr 2002.

Lichtenegger, H.I.M., H. Lammer: Flux and energy distributions of planetary H and O atoms on Venus and Mars, *EGS Meeting*, Nice, Apr 2002.

Macher, W., B. Schraußer, G. Fischer, H.O. Rucker, H. Lammer, C. Kolb, G. Kargl: Analysis of sounding antennas of the Mars-Express MARSIS experiment, *2nd European Workshop on Exo/Astrobiology*, Graz, Sep 2002.

Noda, H., et al.: Electric field pulsations in the Earth's tail lobe, *EGS Meeting*, Nice, Apr 2002.

Noda, H., et al.: Tail lobe convection observed by Cluster/EDI, *EGS Meeting*, Nice, Apr 2002.

Riedler, W., K. Torkar, H. Jeszenszky, J. Romstedt: The instrument MIDAS for atomic force microscopy on cometary dust, *2nd European Workshop on Exo/Astrobiology*, Graz, Sep 2002.

Rucker, H.O., U. Taubenschuss, M. Leitner, A. Lecacheux, A. Konovalenko: Simultaneous observations of Jupiter DAM emissions, *2002 Western Pacific Geophysics Meeting*, Wellington, Jul 2002.

Schwingenschuh, K., H.I.M. Lichtenegger, M. Menvielle, M. Hamelin, W. Magnes, I. Jernej, H.-U. Eichelberger, C. Kolb, H. Lammer, G. Musmann, W. Zambelli, G.J. Molina-Cuberos: Investigations of Water on Mars Using Netlander Electric and Magnetic Experiments, *2nd European Workshop on Exo/Astrobiology*, Graz, Sep 2002.

Steller, M.B., J. Heihsler, H. Ottacher, W. Weiss: From Stars to Habitable Planets, the Austrian Contribution to the COROT Mission, *2nd European Workshop on Exo/Astrobiology*, Graz, Sep 2002.

Torkar, K., et al.: Survey of Cluster plasma measurements supported by active spacecraft potential control, *EGS Meeting*, Nice, Apr 2002.

Torkar, K., M. Fehringer, C.P. Escoubet, A. Fazakerley, S. Szita, K.R. Svenes, H. Rème, I. Dandouras, M. André, P.M.E. Décréau: Improvement of plasma neasurements onboard Cluster due to spacecraft potential control, *COSPAR Assembly*, Houston, Oct 2002.

Valavanoglou, A., et al.: Concept Study and First Realisation of a Sigma-Delta Fluxgate Magnetometer, *High Sensitivity Magnetometers*, Port-Bail, Nov 2002.

Vogl, D.F., W. Macher, G. Fischer, B. Cecconi, P. Zarka, W.S. Kurth, H.O. Rucker, D.A. Gurnett, H.P. Ladreiter: The calibration of the Cassini RPWS antenna system, *Western Pacific Geophysics Meeting*, Wellington, Jul 2002.

Volwerk, M., et al.: Cluster Observations of Neutral Sheet Oscillations, *EGS Meeting*, Nice, Apr 2002.

Volwerk, M., et al.: Discovery of water on the Galilean satellites by the Galileo magnetometer, *2nd European Workshop on Exo/Astrobiology*, Graz, Aug 2002.

Zhang, T.L., et al.: Structures of the neutral sheet observed by Cluster, *COSPAR Assembly*, Houston, Oct 2002.

Zhang, T.L., et al.: Structures of the neutral sheet observed by Cluster, *EGS Meeting*, Nice, Apr 2002.

Zhang, T.L., K.K. Khurana, C.T. Russell, M.G. Kivelson, R. Nakamura, W. Baumjohann: Solar Wind Dynamic Pressure Effect on the Venus Bow Shock, *COSPAR Assembly*, Houston, Oct 2002.

6.8 Co-Authored Presentations

Arshoukova, I.L., N.V. Erkaev, H.K. Biernat, D.F. Vogl: Interchange Instability of the Venusian Ionopause, *COSPAR Assembly*, Houston, Oct 2002.

Bérces, A., G. Kovávs, Gy. Rontó, T. Kerékgyártó, H. Lammer, G. Kargl, N.I. Kömle: Uracil dosimeter in simulated extraterrestrial conditions, *2nd European Workshop on Exo/Astrobiology*, Graz, Sep 2002.

Bérces, A., T. Kerékgyártó, Gy. Rontó, H. Lammer, G. Kargl, N.I. Kömle: Study of the non-linear UV

dosimetry in simulated extraterrestrial conditions, *EGS Meeting*, Nice, Apr 2002.

Del Bianco, A., R. Bertran, C. Kolb, G. Kurat, H. Lammer, V. Laziæ, H.S. Voraberger: In-situ geological and biological analysis of planetary surfaces: A proposal for an integrated instrument, *2nd European Workshop on Exo/Astrobiology*, Graz, Sep 2002.

Cockell, C.S., P. Rettberg, G. Horneck, M.R. Patel, H. Lammer, C. Cordoba-Jabonero: Ultraviolet protection in micro-habitats – lessons from the terrestrial poles applied to Mars, *2nd European Workshop on Exo/Astrobiology*, Graz, Sep 2002.

Ellery, A., A. Ball, C.S. Cockell, P. Coste, D. Dickensheets, H.G.M. Edwards, H. Hu, C. Kolb, H. Lammer, R. Lorenz, G. McKee, L. Richter, A. Winfield, C. Welch: Robotic Astrobiology – the need for sub-surface penetration of Mars, *2nd European Workshop on Exo/Astrobiology*, Graz, Sep 2002.

Fekete, A., K. Módos, M. Hegedüs, Gy. Rontó, G. Kovács, A. Bérces, G. Kargl, N.I. Kömle, H. Lammer: Study of the effect of simulated space environment on nucleoprotein and DNA thin films, *2nd European Workshop on Exo/Astrobioloy*, Graz, Sep 2002.

Fekete, A., Gy. Rontó, M. Hegedüs, K. Módos, A. Bérces, G. Kovács, H. Lammer, N.I Kömle, G. Kargl: Simulation experiments of the effect of space environment on bacteriophage and DNA thin film, *COSPAR Assembly*, Houston, Oct 2002.

Galopeau, P.H.M., M.Y. Boudjada, H.O. Rucker: Occurrence probability of jovian decameter radio emissions: Theoretical evidence of active longitude, *Magnetospheres of the Outer Planets Conference*, Johns Hopkins University, Laurel, Jul 2002.

Gibbs, P., F. Koidl, G. Kirchner: Inter-comparison of various timing devices against a single SR timer (Herstmonceux – D), *13th Int. Workshop on Laser Ranging*, Washington D.C., Oct 2002.

Höggerl, N., G. Stangl: National Report 2001/2002 for Austria, *Symp. of the IAG Subcommission for Europe*, Ponta Delgada, Jun 2002.

Jankovicova, D., Z. Vörös: Neural network prediction of geomagnetic storms: a method using regularity- scaling characteristics, *EGS Meeting*, Nice, Apr 2002.

Konovalenko, A., E. Abranin, V. Zakharenko, V. Lisachenko, V. Melnik, O. Ulyanov, H.O. Rucker, M. Boudjada, A. Lecacheux, C. Rosolen: Observations of new types of the solar sporadic radio emission at decameter wavelengths, *EGS Meeting*, Nice, Apr 2002.

Konovalenko, A., I. Falkovich, N. Kalinichenko, M. Olyak, A. Lecacheux, C. Rosolen, J.-L. Bourgeret, H.O. Rucker, Y. Tokarev: High sensitive scintillation obserations at very low frequencies, *EGS Meeting*, Nice, Apr 2002.

Kurth, W.S., D.A. Gurnett, G.B. Hospodarsky, P. Zarka, A. Lecacheux, M. Desch, M. Kaiser, P. Louarn, H.O. Rucker: Radio Astronomy at Jupiter and Saturn from Cassini, *COSPAR Assembly*, Houston, Oct 2002.

Kurth, W.S., D.A. Gurnett, G.V. Gospodarsky, M.D. Desch, W.M. Farrell, M.L. Kaiser, P. Zarka, A. Lecacheux, H.O. Rucker, P. Galopeau, A. Roux, P. Louarn, C.J. Alexander: Radio and plasma wave observations at Jupiter by Cassini and Galileo, *2002 Western Pacific Geophysics Meeting*, Wellington, Jul 2002.

Leitner, M., H.O. Rucker: A digital broadband waveform receiving system for fast radio emissions in the decametric range, *2002 Western Pacific Geophysics Meeting*, Wellington, Jul 2002.

Leuko, S., G. Weidler, C. Radax, A. Legat, N.I. Kömle, G. Kargl, H. Stan-Lotter: Examining the physico-chemical resistance of halobacteria with the LIVE-DEAD kit, following exposure to simulated martian atmospheric conditions and heat, *2nd European Workshop on Exo/Astrobiology*, Graz, Sep 2002.

Litvinenko, G., V. Vinogradov, M. Leitner, H.O. Rucker, V. Shaposhnikov: Microsecond modulations in the simple Jovian decameter S-bursts, *EGS Meeting*, Nice, Apr 2002.

Matsui, H., J.M. Quinn, R.B. Torbert, V.K. Jordanova, W. Baumjohann, G. Paschmann: Convection measurements in the inner magnetosphere by Cluster, *AGU 2002 Fall Meeting*, San Francisco, Dec 2002.

Matsuoka, A., W. Baumjohann: The magnetic field experiment for Bepi-Colombo MMO, *EGS Meeting*, Nice, Apr 2002.

Molina-Cuberos, G.J., J.A. Morente, J. Portí, K. Schwingenschuh, B.P. Besser, H.I.M. Lichtenegger, H.-U. Eichelberger, A. Salinas: A study of

planetary ionospheric cavity using the TLM numerical method: Schumann resonances, *10th Int. IGTE Symp.*, Graz, Sep 2002.

Morente, J.A., G.J. Molina-Cuberos, J. Portí, K. Schwingenschuh, B.P. Besser, H.I.M Lichtenegger, H.-U. Eichelberger, A. Salinas: Schumann resonances and electromagnetic transparence in the atmosphere of Titan, *COSPAR Assembly*, Houston, Oct 2002.

Nornberg, P., J. Merrison, H.P. Gunnlaugsson, K. Kinch, C. Kolb, W. Goessler, N. Kienzl: Iron oxide soil precipitate as Mars analogue in wind tunnel experiments, *EGS Meeting*, Nice, Apr 2002.

Patel, M.R., J.C. Zarnecki, H. Lammer, C. Kolb, F. Selsis: Seasonal and diurnal variations of UV at the Martian surface, *2nd European Workshop on Exo/Astrobiology*, Graz, Sep 2002.

Patel, M.R., A. Bérces, T. Kerékgyártó, Gy. Rontó, H. Lammer, J.C. Zarnecki: Annual solar UV exposure and biological effective dose rates on the Martian surface, *COSPAR Assembly*, Houston, Oct 2002.

Patel, M.R., A. Bercés, T. Kerékgyártó, H. Lammer, C. Kolb, J.C. Zarnecki, F. Selsis: Annual variation of the biological effective UV dose on the Martian surface, *EGS Meeting*, Nice, Apr 2002.

Petrukovich, A.A., W. Baumjohann, R. Nakamura, A. Balogh, K.-H. Glaßmeier: Plasma sheet structure during strong northward IMF, *COSPAR Assembly*, Houston, Oct 2002.

Pickett, J., M.Y. Boudjada, T.F. Bell, Q.G. Zong, M.L. Adrian, P. Decreau, P. Canu, O. Santolik, A. Masson, H. Laakso, D.A. Gurnett, T.A. Fritz, N. Cornilleau-Wehrlin, M. Andre: Triggered VLF emissions observed by the CLUSTER wideband plasma wave receiver near the plasmapause, *COSPAR Assembly*, Houston, Oct 2002.

Povoden, G., H. Lammer, G. Grampp, F. Stelzer: Experiments and simulation models for the study of prebiotic chemistry in Titan's atmosphere, *2nd European Workshop on Exo/Astrobiology*, Graz, Sep 2002.

Rontó, Gy., A. Bérces, A. Fekete, T. Kerékgyártó, H. Lammer, G. Kargl, N.I. Kömle: Biological samples on the ISS-EXPOSE facility for the ROSE/PUR experiment, *2nd European Workshop on Exo/Astrobiology*, Graz, Sep 2002.

Rontó, Gy., A. Bérces, A. Fekete, G. Kovács, H. Lammer: Biological UV dosimeters in simulated space, *COSPAR Assembly*, Houston, Oct 2002.

Schmieder, B., B. Vincent, W. Baumjohann, T. Ono, S. Basu, L. Lean: Climate and Weather of the Sun Earth system: SCOSTEP's program for 2004-2008, *COSPAR Assembly*, Houston, Oct 2002.

Selsis, F., H. Lammer, I. Ribas, E.F. Guinan, H.I.M. Lichtenegger, L. Lara, M.G. Tehrany, A. Hanslmeier: Radiation and particle exposure of the Martian paleoatmosphere: Implications for the loss of water, *2nd European Workshop on Exo/Astrobiology*, Graz, Sep 2002.

Selsis, F., L.-M. Lara, H. Lammer, I. Ribas, E.F. Guinan: Effects of early X-ray and EUV fluxes on planetary paleoatmospheres, *EGS Meeting*, Nice, Apr 2002.

Taubenschuss, U., M.Y. Boudjada, H.O. Rucker, P.H.M. Galopeau: A 'caustic-like' pattern in the Jovian hectometric spectra, *EGS Meeting*, Nice, Apr 2002.

Tehrany, M.G., H. Lammer, F. Selsis, I. Ribas, E.F. Guinan, A. Hanslmeier: The particle and radiation environment of the early Sun, *10th European Solar Physics Meeting*, Prague, Sep 2002.

Weidler, G., S. Leuko, C. Radax, N.I. Kömle, G. Kargl, H. Stan-Lotter: Viability and DNA damage of halobacteria under physical stress condition, including a simulated martian atmosphere, *2nd European Workshop on Exo/Astrobiology*, Graz, Sep 2002.

7 Teaching & Workshops

7.1 Lecturing

IWF members are actively engaged in teaching at five universities. In summer 2002 and in the current winter term 2002/2003 the following lectures are given, in addition to a number of practical exercises and seminars. The majority of the lectures are given in German.

KFU Graz

Introduction to Geophysics (Bauer)

Introduction to Meteorology (Bauer)

Magnetospheric Coupling (Selected Chapters of Space Physics and Aeronomy) (Biernat)

Plasma Physics (Foundations) (Biernat)

Plasma Physics (Transport) (Biernat)

Solar-Terrestrial Relationships (Waves and Instabilities) (Biernat)

Instruments and Data Processing in Geophysics and Space Physics (Boudjada)

Introduction to Planetology (Kömle, Lammer)

Measurement Methods in Space Physics and Aeronomy (in-situ measurements) (Rucker)

Measurement Methods in Space Physics and Aeronomy (remote sensing) (Rucker)

Planetary Radio and Plasma Waves (Rucker)

TU Graz

HF-Engineering 1 (Riedler)

HF-Engineering 2 (Riedler)

Dynamical Satellite Geodesy (Sünkel)

Satellite Geodesy (Sünkel)

Theory and Practice of Active Plasma Experiments in Space (Torkar)

JKU Linz

Mathematics for Students of Computer Sciences in Economics I (Hausleitner)

LMU München

Space Plasma Physics I (Baumjohann)

Space Plasma Physics II (Baumjohann)

University of Calgary

Advanced Mathematical Methods and Applications in Satellite Geodesy (Sünkel)

Advanced Course

The joint two-years post-graduate university course MAS Space Sciences at both Karl-Franzens University of Graz and Graz University of Technology continued in 2002 with the second and third semester, where candidates get prepared for the master thesis in the fourth semester in 2003. Several scientific members of IWF are supervisors of the participants of the MAS Space Sciences (http://www.spacesciences.oeaw.ac.at).

Summer University

The Summer University “Graz in Space – Current Space Research” has been organized by IWF in cooperation with lecturers from Karl-Franzens University of Graz, Graz University of Technology, Joanneum Research, Vienna University of Technology and Magna Steyr Space Technology. These summer university lecture presentations took place from September 23 – 27, 2002, and provided an extensive overview on Space Physics, Remote Sensing, Space

Communication and Navigation, as well as on Life Sciences. One day was specifically devoted to manned space flight to Mars. Main coordinator and organizer was H.O. Rucker (http://www.grazinspace.oeaw.ac.at).

7.2 Theses

Besides lecturing, IWF members are supervising Diploma/Doctoral Theses and Habilitations. In 2002, the following theses have been completed:

Mühlbachler, S.: Studies of Dayside Magnetic Field Line Erosion Signatures, Doctoral Thesis, KFU Graz (Supervisor: H. Biernat)

Pail, R.: Selected problems in the framework of the GOCE data processing", Habilitation, TU Graz (Supervisor: H. Sünkel)

Pany, T.K.: Entwicklung und Anwendung von Modellen für die troposphärische Laufzeitverzögerung von GPS Signalen basierend auf Modellen der numerischen Wettervorhersage und der Turbulenztheorie, Doctoral Thesis, TU Graz (Supervisor: H. Sünkel)

Steindl, M.J.: Hardware-Entwicklung eines Rangegate-Generators, Diploma Thesis, Fachhochschule Deggendorf/BRD (Supervisor: G. Kirchner/P. Sperber)

Töfferl, H.: Data Preselection using a Lookup Table for the Space Telescope COROT, Diploma Thesis, TU Graz (Supervisors: M.B. Steller, H. Ottacher/B. Rinner)

Valavanoglou, A.: Concept Study and First Realization of a Sigma-Delta Fluxgate Magnetometer, Diploma Thesis, TU Graz (Supervisor: W. Magnes/M. Friedrich)

Wagner, B.: Gravitoelektromagnetismus und Lense-Thirring-Effekt - Bewegung eines Testteilchens in der linearisierten Kerrmetrik, Diploma Thesis, KFU Graz (Supervisor: H.I.M. Lichtenegger/A. Hanslmeier)

7.3 Workshops

From September 16 – 19, 2002, together with the Institute for Geophysics, Astrophysics and Meteorology (IGAM) of the KFU Graz, the IWF hosted the 2nd European Workshop on Exo-/Astrobiology. This workshop was organized by H. Lammer (IWF Graz) together with IGAM, the European Exo/Astrobiology Network Association (EANA) and ESA. About 300 participants from 21 nations have attended this workshop. Corresponding proceedings have been published in November 2002 by ESA.

In addition, H.O. Rucker organized a session at the 2002 Western Pacific Geophysics Meeting in Wellington, New Zealand, and W. Baumjohann organized sessions at the EGS Meeting in Nice, France, and the German Physical Society Meeting in Leipzig.

8 Personnel

Arsov, Kirčo, Dr. (S)
Aydogar, Özer, Dipl.-Ing. (E)
Badura, Thomas, Dipl.-Ing. (S, RFTE)
Bauer, Siegfried J., Prof. em. (P, BMBWK)
Baumjohann, Wolfgang, Prof. (E)
Berghofer, Gerhard, Ing. (E)
Besser, Bruno, Dr. (E)
Biernat, Helfried K., Prof. (P)
Boudjada Mohammed Y., Dr. (P)
Chwoika, Rudolf (S)
Cristea, Elena, Dipl.-Ing. (S, part. UN)
Delva, Magda, Dr. (E)
Eichelberger, Hans U., Dipl.-Ing. (E, BMVIT)
Feldhofer, Helmut, Dipl.-Ing. (E, part. ESA)
Fischer, Georg, Dipl.-Ing. (P)
Flock, Barbara, Mag. (E)
Fremuth, Gerhard, Dipl.-Ing. (E)
Gerler, Oliver, Dipl.-Ing. (E, ESA)
Giner, Franz, Dipl.-Ing. (E)
Graf, Christian, Ing. (S)
Hausleitner, Walter, Dr. (S)
Heihsler, Johann, Dipl.-Ing. (E, BMBWK)
Höck, Eduard, Dipl.-Ing. (S)
Jernej, Irmgard, Ing. (E)
Jeszenszky, Harald, Dipl.-Ing. (E)
Jetzl, Ilse, Dr. (P)
Kargl, Günter, Dr. (P)
Kaufmann, Erika, Mag. (P, FWF)
Khodachenko, Maxim, Dr. (P)
Kirchner, Georg, Dr. (S)
Kögler, Gerald (I)
Koidl, Franz, Ing. (S)
Kolb, Christoph, Mag. (P)
Kömle, Norbert, Dr. (P)
Koren, Wolfgang, Ing. (E)
Kürbisch, Christoph, Ing. (E)
Laky, Gunter, Dipl.-Ing. (E)
Lammer, Helmut, Dr. (P)
Langmayr, Daniel, Mag. (P, FWF)
Leubner, Manfred, Dr. (P, BMBWK)
Lichtenegger, Herbert I.M., Dr. (E)
Macher, Wolfgang, Dipl.-Ing. (P)
Magnes, Werner, Dr. (E)
Močnik, Karl, Dr. (E)
Mühlbachler, Stefan, Dr. (P, FWF & RFTE)
Nakamura, Rumi, Dr. (P)
Neukirchner, Sonja, Ing. (E)
Nischelwitzer-Fennes, Ute, Ing. (E)
Ottacher, Harald, Mag. (E, BMBWK & ESA)
Pešec, Peter, Dr. (S)
Preimesberger, Thomas, Dipl.-Ing. (S, RFTE)
Riedler, Willibald, Prof. em. (E, BMBWK)
Rucker, Helmut O., Prof. (P)
Runov, Andrei V., Dr. (E)
Scherr, Alexandra, Mag. (I)
Schwingenschuh, Konrad, Dr. (E)
Slamanig, Herwig, Dipl.-Ing. (I, BMBWK)
Stachel, Manfred, Ing. (E, ESA)
Stangl, Günter, Dipl.-Ing. (S, BEV)
Steiner, René, Dipl.-Ing. (E, ESA & FWF)
Steller, Manfred, Dr. (E)
Stock, Daniel (E)
Sucker, Michael, Dipl.-Ing. (S)
Sünkel, Hans, Prof. (S, BMBWK)
Torkar, Klaus M., Univ.-Doz. (E)
Valavanoglou, Aris, Dipl.-Ing. (E)
Vogl, Dieter, Dr. (P)
Voller, Wolfgang G., Mag. (P)
Volwerk, Martin, Dr. (E, MPE)
Vörös, Zoltán, Dr. (E)
Wallner, Robert, Ing. (E)
Zehetleitner, Sigrid (S & I)
Zhang, Tie-Long, Dr. (E)

As of December 31, 2002

E: Experimental Space Research, P: Extraterrestrial Physics, S: Satellite Geodesy, I: Institute Administration. Most positions are directly funded through ÖAW, others as indicated by: BEV: Federal Office for Metrology and Surveying, BMBWK: Federal Ministry for Education, Science and Culture, BMVIT: Federal Ministry of Transport, Innovation and Technology, ESA: European Space Agency, FWF: Austrian Science Fund, MPE: Max-Planck Institute for Extraterrestrial Physics, RFTE: Austrian Council for Research and Technology Development, UN: United Nations.